Iron Phosphate Glass–Containing Hanford Waste Simulant

GJ Sevigny
ML Kimura
CM Fischer
MJ Schweiger
CP Rodriguez
D Kim
BJ Riley

January 2012

Pacific Northwest
NATIONAL LABORATORY

Proudly Operated by **Battelle** *Since 1965*

DISCLAIMER

Iron Phosphate Glass–Containing Hanford Waste Simulant

GJ Sevigny
ML Kimura
CM Fischer
MJ Schweiger
CP Rodriguez
D Kim
BJ Riley

January 2012

Pacific Northwest National Laboratory
Richland, Washington 99352

Summary

Resolution of the nation's high-level tank waste legacy requires the design, construction, and operation of large and technically complex one-of-a-kind processing waste treatment and vitrification facilities. While the ultimate limits for waste loading and melter efficiency have yet to be defined or realized, significant reductions in glass volumes for disposal and mission life may be possible with advancements in melter technologies and/or glass formulations.

This test report describes the experimental results from a small-scale test using the research-scale melter (RSM) at Pacific Northwest National Laboratory (PNNL) to demonstrate the viability of iron-phosphate-based glass with a selected waste composition that is high in sulfate (4.37 wt% SO_3). The primary objective of the test was to develop data to support a cost-benefit analysis related to the implementation of phosphate-based glasses for Hanford low-activity waste (LAW) and/or other high-level waste streams within the U.S. Department of Energy complex. The testing was performed by PNNL and supported by Idaho National Laboratory, Savannah River National Laboratory, Missouri University of Science and Technology, and Mo-Sci Corporation.

The RSM is a small, joule-heated melter capable of processing melter feed on a continuous basis. The melter is equipped with Inconel 693 electrodes, Monofrax K-3 refractory, and an Inconel 690 pour spout. For the experiments described here, an electric kiln surrounded the melter body and minimized heat loss from the melter body during operation. The RSM was equipped with an off-gas treatment system that employed quenching, wet scrubbing, and high-efficiency mist elimination. The glass discharge section was heated to facilitate pouring of the glass. The melter cavity was 15 cm in diameter with a nominal glass depth of 7.6 cm. The melter was operated with a glass target temperature of 1030°C and a plenum temperature between 300 and 600°C.

The RSM test was broken into five segments to determine the effects of adding sugar to the feed and subsurface air injection through the molten glass, both of which are included in the current Waste Treatment Plan design. The test segments were:

1.   No sugar, no air bubbler
2.   No sugar, air bubbler short duration
3.   Sugar, no air bubbler
4.   Sugar, air bubbler
5.   No sugar, air bubbler long duration

Overall, the test produced 124 kg of glass. The average glass density was 2.77 g/cm^3.

At the conclusion of the test, the melter and exhaust lines were inspected for particulate deposition and corrosion. The melter electrodes and bubbler tube were removed from the glass in the RSM. The electrodes were examined with an optical microscope and a scanning electron microscope (SEM). The electrodes appeared discolored and without the loss of significant amounts of metal. Before and after measurements indicated a very small reduction in electrode dimension. Differences in the thickness measurements indicated a corrosion rate less than 0.3 mm/year and maximum length differences indicated a maximum corrosion rate of 2.1 mm/yr.

Samples of glass and off-gas condensate were collected during the test for mass balance calculation and glass durability measurements. The data indicate an average sulfur retention in the glass of 70 wt% which is within the requirements for the low-level waste glass. Retention of Re (Tc surrogate) was 80 wt% based on the feed-to-off-gas values and 30 wt% based on the feed-to-glass values. The unaccounted for Re is most likely attributed to inefficiencies of the off-gas scrubbing equipment and scrub solution. The off-gas condensate data, along with the feed-rate and concentration data, also indicate that air bubbling likely decreased overall retention in the melter, but especially reduced retention of S in the melter.

The processing of iron-phosphate-based glass was similar to borosilicate glass, although the melter was operated at a lower average temperature (1030°C) with 4.4 wt% SO_3 compared to typical borosilicate melts at 1150°C and <1.5 wt% SO_3. The average RSM glass production rate was from 0.31 to 1 kg/h resulting in a melter surface area normalized glass generation rates of 411 to 1330 kg/day·m^2. The addition of sugar and/or air bubbling increased the processing rate as expected, with the glass production rate more than doubling with the introduction of both sugar and air bubbling. The product glass met the LAW glass product consistency test (PCT) requirement for both quenched and canister centerline cooling (CCC) treated glasses, with lower PCT performance for CCC treated glasses likely caused by crystallization. The CCC treated samples had greater alteration rate variability than the quenched samples, with three of the CCC treated samples failing the vapor-phase hydration test (VHT) requirement. Whereas all quenched glasses showed little sign of alteration. The failure of some CCC samples to meet VHT requirement may be related to the high crystallinity and low reproducibility of crystallization in CCC samples. The corrosion of melter components was acceptable, and losses to the melter exhaust were typical of other waste glasses.

Acknowledgments

Acronyms and Abbreviations

CCC	canister centerline cooling
CCIM	cold crucible induction melter
DAC	data acquisition and control
EPA	U.S. Environmental Protection Agency
EVS	ejector venturi scrubber
FEP	Iron Phosphate
HEME	high-efficiency mist eliminator
HLW	high-level waste
ICP	inductively coupled plasma
ICP-AES	inductively coupled plasma–atomic emission spectroscopy
ICP-MS	inductively coupled plasma–mass spectrometry
INL	Idaho National Laboratory
JHM	joule-heated melter
LAW	low activity waste
PCT	product consistency test
PNNL	Pacific Northwest National Laboratory
RSM	research-scale melter
SEM	scanning electron microscope
SRNL	Savannah River National Laboratory
TCLP	toxicity characteristic leaching procedure
UDS	undissolved solids
VHT	vapor-phase hydration test
WTP	Hanford Tank Waste Treatment and Immobilization Plant
XRD	x-ray diffraction

Contents

Figures

Tables

1.0   Introduction

Resolution of the nation's high-level tank waste legacy requires the design, construction, and operation of large and technically complex one-of-a-kind processing waste treatment and vitrification facilities. Vitrification technology was chosen to treat the high-level waste (HLW) fraction of tank waste at the U.S. Department of Energy's (DOE's) Hanford and the Savannah River Sites, the low-activity waste (LAW) fraction of tank waste at Hanford, and potentially other defense waste streams such as the sodium-bearing tank waste or calcine HLW at Idaho National Laboratory (INL). Joule-heated melters (JHMs) are being used at the Defense Waste Processing Facility and will be used at the Hanford Tank Waste Treatment and Immobilization Plant (WTP) to vitrify tank waste fractions. While the ultimate limits for waste loading and melter efficiency have yet to be defined or realized, significant reductions in glass volumes for disposal and mission life may be possible with advancements in melter technologies and/or glass formulations.

Advanced glass formulations are needed to take advantage of the next generation melter technologies such as the advanced JHMs or cold crucible induction melters (CCIMs). New glass formulations for increased waste loading and melt rates would substantially reduce the volume of glass produced, stored, transported, and disposed. This would significantly reduce the cost and schedule of tank waste management in the United States.

With respect to advanced glass formulations, phosphate-based glasses offer the potential for significant increases in loading of wastes that are high in troublesome components (e.g., S, Cr, P, F, and Cl) that are difficult to dissolve into silicate melts (Kim et al. 2003). However, phosphate-based glasses are not a mature technology relative to alkali-borosilicate glasses for the vitrification of HLW and LAW. Early research on phosphate-based glasses has shown unacceptable corrosion of melter components and crystallization on slow cooling to form low-durability waste forms (Perez et al. 2001). However, recent studies have shown promise in the ability to formulate iron-phosphate-based waste glasses that may not demonstrate the drawbacks found in earlier phosphate formulation studies (Kim et al. 2003, Kim et al. 2004).

This test report describes the experimental results from a small-scale test using the research-scale melter (RSM), a JHM at Pacific Northwest National Laboratory (PNNL), to demonstrate the viability of iron-phosphate-based glass with a selected waste composition that is high in sulfates. Data are given for the volatility of S and Re (Tc surrogate), and corrosion of melter materials.

A similar study was undertaken at Idaho National Laboratory (INL) to evaluate iron-phosphate-based glass processing in a CCIM (Soelberg and Rossberg 2011). The INL study also showed losses of about 10 mass% S and 35.7 mass% Re. The RSM showed a range of retention from 20 to about 70 percent for both elements depending on processing conditions. These results suggest adequate retention of S and Re can be achieved while processing iron-phosphate-based glass.

2.0   Objectives

The primary objective of the test was to develop data to support a cost-benefit analysis related to the implementation of phosphate-based glasses for Hanford LAW and/or other HLW streams within the DOE complex. Data required for such an assessment included, but were not limited to, successful production of a durable glass and retention of S and Re (Tc surrogate) without causing excessive corrosion to JHM components. This test demonstrated the process flowsheet through a small-scale integrated process test by:

- Obtaining steady feeding operations for a prolonged period using the RSM to determine processing rate and evaluate corrosion of melter electrode and ceramic materials

- Collecting samples from feed, glass, and off-gas components and completing a mass balance to the determine fate of Re, S, P, and other elements provided by inductively coupled plasma (ICP) analyses.

3.0 Task Organization and Responsibilities

Project responsibilities of each contributing group are described below.

- PNNL
  - Provided overall responsibility for the performance of the test
  - provided test facility (RSM system) and support infrastructure (e.g., utilities, electrician, machine shop)
  - provided feed staging
  - prepared test procedure and test instruction
  - provided operational direction during the test series
  - provided RSM process monitors and data logging equipment
  - provided data reduction and test report preparation
  - provided vapor hydration test (VHT) of glass
- Savannah River National Laboratory (SRNL)
  - analyzed glass samples
  - analyzed waste-stream samples
  - performed product consistency test (PCT)
- Mo-Sci Corporation and Missouri University of Science and Technology (MS&T)
  - produced/analyzed phosphate glass composition
  - produced/analyzed start-up glass
  - determined Fe^{+2}/total iron ratios for the glass
- INL
  - provided simulated slurry feed
  - provided glass formers

4.0 Experimental Equipment Descriptions

The RSM processing system used to support the objectives of this study is described in this section.

4.1 RSM System Description

The Process Development Laboratory East building in Richland, Washington, housed the RSM system. Figure 4.1 shows the process flow diagram for the RSM test.
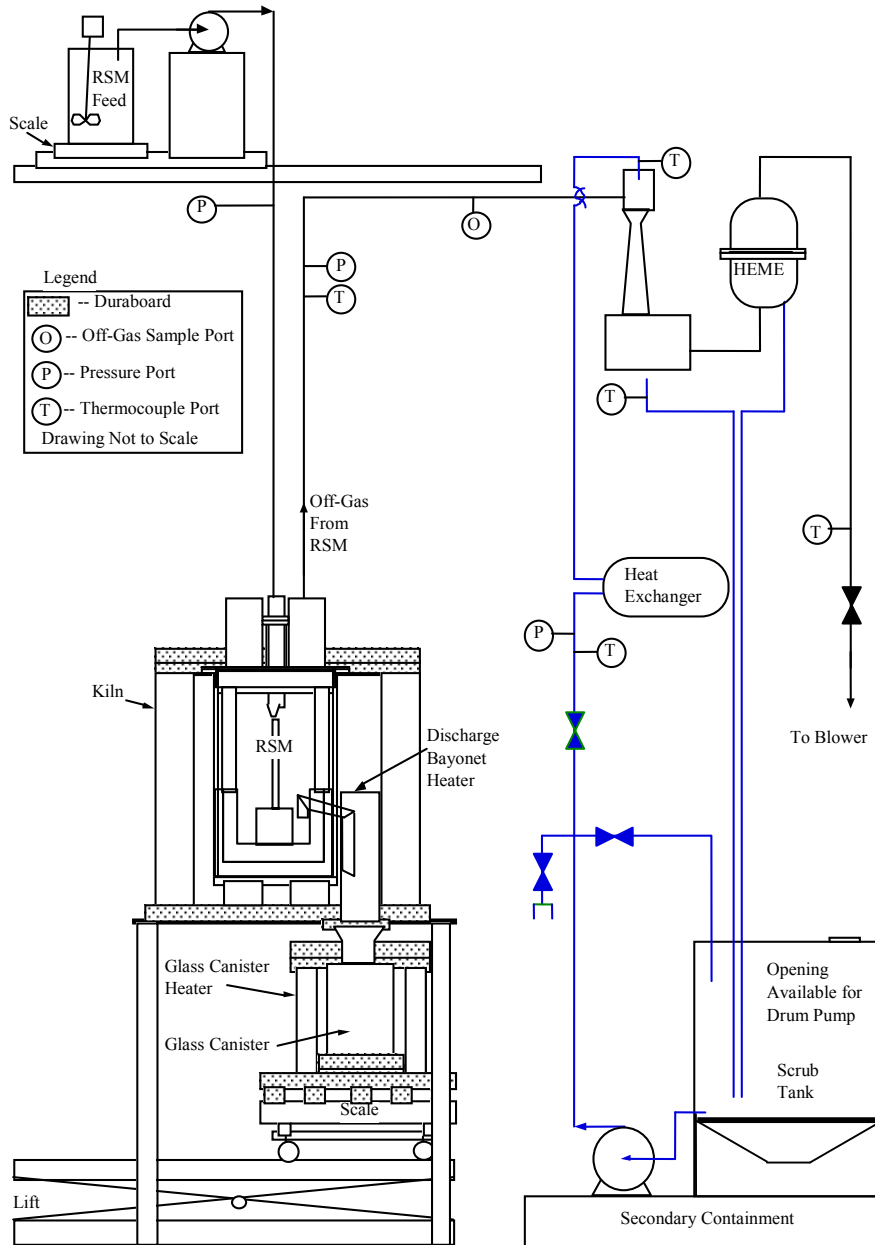
Figure 4.1. Research-Scale Melter Process Flow Diagram

The RSM is a small JHM capable of processing melter feed on a continuous basis. This capability is representative of a full-scale system, which was the key for determining the relationships between the properties of the feed and the final glass produced. Testing in the RSM allowed quantitative measurement of the off-gas stream and performance of parametric studies (e.g., changing one feed component at a time to determine its effect on the process) in a relatively short time. The RSM processing system provided unit off-gas treatment operations of quenching, wet scrubbing, and high-efficiency mist elimination and, therefore, allowed direct assessment of effluent partitioning behavior. The aqueous quench-scrubber was an ejector venturi scrubber (EVS), previously shown to be functionally equivalent to the WTP submerged-bed scrubber technology (Goles 1992). The exhaust of the RSM EVS was treated by a high-efficiency mist eliminator (HEME) that not only demisted the influent stream but efficiently removed sub-micron aerosol matter penetrating the EVS. Table 4.1 provides RSM dimensions and other operational features.

Table 4.1. RSM Dimensions and Operational Features

Parameter	Value
Melter cavity diameter	15 cm
Melter cavity height	17 cm
Melter internal volume	4.5 L
Nominal glass depth	7.6 cm
Maximum operating temperature	1200°C
Nominal operating temperature for borosilicate glass	1150°C
Electrode dimensions	7.6×7.6 cm
Electrode material	Inconel 693
Electrode distance from bottom	0 cm
Electrode current (average)	120 A
Electrode voltage (average)	10-35 V
Electrode current density (average/maximum)	1.6/3.5 A/cm^2

RSM Melter: The body of the RSM was an Inconel-625 closed-ended cylinder lined with Alfrax refractory that contained a Monofrax K3 refractory melt cavity. An Inconel pour spout tube discharged molten glass into a stainless steel canister. An electric kiln surrounded the melter body and minimized heat loss from the melter body during operation. The discharge section was heated to facilitate pouring of the glass. The stainless steel canister sat inside a smaller kiln maintained between 700 and 900°C to promote uniform canister filling. Two top-entering Inconel 693 electrodes submerged in the glass supplied joule-heating power to the RSM.

RSM Feed System: Melter feed was delivered from a feed tank to the RSM feed nozzle by a peristaltic pump. An agitator in the feed tank kept the slurry well mixed. The feed tank sat on a scale monitored by the computer data acquisition and control system. The feed rate to the melter was controlled by a variable speed pump.

EVS: The EVS sprayed solution through a nozzle for direct contact with the melter exhaust. The EVS condensed water from the melter exhaust and removed particulates and some acid gases. The resulting two-phase stream traveled through a separator chamber and the scrubber solution was returned to the scrub tank. The scrubber solution was recirculated from a tank with a pump located adjacent to the RSM platform and through a heat exchanger to remove the heat transferred from the melter exhaust. From the scrubber, the exhaust passed through a HEME to remove condensed-phase aerosols. Collection of the quench scrubber samples was performed periodically during the test.

5.0   Test Conditions

To satisfy the technical objectives of this process flowsheet, approximately 10 days of continuous, 24 h/day melter operation was targeted. The process condition targets used during testing are described below and in Table 5.1.

Table 5.1. Target RSM Operating Conditions

Parameter	Target
Melt surface area	182 cm^2
Melt volume	1.4 L
Glass inventory	4.2 kg
Minimum expected glass rate	0.30 kg/h
Maximum expected glass rate	0.61 kg/h
Minimum expected feed rate	0.55 liters/h
Maximum expected feed rate	1.11 L/h
Glass melt temperature	1030°C
Plenum temperature range	300 to 600°C
Plenum pressure	-0.5 to -1.5 in. water
Post film cooler temperature range	200 to 350°C
Air in-leakage rate	1-3 scfm
Initial scrub solution volume	80 L
Initial scrub solution	6 to 8 pH

5.1   Process Conditions

The major process conditions that were controlled were glass pool temperature, melter vacuum, melt pool bubbling rate, feed composition, processing rate, plenum temperature, off-gas temperature, and quench-scrubber condensate temperature. Strategies for maintaining baseline conditions are discussed below.

Glass Pool Temperature: The 1030°C target temperature was automatically controlled by the RSM control system. The limiting electrode current density of $\leq$3.5A/cm^2 (~200A) was a constraint considered in maintaining the glass temperature. Kiln temperature set points could be adjusted to mitigate potential glass temperature control problems. However, both parameters directly influenced plenum and off-gas temperatures and had to be subsequently adjusted to meet baseline expectations.

Melter Vacuum: The RSM melter pressure was automatically controlled at a set point, nominally between 0.5 and 2 in. water gage below ambient conditions. The RSM blower provided up to 28 in. water gage vacuum (at 200 cfm), most of which occurred across the control valve under standard operating conditions.

Melt Pool Bubbling Rate: Glass pool agitation using subsurface air injection was employed to enhance melter feed processing rates. To accomplish this, a flow meter delivered air at 1 to1.5 L/min through one submerged Inconel-625 tube. Optimizing processing rate was not a primary test objective; bubbling rate was a secondary parameter that did not compromise the attainment of primary operational targets (temperatures).

Feed Composition: One feed composition was used throughout the test with the addition of sugar as a reductant for two test segments.

Processing Rate: Maximum steady-state feed processing rates for the melter were controlled by cold-cap conditions. The target cold-cap coverage was 85 to 95 percent. To achieve glass processing rates within the expectation range of 0.4 to 0.8 MT/day·m^2, feeding rates of 0.55 to 1.1 L/h were necessary.

Glass foaming was the greatest threat to achieving processing rates within the target range. Bubbler flow rate, and/or sugar additions to the melter feed were test parameters used to counteract the limiting influence extent of foaming.

Plenum Temperature: The targeted plenum temperature range was 500 ± 100°C during maximum feeding activities. Under steady-state processing conditions (90 to 95-percent cold-cap coverage), in-leakage, melter kiln temperature, and bubbling rate all were used to influence this steady-state temperature.

Off-Gas Temperature: The post-film-cooler off-gas temperature was constrained to <350°C. The film-cooler air injection rate was used to control temperature of the off-gas and prevent deposition of particulate in the off-gas line. The air injection was the main adjustment used to control temperature before the quench scrubber.

Quench-Scrubber Condensate Temperature: The expected EVS liquor temperature was ~20 to 35°C. If there was a need to increase or decrease this temperature, the cooling flow rate of the condensate heat exchanger was adjusted appropriately.

At a given set of operating conditions, some operating time was needed to allow time for the melt bath composition to approach a new equilibrium after step changes in the feed composition that affected the melt composition (i.e., the addition or removal of sugar). A 6 to 12 h melt cavity turnover frequency was determined to be adequate based on the RSM molten glass volume. Because up to three bath volume turnovers were needed to achieve steady state composition of the melter glass inventory, a minimum of 18 processing hours at a 0.8 MT/day·m^2 production rate was needed to reach true steady-state processing conditions; however, it was expected to take almost 40 h to reach steady conditions at low production rates.

5.2   Simulated Waste and Melter Feed

The surrogate waste processed during the RSM test was representative of waste from the AZ102 tank. The equivalent oxide feed formulation to be processed was composed of ~26 wt% waste oxides and ~74 wt% glass former oxides. Table 5.2 summarizes the AZ-102-tank equivalent waste oxide composition. Table 5.2 also shows the relative proportions of the glass formers used and the resultant

target glass composition to be prepared during melter testing. The raw materials used for the feed preparation are shown in Table 5.3 and Table 5.4. The composition of the feed mixture was based on measured feed properties. Sampling of the melter feed stream during the test provided for post-test analytical validation of batch compositions.

Table 5.2. MS26AZ102F-2 Glass Composition

MS26AZ102F-2				
Oxide (wt%)	Hanford LAW (AZ-102)	26 wt% Hanford LAW (AZ-102)	74 wt% additives	Target Composition
Al2O3	0.27	0.07	13.14	13.21
B2O3	0.10	0.03	0.00	0.03
Cl	0.14	0.04	0.00	0.04
Cr2O3	0.81	0.21	2.49	2.70
Cs2O	0.50	0.13	0.00	0.13
F	0.60	0.16	0.00	0.16
K2O	3.01	0.78	0.00	0.78
Na2O	77.04	20.03	0.00	20.03
P2O5	0.22	0.06	38.00	38.06
Re2O7	0.10	0.03	0.00	0.03
SiO2	0.43	0.11	5.47	5.58
SO3	16.79	4.37	0.00	4.37
Total	100.01	26.00		
Bi2O3			1.77	1.77
CaO			1.06	1.06
Fe2O3			7.10	7.10
La2O3			0.71	0.71
ZnO			3.55	3.55
ZrO2			0.71	0.71
Total			74.00	100.00

Table 5.3. Simulant Recipe

LAW AZ-102 Simulant Recipe at 7 Molar Sodium (Hansen, 2010).

Target volume of simulant: 2 L

Expected simulant density: 1.320 g/ml

Envelope Constituents	Mole wt	1.3 M Na Simulant target		7 M Na Simulant target		7 M Na Simulant calculated from ingredients		Glass Oxide	Mole wt	TRR-PLT-073 Target Glass Oxide		Glass Oxide calculated from ingredients		Source in Simulant	Order for Addition	Formula Weight	Assay*	Target Weight (g)
-	-	mg/L	M	mg/L	M	mg/L	M	-		mg/L	wt%	mg/L	wt%	DI water	1	18	1	800.000
Al	26.98	75.8	0.003	408	0.016	408	0.015	Al₂O₃	101.96	143	0.27	772	0.27%	Al(NO3)3*9H2O	8	375.14	0.980	11.586
B	10.81	15.6	0.001	84	0.005	84	0.008	B₂O₃	69.62	50	0.10	272	0.10%	H3BO3	5	61.83	1.005	0.961
Cr	52	288.8	0.006	1,555	0.032	1,556	0.030	Cr₂O₃	151.99	422	0.81	2,274	0.81%	Na2CrO4*4H2O	3	234.04	0.990	14.146
Cs Spike $	132.91	247	0.002	1,330	0.011	1,331	0.010	Cs₂O	281.81	262	0.50	1,411	0.50%	CsNO3	4	194.91	0.995	3.922
K	39.1	1306.2	0.033	7,033	0.178	7,037	0.180	K₂O	94.2	1,573	3.01	8,477	3.01%	KOH	7	56.10	0.887	22.766
Na	22.99	29887	1.300	160,930	7.000	161,006	7.003	Na₂O	61.98	40,287	76.96	217,032	76.96%	NaOH, 50% sol. d=1.53	6	40.00	0.502	61.148
Si	28.09	105.4	0.004	568	0.022	568	0.020	SiO₂	60.08	225	0.43	1,215	0.43%	SiO2	16	60.09	0.995	2.442
Cl	35.45	73.6	0.002	396	0.011	396	0.011	Cl	35.45	74	0.14	396	0.14%	NaCl	10	58.45	1.000	1.307
F	19	311.4	0.016	1,677	0.086	1,677	0.088	F	19	311	0.59	1,677	0.59%	NaF	11	42.00	0.998	7.430
I spike	126.9	---	---	282	0.00222	282	0.002	I	126.9	52	0.10	282	0.10%	NaI	17	149.89	1.000	0.665
PO4	94.97	152.4	0.002	821	0.011	821	0.009	P₂O₅	141.94	114	0.22	614	0.22%	Na3PO4*12H2O	9	380.12	1.000	6.572
SO4	96.06	10535	0.110	56,727	0.592	56,744	0.591	SO₃	80.06	8,780	16.77	47,293	16.77%	Na2SO4	12	142.06	0.992	169.188
Re Spike $	186.21	40.3	0.0002	217	0.0011	217	0.0012	Re₂O₇	484.41	52	0.10	282	0.10%	NaReO4	17	273.19	1.000	0.637
NO2	46.01	14572	0.317	78,465	1.707	78,503	1.706	-		-	-			NaNO2	13	69.00	0.997	236.165
NO3	62	4820	0.078	25,954	0.420	25,965	0.419	-		-	-			NaNO3	14	84.99	0.999	71.257
CO3	60.01	16471	0.274	88,690	1.475	88,739	1.479	-		-	-			Na2CO3	15	105.99	1.000	313.461
Org. Carbon	12.01	374.8	0.031	2,018	0.167	-	-	-		-	-			-	-	-	-	-
Oxalate	88.02	1383	0.016	7,447	0.086	7,451	0.085	-		-	-			Sodium Oxalate (Na2C2O4	2	134.00	0.990	22.916
-		-	-					-		-	-			remaining DI water	last	18	1	893.714
-		-	-					SUM		52,347	100.00	281,995	100.00%	Total simulant wt.				2,640.283

Notes:	
1. "-" Empty data field.	Total DI water · 1,693.714
2. Assay refers to the purity of the raw material as specified by the vendor.	Calculated simulant density, g/L · 1.320
3. Cs, I, and Re are spiked at concentrations to provide 0.5 wt% Cs2O, 0.1 wt% I, and 0.1 wt% Re2O7 in simulant oxide composition.	Measured simulant density, g/L (NOAH 15 November 2010 · 1.32
4. The order of addition was adjusted so CsNO3 is added right after sodium chromate, and NaRe2O4 is added last	[CCIM OGSE sample RFA 28jan09.xls]srnl rfa

Table 5.4. Glass Forming Chemicals

GFCs	Ingredient	mole wt	g/L simula	total kg	assay	Oxide basis				Elemental basis			
AZ-102 simulant Na molarity	7 M					oxide	mole wt	gm/L	wt%	element	mole wt	g/L	wt%
Chromium oxide (ACROS 19208-500)	Cr2O3	152	27.241	23.496	0.990	Cr2O3	152	26.969	3.41	Cr	52	18.452	2.33
Silica oxide	SiO2	60.09	58.348	50.326	1.000	SiO2	60.09	58.348	7.38	Si	28.09	27.276	3.45
Bismuth hydroxide	H3BiO3	260	21.394	18.453	0.990	Bi2O3	466	18.981	2.40	Bi	209	17.026	2.15
Calcium phosphate	HCaPO4	183.02	28.344	24.447	0.980	CaO	56.08	8.511	1.08	Ca	40.08	6.083	0.77
Iron oxide (Prince 5001)	Fe2O3	159.7	79.275	68.376	0.990	Fe2O3	159.7	78.482	9.93	Fe	55.85	54.893	6.95
Lanthanum oxide	La2O3	325.8	7.697	6.639	0.999	La2O3	325.8	7.689	0.97	La	138.9	6.556	0.83
Zinc oxide	ZnO	81.39	38.526	33.229	0.998	ZnO	81.39	38.449	4.87	Zn	65.39	30.890	3.91
Zirconium oxide	ZrO2	123.22	7.690	6.633	1.000	ZrO2	123.22	7.690	0.97	Zr	91.22	5.693	0.72
Aluminum hydroxide to replace AlPO4	Al(OH)3	77.98	67.722	58.412	0.995	Al2O3	101.96	138.785	17.56	Al	26.98	73.449	9.29
total aluminum metaphosphate	Al(PO3)3	263.89	503.457	434.242	0.974	P2O5	141.94	406.406	51.42	P2O5	141.94	406.406	51.42
total simulant, L	862.5 L					sum		790.309	100.00	sum		646.724	81.832

[CCIM OGSE sample RFA 28jan09.xls]srnl rfa

5.5

6.0   Run Description

The RSM test to produce iron-phosphate glass was broken into five segments to determine the effects of adding sugar to the feed and subsurface air injection through the molten glass, both of which are included in the current WTP plant design. Sugar was added as a reductant to the RSM feed reservoir during test segments where its effect was under consideration. The air bubbler was fabricated from Inconel-625 alloy tubing. The bubbler tip was submerged in the molten glass pool to promote convective mixing of the glass for some test segments. The test segments are listed below:

1. No sugar, no air bubbler
2. No sugar, air bubbler (short duration)
3. Sugar, no air bubbler
4. Sugar, air bubbler
5. No sugar, air bubbler (same as Segment 2 but for a longer duration and slightly higher bubbling rate).

The glass in all test segments was melted under similar operating conditions as discussed in Section 4.0 and shown graphically in Appendix D. A summary of the main operating parameters during each segment is given in Table 6.1.

Table 6.1. RSM Operations Summary

Seg #	Start Date (2010)	Start Time	Total Hours	Sugar (g/L)	Avg. Plenum Temp (°C)	Avg. Melt Temp (°C)	Bubbler rate (L/m)	Stable Feed Rate[a] (L/h)	Avg. Glass Production Rate (kg/h)
1	11/30	1053	34	0	594	1024	0	0.54	0.41
2	12/1	2000	14.7	0	572	1028	1	0.64	0.55
3	12/2	1043	92.4	50	534	1030	0	0.86	0.46
4	12/6	0705	54.7	50	571	1027	1-1.5	1.07	0.96
5	12/8	1348	43.7	0	549	1030	1.5	0.82	0.57

(a) Stable feed rate was calculated during relatively steady melter operating conditions with no feed-line plugging problems.

The RSM operating segments were targeted to have at least three melter turnovers of glass and a prolonged period of operation at a consistent feed rate. The operation of the melter was sufficient to satisfy the melter-related objectives and to obtain basic operational data. The maximum steady feed rate was attempted but was not optimized in all segments. Feed-line and feed-nozzle plugging problems were the primary cause of disruption during processing and the limitation to obtaining a steady equilibrium melt rate. The feed did not seem to settle in the feed tank, as evidenced by a lack of material in the bottom of the tanks when the tanks were emptied after test completion. Feed-line plugging for the RSM was an operating challenge because of the low RSM feed rates. The feed-line velocities were very slow and allowed some undissolved solids (UDS) to caused plugging problems in the feed line. Smaller line sizes could not practically be employed for slurry transfers to increase the velocities. Plugging of slurry systems can be remediated with appropriate flow velocities and therefore, plugging is not expected in a larger scale system.

The test started on November 30, 2010 (at 1053 h) and ended on December 10, 2010 (at 0930 h); 124.4 kg of glass was produced. Before the actual feed processing started, the melter was loaded with 2.27 kg of start-up glass (targeting the MS26AZ102-F-2 composition; Day et al. 2011) provided by Mo-Sci/MS&T and heated with the melter kiln heater to bake out the castable refractory installed behind the Monofrax K-3. The melter was then allowed to cool over a 4-day holiday weekend. The melter kiln heater was restarted on Monday, November 29, 2010, to melt the solidified start-up glass in the melter refractory prior to initiating joule heating of the glass. The kiln was operating at 100 percent power, and the glass temperature was 700°C before joule heating was started at 1458 hrs. The melter reached the targeted temperature of 1030°C at 1721 hrs. Shakedown testing with feed began at 1854 h and continued until 2150 h on Monday, and then restarted on Tuesday, November 30, 2010. Testing operations were initiated at 1053 h although refinements to the processing continued during testing. Erroneous melter temperature readings were observed on one thermocouple during the start of testing and it was determined that the melter electrode power was interfering with the melter temperature measurement taken by thermocouples inserted in each electrode pipe. This was not observed earlier and was corrected by isolating the thermocouples from each other, reading one temperature on a handheld device while collecting the other using the data acquisition system discussed in Section 7.0. Plots of melter power, melter feed rate, plenum temperature, glass temperature, and off-gas temperature are shown in Figure 6.1 and Figure 6.2.

Segment 1 (no sugar, bubbler off) commenced on November 30, 2010, at 1053 h with an initial feed rate of 1 L/h based on rates achieved during shakedown testing; however, excessive glass foaming quickly became an issue, requiring a significant decrease in the feed rate. The average glass temperature was 1024°C.

During Segment 1, a relatively thick layer of foam developed outside the main cold cap and formed a cold area around the perimeter of the molten glass surface (Figure 6.3). This cold area became a cold glass bridge that quickly grew to cover the entire surface. The feed was discontinued temporarily to allow the residual heat in the molten glass pool to dissolve the frozen glass bridge. The foaming/freezing cycle continued throughout Segment 1. An average feed rate for Segment 1 during stable processing was 0.54 L/h. The overall average feed rate including feed outages was 0.36 L/h with a glass production rate of 0.41 kg/h (544 kg/day·m^2). The glass processing rate was determined based on the weight of poured glass collected and the pour events were cyclic in response to melter level, plenum vacuum and cold-cap behavior, complicating accurate process rate determinations for the separate segments.

For Segment 2 (no sugar, bubbler on), an air bubbler was introduced into the melter on December 1, 2010, at 2000 h with a flow rate of approximately 1 L/min. This segment ran for about 15 h and achieved a significantly higher feed rate than the test without bubbling. The stable feed rate for Segment 2 was 0.64 L/h. The overall feed rate including feed outages was 0.60 L/h with a glass production rate of 0.55 kg/h (733 kg/day·m^2). To confirm the feed rate, this condition was repeated in Segment 5 for a longer duration.

Segment 3 (sugar, bubbler off) started on December 2, 2010, at 1043 h and required the addition of 50 g/L of sugar to the feed. Melter operation became more stable, and a higher feed rate was achieved than in Segment 1 (without sugar). The bubble diameter in the layer of foam at the periphery of the cold cap on the molten glass surface appeared to be larger, and bubbles rose and collapsed continuously (Figure 6.4). The average feed rate for a stable processing period for Segment 3 was 0.86 L/h. The overall feed rate including feed outages was 0.81 L/h with a glass production rate was 0.46 kg/h (611 kg/day·m^2).
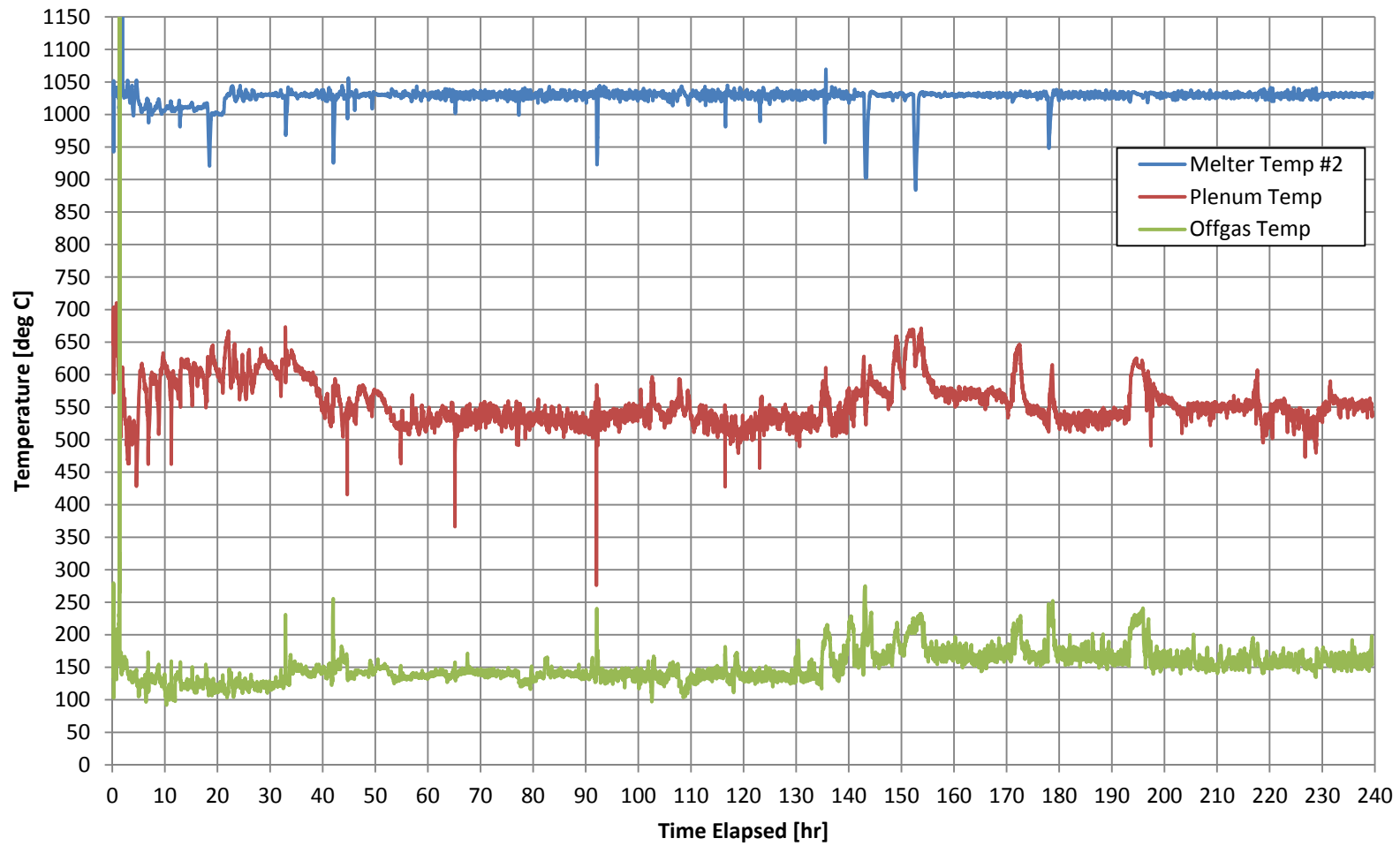
Figure 6.1. Melter Glass, Plenum, and Off-Gas Temperatures
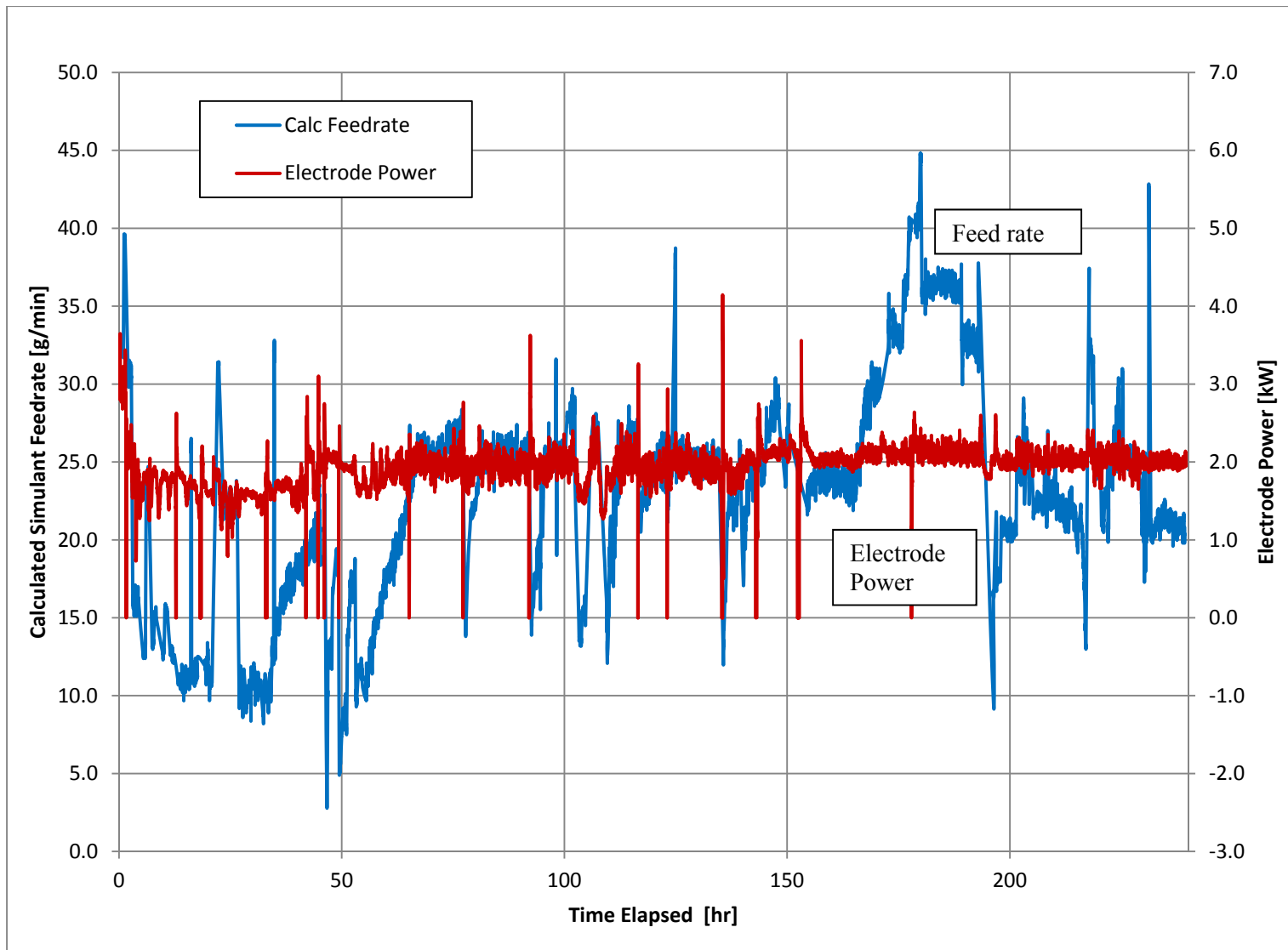
Figure 6.2. RSM Feed Rate and Electrode Power

Figure 6.3. Small Cold Cap (left). Dark perimeter is 'cold' foam. Feed nozzle is top center of photo.
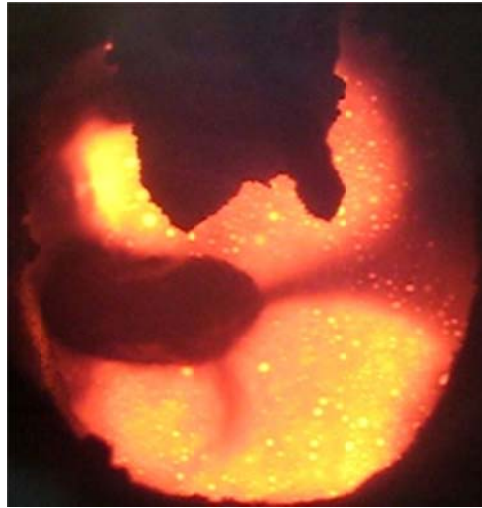
Figure 6.4. Segment 3 Molten Glass Surface

The highest feed rates were achieved in Segment 4 (sugar added, bubbler on), which started on December 6, 2010, at 0705. For this segment, the air bubbler was used, and 50 g/L sugar was added to the feed. Without a mass flow controller, it was difficult to control the bubbler rate using only a 0 to 10 L/min rotometer. At times, bubbler rates higher than the designated 1 L/min were observed during data collection (there was also no automatic data collection of the bubbler rate). Vigorous bubbling was observed in the molten glass surrounding the cold cap (Figure 6.5). So much activity existed that a few times the entire cold cap rolled and was engulfed in the molten glass. The feed rate was increased until a large, thick cold cap almost fully covered the molten glass, at which time the rate was decreased and steady state was achieved. The stable feed rate for Segment 4 was 1.07 L/h. The overall average feed rate including feed outages was 0.92 L/h with a glass production rate was 0.96 kg/h (1265 kg/day·m^2). The higher bubbler flow rates resulted in higher feed rates and glass production rates.

Figure 6.5. Large, Highly Mobile Cold Cap in Segment 3

Segment 5, the final segment (no sugar, bubbler on), was initiated on December 8, 2010, at 1348 hrs. Glass was produced under similar conditions to those in Segment 2 (no sugar, bubbler on) except for a longer duration and a slightly higher bubbling rate. The bubbling rate averaged about 1.5 L/min but the feed rate was still lower than the rate achieved in Segment 4 when bubbling and sugar were used. The glass production rate was similar to Segment 2 and may be slightly higher because there were fewer feed outages. The stable feed rate for Segment 5 was 0.82 L/h. The overall average feed rate was 0.80 L/h, and the glass production rate was 0.57 kg/h (754 kg/day·m^2).

6.1 Melter System Inspection

At the conclusion of the test, the melter and exhaust lines were inspected. The melter electrodes and bubbler tube were removed from the melt while the glass was hot. After the glass cooled, the melter lid and first section of the exhaust line were disassembled. The electrodes looked discolored, but it did not appear that a significant amount of metal had been removed. The edges of the electrodes were sharp (as shown in Figure 6.6). Electrode dimensional measurement after cleaning the electrode showed maximum losses <2.5 mm/y as described in Section 7.5. Green material on the electrodes came from contact between the electrodes and deposits on the side of the melter and exhaust plenum during removal. The cause of the green color was not identified. In addition, some glass was still attached to the electrode. Overall, the electrodes appeared to be in relatively good condition. The bubbler tube, which was made from thin-wall Inconel 625 tubing, was heavily oxidized, but still intact and retained some ductility.

Inspection of the melter lid showed that a large amount of entrained material adhered to the underside and to the exhaust piping. Some deposits on the lid appeared stratified, with a green color on the outer most deposits and the inner deposits mostly brown. The green deposits most likely formed after the cold cap melted at the end of testing and the bare glass surface with the higher temperature volatilized some material. Green deposits were not identified using x-ray diffraction (XRD) analyses and an inductively coupled plasma-mass spectroscopy (ICP-MS). The analysis was inconclusive for Ni as the sample fusion crucible was Ni based. The composition of the deposits with assumed oxide forms is provided in Table 6.2. The total in Table 6.2 does not add up to 100 percent because anions and water content are not included. The deposited material was enriched 2 to 5 times for S and depleted up to 50 percent in Zn, Na, and P, as compared to the glass composition. The ratio of the Na and P indicated the possibility of significant amounts of sodium phosphate. The deposits were probably also enriched in Cl and F like the scrubber solution from this test.

**Figure 6.6**. Melter Electrodes Pulled From the Glass Melt

Table 6.2. Plenum and Exhaust Line Deposit Composition[a]

Compound	Melter Lid (wt%)	Exhaust Pipe (wt%)	Green Powder Inside Melter (wt%)
Al_2O_3	13.91	6.42	9.43
Bi_2O_3	0.78	0.96	1.54
Cr_2O_3	1.86	1.31	2.02
Fe_2O_3	6.64	3.21	5.19
Na_2O	8.80	9.57	13.74
P_2O_5	14.05	17.97	27.73
SO_4	27.39	28.71	13.80
SiO_2	5.13	2.99	4.41
ZnO	1.41	1.53	2.38
Other cations	0.89	0.35	0.33
Total mass	51.15 g	50.06 g	4.96 g
(a) Analyzed by ICP-MS and converted to oxides. No anion analysis.			

The exhaust gas scrubber solution analysis results are presented in Section 7.4. The solution was highly enriched in sulfates, nitrates, Cl, F, and I). The anions made an acidic scrub solution with a pH <1. The most abundant cations in the scrub solution were Na and P with a ratio that indicated sodium phosphate compounds may have been released from the melter.

The overall operation of the melter was steady with the exception of the bubbler rate, which drifted upward during segments 4 and 5 to levels higher than desired for the small melter. The high bubbler flow rates probably caused most of the particulate entrainment. The bubbler flow rate for the tests varied as shown in Figure 6.7. Optimizing the bubbler flow would likely improve long-term operation.
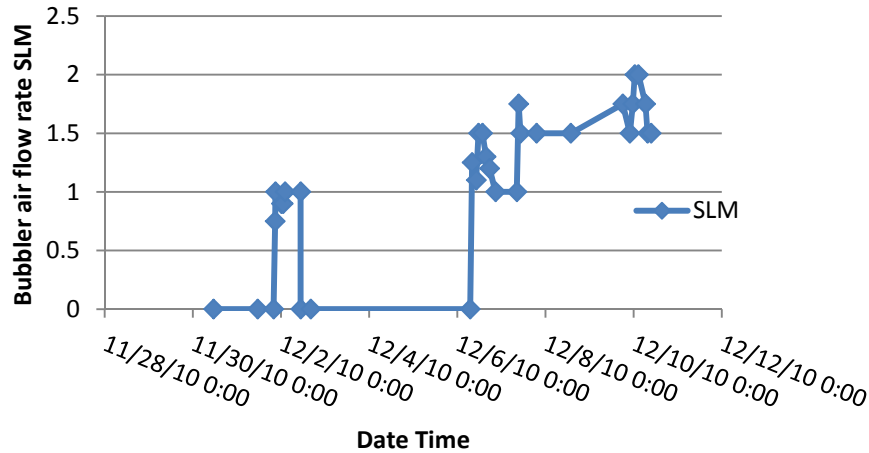
Figure 6.7. Bubbler Flow Rates Throughout the Test

The Inconel 690 pour spout down-comer was missing at the end of the test; however, it appears that a small seal weld connecting it to the rest of the pour spout probably failed. The rest of the pour spout was heavily oxidized but in relatively good condition.

A core of the glass left in the Monofrax K-3 crucible was removed from the melter at the end of the test to visually inspect for crystals or reduced metals. No crystals or reduced metals were observed in the melter.

6.2   Operational Summary

The RSM test segments were successful in providing glass samples and basic operational data for the iron-phosphate-based glass feed. Optimum steady-state processing may not have been attained in some cases, but system optimization was not a priority in this initial test. Additional testing will be required to optimize operating conditions.

The melter, plenum gas and quenched off-gas temperatures, recorded for the time interval covering all the test segments (~240 hours), are presented in Figure 6.1. The blue data represents the melt temperature as recorded by a thermocouple inserted in one of the electrodes. The red data is the temperature of the plenum gas, as recorded above the melter and before the film cooler injection air and the green data is the temperature of the quenched off-gas prior to venting to the atmosphere.

The calculated slurry feed rate and power output by the electrode, over the entire test, is presented in Figure 6.2. The power consumption is shown to trend with the slurry feed rate with a test average power load of about 2 kW.

7.0 Data Collection and Sample Collection/Analysis

Characterization activities supporting experimental test objectives included the collection of operational, monitoring, and control data as well as process stream compositional information.

7.1 Data Collection and Process Controls

The collection of process operational and control data was performed primarily by the RSM data acquisition and control (DAC) system, which monitors, controls, and electronically logs key system variables. Process data not electronically logged by this system and selected parameters of greatest interest were recorded manually on operator datasheets.

Table 7.1 identifies the process information that was electronically logged by the RSM DAC system and/or manually logged on RSM operation datasheets. The data documented important operational conditions associated with the melter, off-gas system, feed, glass, and secondary waste streams. Routine datasheets from the operating procedure were completed on an hourly basis throughout the duration of testing.

Table 7.1. RSM Process Data Electronically ("A," 1-s) or Manually ("M," 1-hr) Logged

Parameter	Units	Range	Electronic Log	Manual Log
Melt temperature (T1, control, T2, backup)	°C	1000 to 1050	X	X
Plenum temperature	°C	200 to 500	X	X
Feed pump setting	%		X	X
Cold cap coverage	%	>75	---	X
Number of vents	#		---	X
Electrode potential	V	10 to100	X	X
Electrode current	A	<200	X	X
Electrode power	kW		X	X
Melt (electrode) set-point temperature	°C		X	X
Kiln power	kW		X	X
Kiln set-point temperature	°C		X	X
Kiln actual (middle) temperature	°C		X	X
Kiln control mode	A or M		X	X
Discharge can power	kW		X	X
Discharge can set-point temperature	°C		X	X
Discharge can actual temperature	°C		X	X
Discharge can power output	%		X	X
Pour spout heater set-point temperature	°C		X	X
Pour spout heater temperature	°C		X	X
Pour spout heater power output	%		X	X
Feed nozzle cooling flow	gpm	0.5	---	X
Film cooler air flow rate (indicated)	scfm	1 to 10	---	X
Film cooler back pressure	psi	0 to 60	---	X
Melter vacuum-Magnehelic gage	in. H$_2$O	0.1 to 2.0	---	X

Table 7.1. (contd)

Parameter	Units	Range	Electronic Log	Manual Log
EVS heat exchanger cooling flow	gpm	1 to 5	---	X
EVS scrub tank volume	L	20 to 220	---	X
EVS nozzle pressure	psi	50 to 55	---	X
Off-gas temperature	°C	<250	X	X
Post-EVS off-gas temperature	°C	<50	X	X
Scrub liquid EVS inlet temperature	°C	<50	X	X
Heat exchanger temperature	°C	<50	X	X
Feed line pressure	psi		X	X
Feed tank weight	kg	decreasing	X	X
Pour spout temperature	°C	900 to 1000	X	X
Discharge can temperature	°C	700 to 850	X	X
Glass scale	kg	<10	---	X

Other items noted in the RSM logbook included visual observations of the operating behavior of the feed system, melter, and off-gas system; processing anomalies involving the cold-cap, glass conditions, off-gas behavior, corrosion, or salt formation; and all feed rate adjustments, operational problems, and optimizations activities.

At the completion of testing, the melter system was shut down according to procedure. The melter electrodes, feed-nozzle, and off-gas system were visually examined for any wear, pitting, and/or corrosion. Off-gas debris in segments of the melter/EVS off-gas jumper was measured and subsequently combined, homogenized, and analyzed. Neither the melter operation nor the glass product characteristics suggested the presence of a separate metal phase; however, the RSM melt cavity was examined in only one location for possible accumulation of reduced metals.

7.2   Process Sample Collection and Analysis

Routine sampling of the feed, glass, and secondary waste streams was conducted based on instructions in the test procedure. The melter feed distribution panel allowed for direct sampling of the melter feed stream. Glass samples were collected from the melter pour spout stream with a rectangular graphite boat. Because the newly formed glass bar could shatter and create a sharp projectile hazard, glass samples were shielded while cooling. These samples were used as the rapidly cooled "quenched" samples for the VHT tests. The EVS condensate drain samples were directly extracted from valves on the condensate recirculation line. The HEME run off was manually recycled back to the EVS recirculation tank. Analyses of the condensate samples were performed by separating the solids and the supernate to facilitate characterization of the materials.

Process samples collected for analysis included the feed slurry, glass product, off-gas line accretions, and secondary off-gas system waste streams, including EVS scrubbing liquid, UDS, and HEME run-off. In general, process samples were collected at least once per day and for every identified 'stable' operating condition (except for off-gas line deposits and the EVS UDS, which were collected only at the conclusion of testing). Sample analyses were conducted to characterize the quantities, compositions, and properties of these process streams.

Glass sample analyses included the elemental composition, and also leachability and density. Leachability was measured using the PCT and VHT tests.

Although feed, glass, off-gas waste stream, and pipe-accretion samples were collected according to the frequency indicated, only those samples considered to be most representative of selected test conditions were analyzed. Furthermore, not all analytical samples of a particular type were subjected to identical analytical schedules. For example, some glass samples analyzed for elemental composition were not analyzed for leachability or other properties. However, at least one glass and two EVS samples were analyzed for each test segment.

Sample Identification: Process stream samples were collected as detailed in the test instruction[1]. All samples were identified according to the following unique sequential labeling scheme (starting with RSM-FEP-001) and logged with the descriptive information listed below:

- date and military time

- sample description (e.g., feed, condensate, glass sample)

- initials of operations staff obtaining sample.

This information was recorded on sample log sheets and all sample containers were similarly labeled.

7.3 Sample Analysis Procedures and Equipment

Process and off-gas samples were analyzed, as applicable, for elemental composition, leachability, and density. Some analyses were contemporaneous with test operations, while most others incurred delays of several hours or days, depending on the kind of analysis performed, the sample preparation required prior to analysis, and the location of the analytical equipment. Table 7.2 briefly describes the different analyses included in this test program.

Table 7.2. Sample Analysis Methods for Process and Off-Gas Samples

Analysis	Sample Matrix	Analysis Method	Analysis Description
Cations	Solid or liquid	ICP for metals	Analysis of total amount of element, regardless of speciation
Anions	Solid	X-ray fluorescence	Cl^-, F^-, I^-
	Liquid	Ion Chromatography, Specific ion electrode	Cl^-, F^-, I^-, nitrate, nitrite, and phosphate
Leachability		PCT and VHT	
Density	Solid	---	Gas with a known mass or liquid displacement

As mentioned in the section above, many samples were taken to characterize the tests as shown in Table 7.3 and Table 7.4.

---

[1] Sevigny GJ. 2010. *Iron Phosphate Glass Containing Hanford Waste Simulant*, Test Instruction: TP-511EM31-2010, Pacific Northwest National Laboratory, Richland, Washington.

Table 7.3. List of Glass Samples Analyzed

Seg #[a]	ID	Date	Time	Analyses			
1	RSM-FEP-6	12/1/2010	0315			VHT c,q	
1	RSM-FEP-7	12/1/2010	1052	Comp			XRD q
1	RSM-FEP-10	12/1/2010	1613	Comp	PCT c		
2	RSM-FEP-12	12/2/2010	0340	Comp	PCT q		XRD q
2	RSM-FEP-15	12/2/2010	1041				XRD q
1	RSM-FEP-16[b]	12/1/2010	1412			VHT q	
3	RSM-FEP-18	12/3/2010	0137	Comp	PCT c		
3	RSM-FEP-24	12/3/2010	1730	Comp	PCT c,q		
3	RSM-FEP-30	12/4/2010	1125	Comp	PCT q		
3	RSM-FEP-31	12/4/2010	1407			VHT q	
3	RSM-FEP-34	12/4/2010	1621	Comp	PCT c		XRD c
3	RSM-FEP-37	12/4/2010	2110				XRD q
3	RSM-FEP-38	12/5/2010	0120	Comp	PCT c,q		
3	RSM-FEP-46	12/6/2010	0438				XRD q
4	RSM-FEP-48	12/6/2010	1400	Comp	PCT c		
4	RSM-FEP-54	12/7/2010	1037	Comp	PCT q	VHT c,q	XRD q
4	RSM-FEP-59	12/7/2010	2345	Comp	PCT c,q		XRD c,q
4	RSM-FEP-61	12/9/2010	1058	Comp	PCT c,q		XRD c,q
4	RSM-FEP-63	12/8/2010	1030	Comp	PCT c	VHT c	
5	RSM-FEP-65	12/8/2010	2026	Comp	PCT c,q		XRD c,q
5	RSM-FEP-68	12/9/2010	0011	Comp	PCT c,q		
5	RSM-FEP-70	12/9/2010	1058			VHT c	
5	RSM-FEP-72	12/9/2010	1723	Comp	PCT c		
5	RSM-FEP-74	12/10/2010	0545	Comp	PCT c,q		XRD c,q
5	RSM-FEP-76	12/10/2010	0930	Comp	PCT c		XRD c,q

Comp: glass composition including redox (RSM-FEP-10 redox only).
q: quenched; c: canister centerline cooling (CCC) treated, XRD: X-ray Diffraction.
(a) determined based on redox results given in Table 8.3.
(b) large amount of glass poured in a discharge canister.

Table 7.4. List of Off-Gas Samples Analyzed

ID	Date	Time
RSM-FEP-2	11/30/2010	717
RSM-FEP-17	12/2/2010	1620
RSM-FEP-28	12/4/2010	723
RSM-FEP-42	12/5/2010	1809
RSM-FEP-51	12/6/2010	2207
RSM-FEP-58	12/7/2010	2121
RSM-FEP-66	12/8/2010	2020
RSM-FEP-78	12/10/2010	1050

7.4 Analyses of Off-Gas Condensate

Scrubber solutions were analyzed at SRNL with inductively coupled plasma-atomic emission spectroscopy (ICP-AES) for Al, Bi, B, Ca, Cr, Fe, K, La, Na, Ni, P, S, Si, Zn, and Zr, and with ICP-MS for Cs, I, and Re. Prior to analyses, the solutions were filtered to remove any particles, which were analyzed separately. Table 7.5 represents a composite of the soluble and insoluble sample analyses.

7.5 Corrosion Observations

Distance measurements were taken of the sides (top, bottom, right, and left) and thickness (at locations A, B, C, and D) of the electrode (see Figure 7.1) before and after the test for comparison (see Table 7.6). The differences in electrode dimensions presented in Table 7.6 show minor changes between the before and after states. The average thickness measurements suggest a decrease in thickness for electrode A (-0.010 mm) and an average increase in thickness for electrode B (0.006 mm). Both of these values are so low that they could, potentially, be attributed to inconsistent measurement position or to oxidation layer buildup and small amounts of material loss. Measurements of the four sides of the electrodes indicate an averaged change in length contrary to the changes observed for electrode thickness results. An increase in averaged lengths was observed for electrode A (0.01 mm) and a decrease in averaged lengths for electrode B (-0.06 mm). The negative values, or material losses, of -0.01 mm and -0.06 mm equate to estimated (projected) losses of 0.33 mm/y and 2.1 mm/y, respectively.

Previous studies have demonstrated the corrosion resistance of Inconel 693 against iron-phosphate-based glasses (Zhu et al. 2005; Gan et al. 2011; Day et al. 2011). In a study by Zhu (2005), coupons of Inconel 690 and 693 were placed in iron-phosphate melts for 155 days at 1050°C. The results for the test showed that the corrosion resistance of the Inconel 693 was approximately two times higher than that of the Inconel 690, where 8 percent and 14 percent mass losses were observed, respectively.

Additionally, Gan et al. (2011) included tests conducted at 1050, 1100, and 1150°C. In contrast to the Zhu et al. (2005) study, the studies by Gan et al. showed that Inconel 690 behaved similarly to the Inconel 693 at temperatures of 1050 and 1100°C. However, Inconel 690 performed badly at 1150°C. It is worth noting that Gan et al. (2011) performed a separate study where a current, with an applied current density of 0.016 A/mm^2 (at the center pin electrode on the Inconel sample), was directed through an Inconel 693 electrode during a corrosion tests. Following this test, several phosphide and nitride secondary phases were observed at the glass-electrode interface. These secondary phases were not observed in the experiments without the applied electric current.

The corrosion results presented by Gan et al. (2011) were based on grain-boundary attack within the Inconel structure, which are observations that can only be made on polished cross sections of the electrodes. No direct comparisons can be made between the corrosion results from Gan et al. and this study because polished cross sections of the electrodes were not made in this study.

Table 7.5. Results of Condensate Analyses (wt%)

Sample ID	Al_2O_3	B_2O_3	Bi_2O_3	C_2O_4	CaO	Cl	Cr_2O_3	Cs_2O	F	Fe_2O_3	I
RSM-FEP-2	1.1E-03	<Detect	<Detect	<Detect	4.1E-03	<Detect	1.0E-04	3.1E-05	<Detect	3.9E-04	3.0E-04
RSM-FEP-17	8.4E-03	5.8E-04	7.9E-04	<Detect	4.9E-03	<Detect	9.2E-04	3.3E-04	1.2E-02	3.4E-03	5.1E-04
RSM-FEP-28	1.2E-02	5.9E-04	2.0E-03	<Detect	5.2E-03	<Detect	1.1E-03	5.0E-04	1.5E-02	3.7E-03	1.2E-03
RSM-FEP-42	1.5E-02	6.7E-04	1.0E-03	<Detect	5.3E-03	<Detect	1.3E-03	6.2E-04	1.7E-02	4.8E-03	1.9E-03
RSM-FEP-51	1.7E-02	6.6E-04	8.6E-04	<Detect	5.5E-03	<Detect	1.3E-03	7.3E-04	2.0E-02	5.0E-03	2.8E-03
RSM-FEP-58	2.0E-02	7.0E-04	9.6E-04	<Detect	5.5E-03	<Detect	1.4E-03	8.8E-04	2.4E-02	5.7E-03	2.9E-03
RSM-FEP-66	2.0E-02	7.1E-04	1.1E-03	<Detect	5.5E-03	1.1E-02	1.4E-03	9.6E-04	2.7E-02	6.3E-03	3.2E-03
RSM-FEP-78	2.2E-02	7.6E-04	1.6E-03	<Detect	5.4E-03	1.8E-02	1.6E-03	9.7E-03	3.4E-02	7.4E-03	3.5E-03

Sample ID	K_2O	La_2O_3	NO_2	NO_3	Na_2O	P_2O_5	Re_2O_7	SO_3	SiO_2	ZnO	ZrO_2
RSM-FEP-2	6.3E-04	<Detect	<Detect	1.8E-02	3.5E-03	<Detect	9.5E-05	2.4E-02	1.4E-03	7.0E-04	6.9E-05
RSM-FEP-17	1.9E-03	2.5E-04	<Detect	3.7E-01	3.3E-02	2.5E-02	1.0E-03	2.3E-01	2.5E-03	6.3E-03	2.2E-04
RSM-FEP-28	2.8E-03	5.8E-04	<Detect	3.5E-01	4.6E-02	3.2E-02	1.7E-03	7.2E-01	2.2E-03	9.4E-03	2.0E-04
RSM-FEP-42	3.2E-03	8.3E-04	<Detect	4.2E-01	5.4E-02	4.5E-02	2.2E-03	1.1E+00	2.8E-03	1.1E-02	5.0E-04
RSM-FEP-51	3.8E-03	9.2E-04	<Detect	4.2E-01	6.3E-02	4.8E-02	2.6E-03	1.0E+00	2.7E-03	1.2E-02	2.6E-04
RSM-FEP-58	4.2E-03	1.0E-03	<Detect	4.1E-01	7.0E-02	5.3E-02	3.2E-03	1.4E+00	2.7E-03	1.4E-02	2.6E-04
RSM-FEP-66	4.6E-03	1.0E-03	<Detect	4.0E-01	7.3E-02	5.6E-02	3.6E-03	1.6E+00	2.6E-03	1.5E-02	2.6E-04
RSM-FEP-78	5.0E-03	1.1E-03	<Detect	5.4E-01	7.6E-02	6.4E-02	4.1E-03	1.7E+00	4.3E-03	1.6E-02	1.2E-03
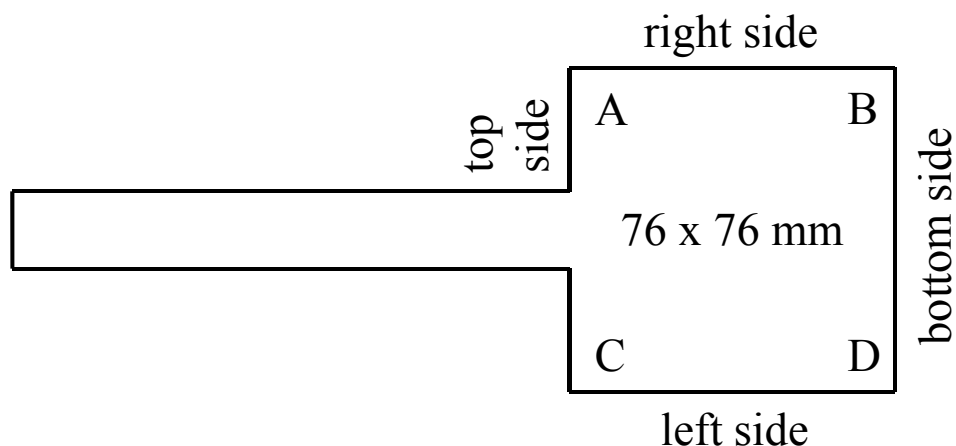
Figure 7.1. Schematic of Electrode

Table 7.6. Electrode Dimensions Before and After Testing

Electrode	A (left)			B (right)		
Location	Before (mm)	After (mm)	Diff.[a] (mm)	Before (mm)	After (mm)	Diff. (mm)
A	8.840	8.840	0.000	8.814	8.827	0.013
B	8.839	8.801	-0.038	8.839	8.814	-0.025
C	8.788	8.738	-0.051	8.788	8.814	0.025
D	8.763	8.814	0.051	8.788	8.801	0.013
Average	**8.807**	**8.800**	**-0.010**	**8.807**	**8.814**	**0.006**
Height/RS	76.17	76.11	-0.06	76.20	76.12	-0.08
Height/LS	76.12	76.15	0.03	76.25	76.14	-0.11
Width/TS	76.23	76.16	-0.06	76.10	76.10	0.00
Width/BS	76.10	76.24	0.14	76.20	76.14	-0.06
Average	**76.16**	**76.17**	**0.01**	**76.19**	**76.12**	**-0.06**

Location describes where the measurements were taken.
RS = right side; LS = left side; TS = top side; BS = bottom side.
(a) calculated as "After" – "Before." Negative values show material losses whereas
    positive values show material gain (due to oxidation or residual glass at the
    measurement location).

8.0   Glass Characterization

8.1   Heat Treatment of Glass Following Canister Centerline Cooling Profile

Selected glass samples were heat treated following the LAW canister centerline cooling (CCC) profile from Petkus (2003), but modified for iron-phosphate-based glass by starting the heating at 1000°C rather than 1115°C (see Table 8.1 and Figure 8.1). Glass samples were placed in a Pt-5%Au crucible, covered with a lid and placed in a high temperature furnace at 1000°C for 1 h. They were then cooled by a programmable furnace controller following the CCC schedule shown in Table 8.1. Some of the samples from the CCC heat treatment were characterized by XRD and durability tests (PCT and VHT).

Table 8.1. CCC Schedule for Iron-Phosphate Glasses Melted at ~1000°C

Segment	Time (min)	Start Temp (°C)	Rate (°C/min)
1	0 – 57	1000	-1.754
2	57 – 179	900	-0.615
3	179 – 339	825	-0.312
4	339 – 624	775	-0.175
5	624 – 1584	725	-0.13
6	1584 – 3694	600	-0.095
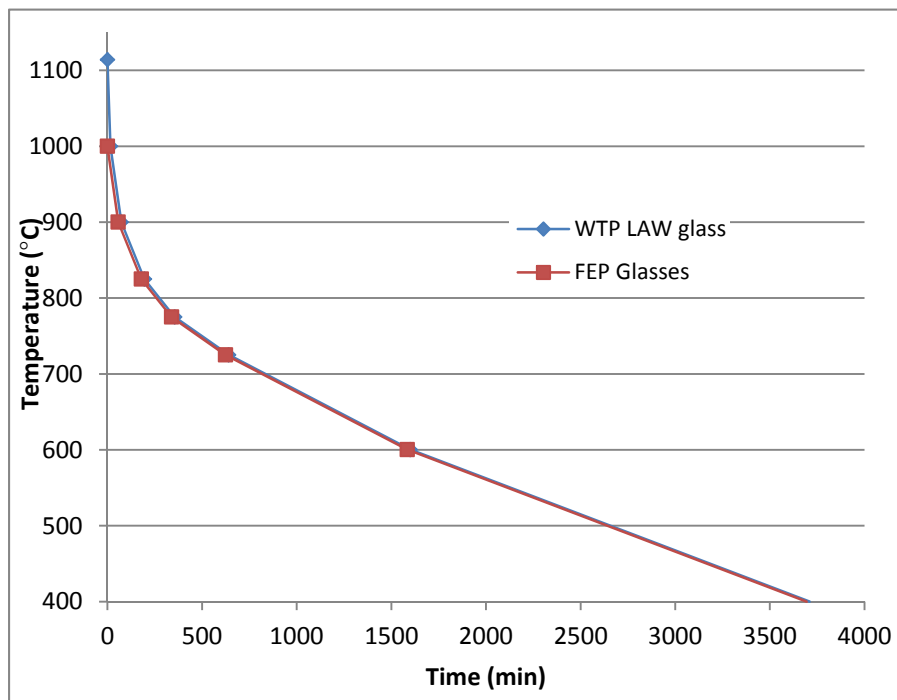
Figure 8.1. Graph of CCC Heat Treatments of Both Iron Phosphate (FEP) and LAW Glass

8.2   Analyses of Glass for Chemical Composition and Iron Redox

To confirm that the fabricated glasses correspond to a target composition, a representative sample of each glass was chemically analyzed at the SRNL. Samples were prepared by the following dissolutions: lithium metaborate, peroxide fusion, mixed acid, and inverse aqua regia. ICP-AES[1] was used to analyze the resulting dissolutions for Al, Bi, B, Ca, Cr, Fe, K, La, Na, Ni, P, S, Si, Zn, and Zr concentrations. ICP-MS[2] was used for Cs, Re, and neutron activation analysis[3,4] for iodine. A low-level waste reference, approved reference material, and standard solutions of Cs and Re were included in the analyses to assess the performance of the ICP-AES and ICP-MS. The analytical results are summarized in Table 8.2. Iodine (target 0.026 wt%) and B (target 0.026 wt%) were below detection for all samples. Fluorine (target 0.16 wt%) and Cl (target 0.036 wt%) were not analyzed. Elemental concentrations were converted to oxide concentrations by multiplying the values for each element by the gravimetric factor for the corresponding oxide.

Iron redox of the glass was also determined at SRNL using a colorimetric technique with UV-Vis spectroscopy[5] according to procedure ITS-0042.[6] Crushed glass samples were dissolved in a sulfuric-hydrofluoric acid mixture, containing ammonium metavanadate. Boric acid was added to the mixture to destroy any iron-fluoride complexes. The solution was added to a buffered ferrozine reagent and the absorbance at 562 nm was measured to determine the Fe^{2+} content. A second absorbance measurement was conducted at 562 nm after ascorbic acid had been added, which determined the total Fe content. Table 8.3 displays the results of the analyses. For the two segments with sugar addition (#3 and #4), the iron redox results were lower than for the segment with bubbling (#4), which is likely a result of oxidizing effect by air bubbles.

Table 8.2 shows that the analyzed composition matched well with the target concentrations, except for K_2O which is known for high analytical uncertainty by ICP-AES method and Re_2O_7 and SO_3 which are highly volatile. Figure 8.2 through Figure 8.4 show the analyzed concentrations of Re_2O_7, SO_3, and Cs_2O as a function of iron redox defined as $Fe^{2+}/(Fe^{2+} + Fe^{3+})$. The analyzed concentrations of Re_2O_7 and SO_3, showed clear correlation with glass redox whereas that of Cs_2O did not. The concentration of Re_2O_7 increased, but that of SO_3 decreased as the iron redox of glass increased. Figure 8.5 shows the retention (analyzed concentration divided by target) of Re_2O_7 and SO_3 as a function of iron redox. The RSM-FEP-7 glass showed outlying concentration for both Re_2O_7 and SO_3 as indicated in Figure 8.2 and Figure 8.3. The RSM-FEP-7 was one of the glass samples taken in the early stage of the RSM operation and XRD scan identified Na_2SO_4 as a potential phase (see Section 8.4) suggesting that the glass could have contained sulfate inclusions enriched with Re.

---

[1] Varian Vista AX - ICP-AES.

[2] Fisons PQ-II.

[3] Californium source.

[4] Canberra LABSOCS, Model GC13023.

[5] Thermo Spectronic Genesys 6.

[6] "Determining Fe^{2+}/Fe^{3+} and Fe^{2+}/Fe (total) Using UV-Vis Spectrometry," ITS-0042, Savannah River National Laboratory, Aiken, SC, latest revision.

Table 8.2. Analyzed Composition of RSM Glasses Compared with Target Composition (wt%)

Sample ID[a]	Al₂O₃	Bi₂O₃	CaO	Cr₂O₃	Cs₂O	Fe₂O₃	K₂O	La₂O₃	Na₂O	P₂O₅	Re₂O₇	SiO₂	SO₃	ZnO	ZrO₂
RSM-FEP-7	13.74	1.77	1.15	2.11	0.126	6.80	1.06	0.55	20.72	37.56	0.0143	5.95	3.43	3.51	0.44
RSM-FEP-12	13.85	1.84	1.14	2.88	0.126	7.14	1.07	0.59	20.59	37.67	0.0082	5.97	2.80	3.41	0.74
RSM-FEP-18	14.17	1.94	1.17	2.71	0.141	7.30	1.21	0.61	20.52	39.50	0.0155	6.16	1.08	3.58	0.78
RSM-FEP-24[b]	14.15	1.96	1.22	2.73		7.30	1.18	0.62	20.66	39.39		6.31	1.13	3.60	0.86
RSM-FEP-30	14.21	1.99	1.23	2.92	0.135	7.53	1.24	0.63	20.72	36.87	0.0182	6.12	1.16	3.57	0.76
RSM-FEP-34	13.69	1.93	1.23	2.84	0.128	7.40	1.26	0.62	20.72	37.21	0.0154	6.09	1.32	3.67	0.72
RSM-FEP-38	13.82	1.94	1.24	2.90	0.135	7.45	1.16	0.64	21.06	37.90	0.0182	6.17	0.99	3.62	0.78
RSM-FEP-48	13.55	1.99	1.17	2.85	0.123	7.50	1.10	0.64	21.06	38.82	0.0083	5.93	1.16	3.70	0.76
RSM-FEP-54B	13.52	2.00	1.19	2.81	0.137	7.50	1.12	0.65	21.33	37.79	0.0081	6.01	1.24	3.66	0.74
RSM-FEP-59	14.80	1.97	1.19	2.84	0.132	7.35	1.24	0.62	20.18	38.13	0.0110	6.17	1.47	3.67	0.63
RSM-FEP-61	14.81	2.00	1.20	2.77	0.135	7.55	1.17	0.64	18.97	38.47	0.0097	6.18	1.27	3.81	0.66
RSM-FEP-63B	14.97	2.00	1.20	2.78	0.127	7.34	1.23	0.63	20.18	39.50	0.0104	6.31	1.35	3.84	0.69
RSM-FEP-65	14.71	1.57	1.20	2.74	0.129	7.10	1.28	0.61	20.66	39.73	0.0074	6.41	2.22	3.78	0.62
RSM-FEP-68	14.38	1.93	1.19	2.66	0.133	7.15	1.18	0.64	20.79	39.04	0.0067	6.24	2.38	3.79	0.68
RSM-FEP-72B	14.31	1.89	1.21	2.63	0.132	6.53	1.29	0.61	20.66	38.70	0.0078	6.21	2.48	3.88	0.64
RSM-FEP-74	14.47	1.91	1.20	2.72	0.129	7.28	1.15	0.64	20.45	38.59	0.0075	6.26	2.41	3.86	0.67
RSM-FEP-76	14.04	1.89	1.23	2.55	0.135	7.05	1.15	0.64	19.91	39.50	0.0074	6.11	2.42	3.90	0.65
Average	14.19	1.91	1.20	2.73	0.131	7.25	1.18	0.62	20.54	38.49	0.0109	6.15	1.78	3.70	0.70
Target	13.21	1.77	1.06	2.7	0.130	7.10	0.78	0.71	20.03	38.06	0.0260	5.58	4.37	3.55	0.71

(a) "A" or "B" designation represents different part of the as-collected sample when it was split for various analyses, e.g., RSM-FEP-54A was used for VHT.

(b) There were not enough samples for measurement of Cs and Re.

Table 8.3. Iron Redox of RSM Glasses

Sample ID	Fe^{2+}	Fe^{3+}	Fe^{total}	$\dfrac{Fe^{2+}}{Fe^{3+}}$	$\dfrac{Fe^{2+}}{Fe^{total}}$	Condition
Environmental Assessment	0.07	0.28	0.35	0.23	0.19	NA
RSM-FEP-7	0.02	0.25	0.26	0.06	0.06	No sugar/No bubbling
RSM-FEP-10	0.01	0.22	0.23	0.05	0.05	
RSM-FEP-12	0.01	0.28	0.29	0.04	0.04	
RSM-FEP-18	0.14	0.18	0.32	0.78	0.44	Sugar/No bubbling
RSM-FEP-24	0.12	0.13	0.25	0.87	0.46	
RSM-FEP-30	0.14	0.15	0.29	0.92	0.48	
RSM-FEP-34	0.15	0.19	0.34	0.76	0.43	
RSM-FEP-38	0.15	0.14	0.29	1.09	0.52	
RSM-FEP-48	0.09	0.21	0.29	0.41	0.29	Sugar/Bubbling
RSM-FEP-54B	0.09	0.21	0.30	0.42	0.30	
RSM-FEP-59	0.10	0.19	0.28	0.53	0.34	
RSM-FEP-61	0.10	0.22	0.32	0.44	0.31	
RSM-FEP-63B	0.08	0.16	0.24	0.49	0.33	
RSM-FEP-65	0.01	0.30	0.31	0.04	0.04	No sugar/Bubbling
RSM-FEP-68	0.01	0.27	0.28	0.04	0.04	
RSM-FEP-72B	0.02	0.25	0.27	0.06	0.06	
RSM-FEP-74	<0.01	0.29	0.29	<0.03	<0.03[1]	
RSM-FEP-76	<0.01	0.26	0.26	0.04	0.04	

[1]0.03 was used for data plots
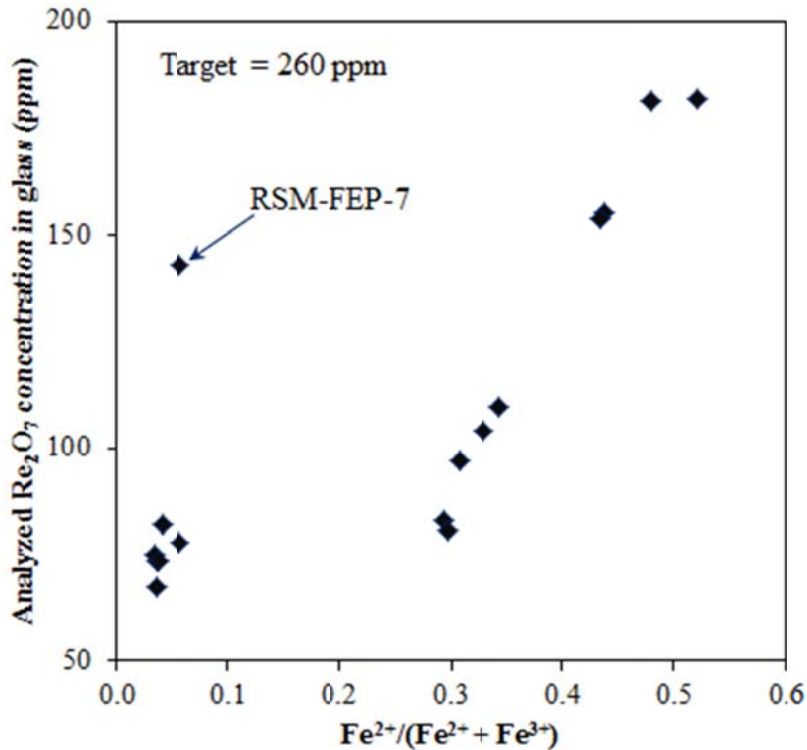
Figure 8.2. Analyzed Re_2O_7 Concentration in Glass Versus Iron Redox of Glass

8.4
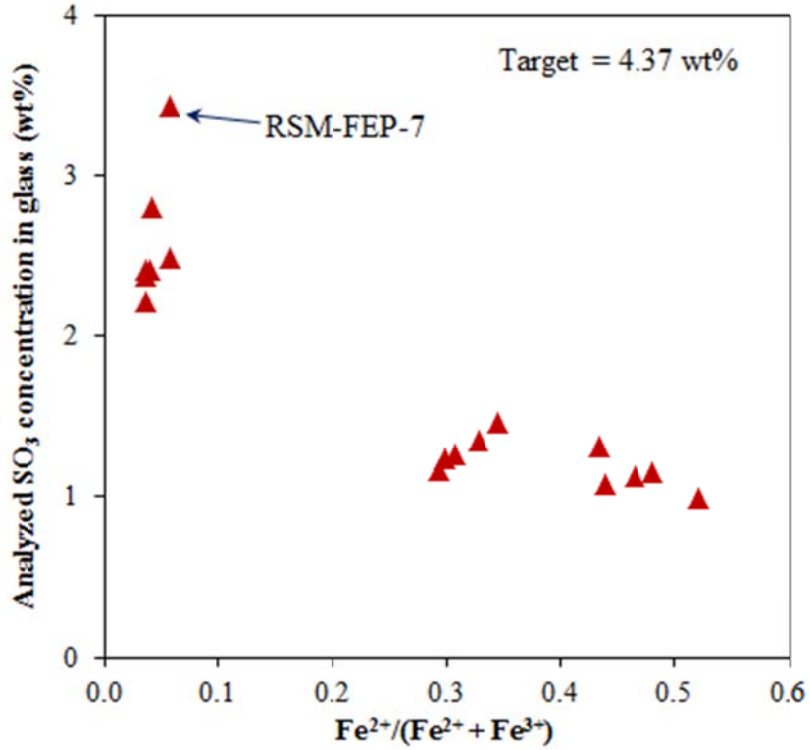
Figure 8.3. Analyzed SO_3 Concentration in Glass Versus Iron Redox of Glass
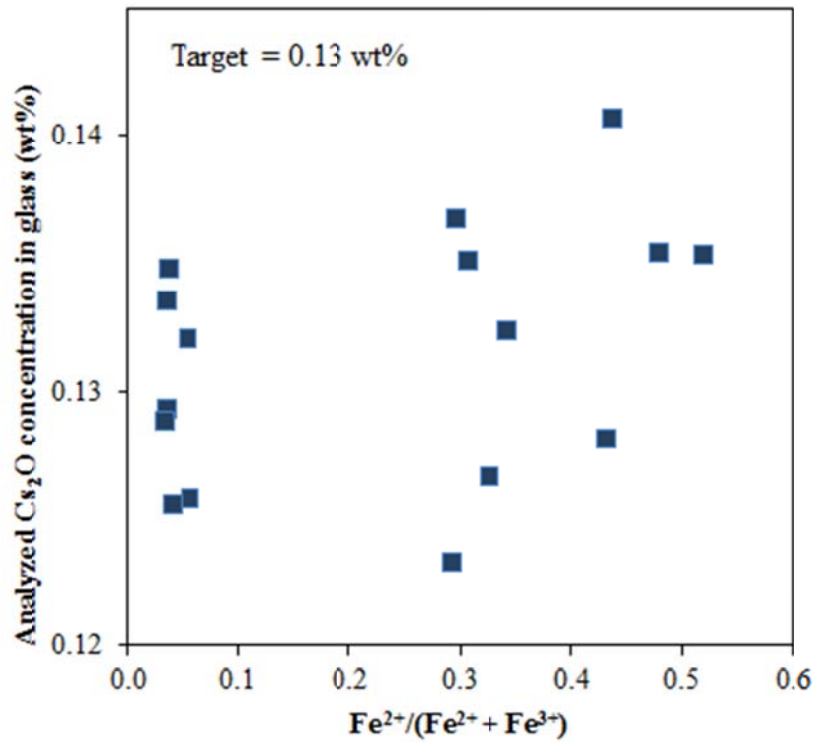
Figure 8.4. Analyzed Cs_2O Concentration in Glass Versus Iron Redox of Glass
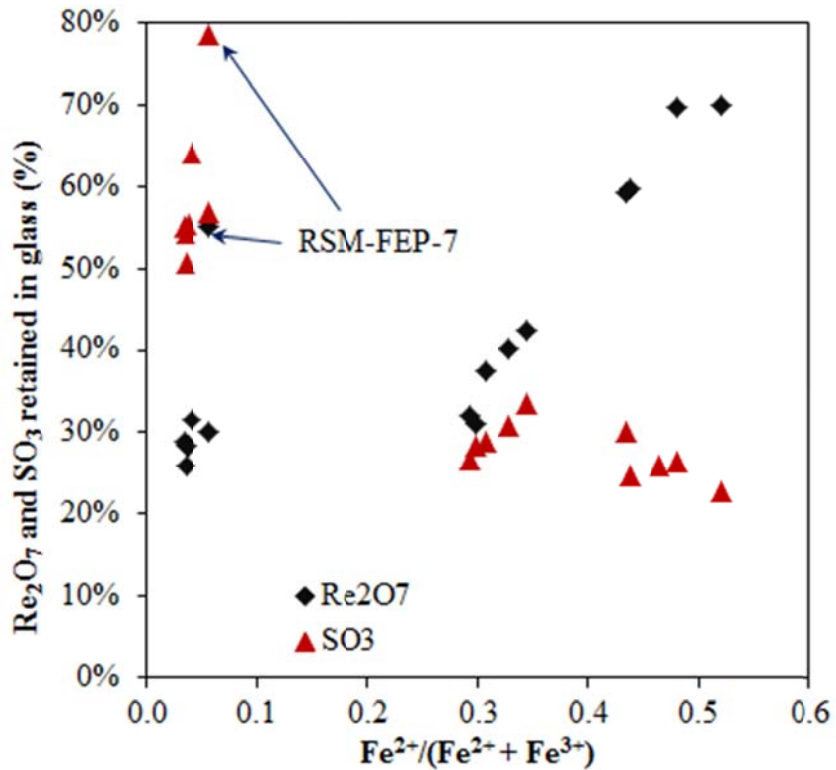
Figure 8.5. Retention of Re_2O_7 and SO_3 in Glass Versus Iron Redox of Glass

The analyzed concentrations of Cs_2O were close to or higher than the target concentration, i.e., Cs_2O retention in glass was close to 1. The decontamination factors for the melter calculated in Section 9.0 also provide support that greater than 99 percent of the Cs was retained in the glass.

The retention of Re_2O_7 and SO_3 can also be affected by the bubbling. Figure 8.6 and Figure 8.7 show the retention of Re_2O_7 and SO_3 as a function of test segment with varied conditions for sugar addition and bubbling. For segments with sugar addition (3 and 4), the bubbling decreased the Re_2O_7 retention substantially but had either zero or no significant effect on the SO_3 retention. For segments with no sugar addition the result is inconclusive because there is only one data point for no sugar/no bubbling segment.

In summary, the sugar addition increases Re_2O_7 retention in glass while it decreases SO_3 retention. This is expected based on the higher volatility of the Re_2O_7 compared to less oxidized species and the lower volatility of SO_3 as compared to more reduced SO_2. The bubbling showed a strong impact on decreasing the Re_2O_7 retention when sugar was added while bubbling had either zero or no significant effect on SO_3 retention.
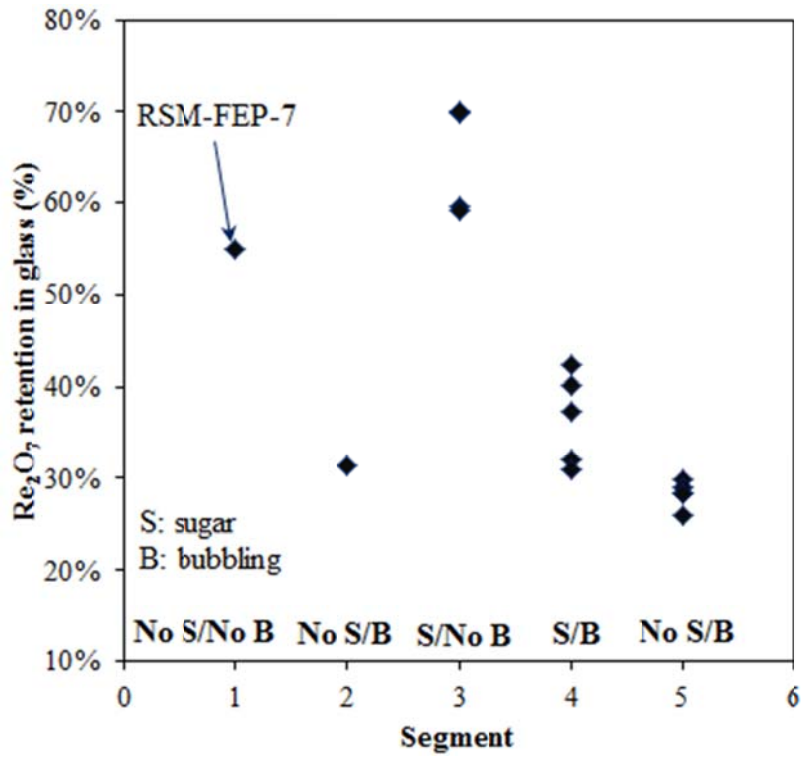
Figure 8.6. Retention of Re_2O_7 in Glass Versus Test Segment
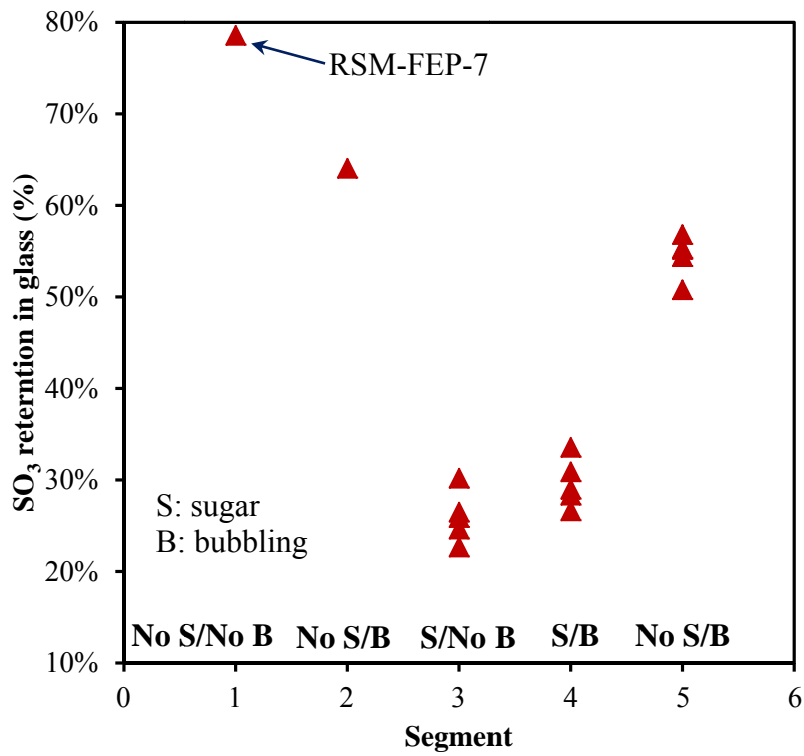
Figure 8.7. Retention of SO_3 in Glass Versus Test Segment

8.3 Glass Density

The density of each glass sample was measured at SRNL by helium pycnometry[1] and the results given in Table 8.4. The average glass density was 2.77 g/cc.

Table 8.4. Density of Selected Glass Samples

Sample	Density (g/cc)	
RSM-FEP-7	2.80	
RSM-FEP-10	2.78	
RSM-FEP-12	2.77	
RSM-FEP-18	2.81	
RSM-FEP-24	2.78	
RSM-FEP-30	2.74	
RSM-FEP-34	2.82	
RSM-FEP-38	2.79	
RSM-FEP-48	2.80	+/- 0.03
RSM-FEP-54B	2.76	
RSM-FEP-59	2.79	
RSM-FEP-61	2.80	
RSM-FEP-63B	2.75	
RSM-FEP-65	2.74	
RSM-FEP-68	2.77	
RSM-FEP-72B	2.75	
RSM-FEP-74	2.74	
RSM-FEP-76	2.75	

8.4 Crystallinity by X-Ray Diffraction

XRD data were collected at SRNL and at PNNL, both on a Bruker D8 X-Ray Diffractometer by step scanning over the range of 5-70°2Θ with a step size of 0.02° and a dwell time of 1 s at SRNL and a step size of 0.015° and a 0.3 s dwell at each step at PNNL. The XRD scans with matching crystal patterns are presented in Appendix B. Data at PNNL were analyzed with Jade 6.0 Software (from MDI, Inc.) for phase identification.

All quenched samples identified a relatively small fraction (qualitative) of eskolaite (Cr_2O_3) phase. The RSM-FEP-07Q sample had weak peaks that suggest thenardite (Na_2SO_4). Some other quenched samples included weak peaks that were not positively matched with likely phases. All CCC heat-treated samples identified eskolaite, sodium iron phosphate, sodium bismuth phosphate, and iron zirconium phosphate as likely crystalline phases but also included peaks that could not be matched with any candidate phases.

---

[1] Quantachrome Multipycnometer.

8.5 Toxicity Characteristic Leaching Procedure

A sample of quenched glass, RSM-FEP-16, was sent to Southwest Research Institute for toxicity characteristic leaching procedure (TCLP) analysis, following U.S. Environmental Protection Agency (EPA) Test Method 1311. Table 8.5 gives the results of the analysis and the EPA criterion for meeting landfill disposal requirements. The RSM-FEP-16 sample concentrations were lower than the EPA limit by nearly three orders of magnitude.

Table 8.5. TCLP Concentrations for RSM-FEP-16Q

CAS No.	Analyte	Concentration (µg/L)	EPA Regulator Levels (µg/L)
7440-38-2	Ar	10.0	5000
7440-39-3	Ba	10.0	100,000
7440-43-9	Cd	5.0	1000
7440-47-3	Cr	5.0	5000
7439-92-1	Pb	14.7	5000
7439-97-6	Hg	0.2	200
7782-49-2	Se	10.0	1000
7440-22-4	Ag	5.0	5000

8.6 Chemical Durability by Product Consistency Test

Duplicate PCTs were performed at SRNL on quenched and CCC glasses following the standard procedure (ASTM 2008). Samples were ground, washed, and prepared according to the standard procedure. The resulting solutions were sampled (i.e., filtered and acidified) and analyzed. The normalized elemental mass release, r_i, is calculated from:

$$r_i \ (\text{g/L}) = \frac{c_i}{f_i}$$

(1)

where c_i is the concentration of the ith element in the leachate (g/m^3 = ppm = µg/mL = mg/L assuming a solution density of 1 g/mL) and f_i is the mass fraction of the ith element in glass (unitless), which is calculated from target glass composition.

The PCT normalized releases are summarized in Table 8.6. All quenched and CCC treated glasses pass the PCT requirement of 4 g/L for normalized Na releases for Hanford LAW glasses (DOE 2000).[1] Figure 8.8 shows the effect of glass iron redox on the PCT normalized Na releases for both quenched and CCC treated glasses (note that the iron redox in Figure 8.8 is for quenched glasses only). Figure 8.8 shows that the PCT Na release increases as the iron redox of the glass increases, i.e., replacing Fe$_2$O$_3$ in glass by FeO decreases glass chemical durability by PCT. The CCC treated glasses that contain various crystalline phases (see Section 8.4) resulted in higher normalized Na release than quenched glasses.

---

[1] Current WTP PCT requirements are for B, Na, and Si. However, B and Si are not major components in the phosphate glasses studied in this report (unlike in the WTP baseline borosilicate glass), and therefore, the normalized Na release was used as a prime PCT criterion.

Figure 8.9 shows the PCT normalized Na releases as a function of test segment with varied conditions for sugar addition and bubbling. For segments with sugar addition (3 and 4), the bubbling decreased the normalized Na release for quenched glasses, which may simply be a result of lower glass redox caused by air bubbling. The effect of bubbling on the PCT of CCC treated glasses was not discernable with large scatter of data. For segments with no sugar addition, the bubbling did not show any noticeable effect on PCT within limited data.

Table 8.6. PCT Normalized Releases from Selected RSM Glasses

Glass ID	Normalized Release (g/L)							
	Al	B	Cr	Fe	Na	P	S	Si
RSM-FEP-10ccc	0.87	<Detect	<Detect	<Detect	1.66	0.68	1.01	1.00
RSN-FEP-12	0.47	<Detect	<Detect	<Detect	1.42	0.68	<Detect	0.57
RSM-FEP-18ccc	1.14	<Detect	<Detect	<Detect	1.98	0.93	<Detect	1.08
RSM-FEP-24	0.68	<Detect	<Detect	<Detect	1.80	0.91	<Detect	0.68
RSM-FEP-24ccc	1.39	<Detect	<Detect	<Detect	2.29	1.15	<Detect	1.09
RSM-FEP-30	0.68	<Detect	<Detect	<Detect	1.83	0.93	<Detect	0.67
RSM-FEP-34ccc	1.51	<Detect	<Detect	<Detect	2.56	1.30	<Detect	1.05
RSM-FEP-38	0.78	<Detect	<Detect	<Detect	2.04	1.04	<Detect	0.73
RSM-FEP-38ccc	1.55	<Detect	<Detect	0.01	2.64	1.33	<Detect	1.13
RSM-FEP-48ccc	1.30	<Detect	<Detect	<Detect	2.02	1.02	<Detect	1.24
RSM-FEP-54B	0.63	<Detect	<Detect	<Detect	1.67	0.86	<Detect	0.60
RSM-FEP-59	0.64	<Detect	<Detect	<Detect	1.54	0.76	<Detect	0.51
RSM-FEP-59ccc	1.44	<Detect	<Detect	<Detect	2.35	1.16	<Detect	1.19
RSM-FEP-61	0.64	<Detect	<Detect	<Detect	1.59	0.76	<Detect	0.59
RSM-FEP-61ccc	1.32	<Detect	<Detect	<Detect	2.13	1.03	<Detect	1.22
RSM-FEP-63Bccc	1.33	<Detect	<Detect	<Detect	2.26	1.10	<Detect	1.10
RSM-FEP-65	0.52	<Detect	<Detect	<Detect	1.51	0.77	<Detect	0.55
RSM-FEP-65ccc	0.85	<Detect	<Detect	<Detect	1.61	0.63	1.05	1.08
RSM-FEP-68	0.48	<Detect	<Detect	<Detect	1.39	0.71	<Detect	0.54
RSM-FEP-68ccc	0.85	<Detect	<Detect	<Detect	1.64	0.66	1.12	1.10
RSM-FEP-72Bccc	0.83	<Detect	<Detect	<Detect	1.65	0.68	1.23	1.05
RSM-FEP-74	0.49	<Detect	<Detect	<Detect	1.31	0.64	<Detect	0.46
RSM-FEP-74ccc	0.89	<Detect	<Detect	<Detect	1.62	0.65	<Detect	1.07
RSM-FEP-76ccc	0.82	<Detect	<Detect	<Detect	1.56	0.62	1.10	1.04
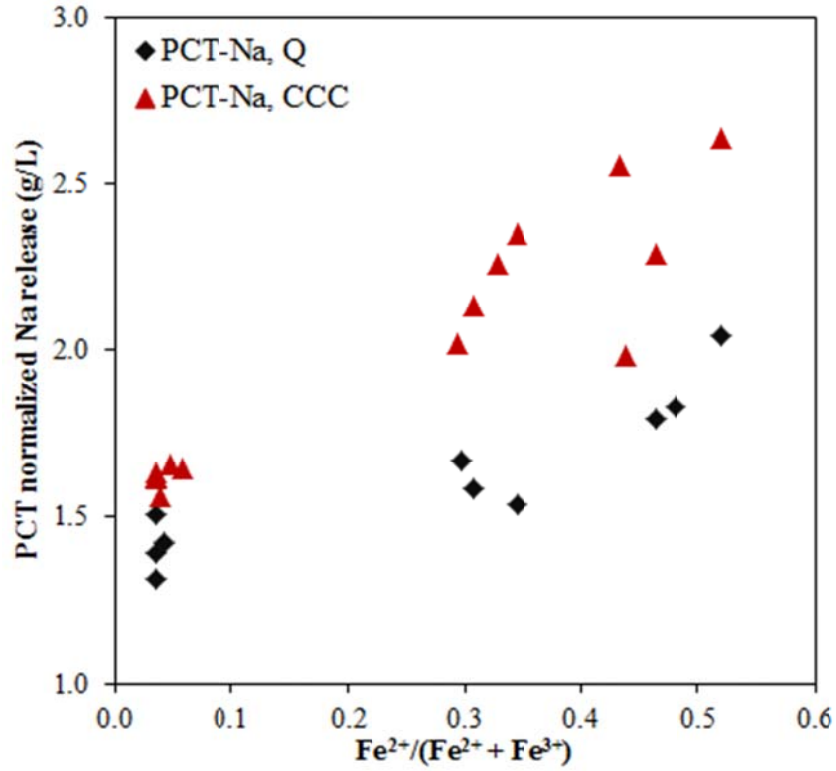
Figure 8.8. PCT Normalized Na Releases Versus Iron Redox of Glass
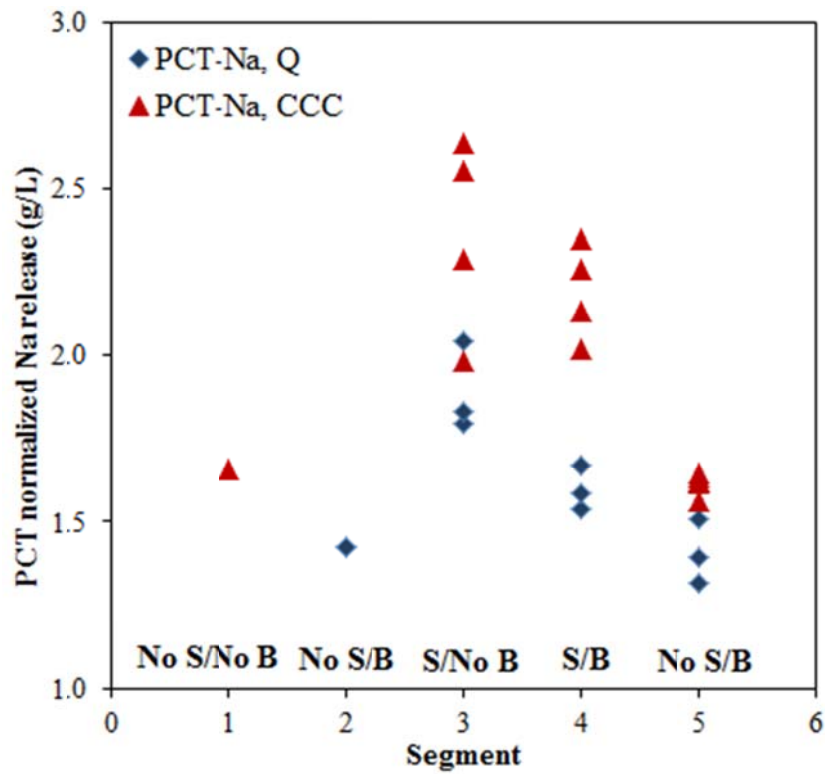
Figure 8.9. PCT Normalized Na Releases Versus Test Segment

8.7 Chemical Durability by Vapor Hydration Test

In the VHT (ASTM 2009), monolithic samples were exposed to water vapor at 200°C in sealed 22-mL, stainless-steel vessels (Type 304L). A diamond-impregnated saw was used to produce $10 \times 10 \times 1.5$ mm ($0.4 \times 0.4 \times 0.06$ in.) samples. The cut samples were polished to 600-grit surface finishes with silicon carbide paper. In the vessels, samples were suspended on a platinum wire above 0.20 g of deionized water and held at 200°C for 7 days. Following the test, the specimens were sectioned through the center of the sample for optical microscopy coupled with image analysis evaluation. Image analysis measurements of the average alteration thickness at 10 locations were used to calculate alteration rate. The VHT alteration rate, r_a (g/day·m^2), of the specimen was calculated from the equation:

$$r_a = \frac{\rho d_a}{t}$$

(2)

where d_a is the alteration layer thickness (µm), t is the duration of test (day), and ρ is the density of glass (g/cc). The average density of 2.77 g/cc (see Section 8.3) was used for all glasses. The VHT results are listed in Table 8.7. Selected samples were examined by SEM analysis. Photos of samples before and after VHT, optical micrographs showing alteration thickness measurement, and SEM micrographs are presented in Appendix A.

Table 8.7. VHT Alteration Thickness and Alteration Rate for Selected RSM Glasses

Sample Identification	Quenched or CCC	Alteration thickness d_a (µm)	Alteration rate r_a (g/day·m^2)
RSM-FEP-6	Quenched	<14[b]	<6
RSM-FEP-6(1)[a]	CCC	293	116
RSM-FEP-6(2)[a]	CCC	118	47
RSM-FEP-6(3)[a]	CCC	81	32
RSM-FEP-16	Quenched	19	8
RSM-FEP-31	Quenched	<14[b]	<6
RSM-FEP-54A	Quenched	<14[b]	<6
RSM-FEP-54A	CCC	150	60
RSM-FEP-63A	CCC	106	42
RSM-FEP-70	CCC	232	92

[a]Three separate VHT samples were taken from the same CCC treated glass block.
[b]Estimated minimum thickness required for measurement via optical microscopy.

All quenched samples passed the VHT requirement of 50 g/day·m^2 for alteration rate for Hanford LAW glasses (DOE 2000). The CCC treated samples resulted in greater alteration rate variability than the quenched samples with three of six samples failing the VHT requirement. The higher VHT alteration rates in some of the CCC samples is likely linked to higher crystallinity in the CCC treated samples, as described in Section 8.4. and this difference is the source of the large variability, as illustrated by the irregular alteration thickness as seen in the cross-section micrographs of the CCC glasses displayed in Appendix A. However, the failure of VHT requirement is surprising because the CCC treated glasses of the same composition prepared in crucible scale (21 g/day·m^2, see Day et al. 2011) and produced from

CCIM tests (37 and 23 g/day·m^2, see Soelberg and Rossberg 2011) passed the VHT requirement and the chemical analyses of the RSM glass samples did not show any noticeable deviation from target composition (see Section 8.2). It is suspected that the large scatter of VHT data for CCC samples may be related to the high crystallinity and low reproducibility of crystallization, e.g., inconsistency in the fraction and type of crystals and in the fraction and distribution of voids.

9.0 Material Balance

A material balance of selected volatile and non-volatile species was performed along with decontamination factors based on glass produced and material collected in the scrub tank. The testing envelope was made using the glass analysis presented in Table 8.2, the simulant recipe listed in Table 5.3 for the feed, and the scrubber analysis shown in Table 7.5 for the overhead losses. The average feed, glass and melter exhaust rates of some key components are shown in Figure 9.1. As expected, non-volatile components such as Al, Cr, Fe, and La remained in the glass phase. Sulfur data was converted to elemental S for the purpose of comparison. Discrepancies in the glass and off-gas totals as compared to the feed for the non-volatile species may be related to either the scrubbing efficiency or the problems caused by the feeding disruptions. The additional losses that appear for the Re may be due to inefficiencies of the off-gas scrubbing equipment, which uses highly acidic condensate for scrubbing. The data show significant losses of S from the melter, but are within the requirements for the low-level waste melter. The scrub solution data versus the feed rate and concentration data also indicate that air-bubbling likely increases the losses of S from the melter. The glass composition data indicate that the sugar may increase losses of S from the melter, probably through reduction of SO_4 to SO_3 or SO_2.

The decontamination factors for the test, defined as the weight of a component in the feed divided by the weight of the same component collected in the off-gas scrubber for a unit of time within a segment, are shown in Table 9.1.

Table 9.1. Decontamination Factors

	Values based on Feed Composition				
Segment #	2	3	4	5	average
Al	440	360	730	510	510
B	12	54	89	42	49
Bi	630	2,800	14,000	640	4,400
$Ca^{(a)}$	180	210	570	310	320
Cr	910	2,200	4,300	1,800	2,300
Cs	120	160	130	5	100
F	4	9	6	3	5
Fe	650	1,400	1,700	770	1,200
I	30	7	8	7	12
K	150	200	190	150	180
La	780	480	800	770	710
Na	70	120	110	120	110
PO_4	430	660	980	580	660
Re	8	8	6	5	7
S	6	2	3	2	3
$Si^{(a)}$	1,100	1,600	15,000	700	4,600
Zn	15	13	29	18	19
Zr	1,200	890	NA	240	780
(a) Based on glass composition instead of feed composition.					
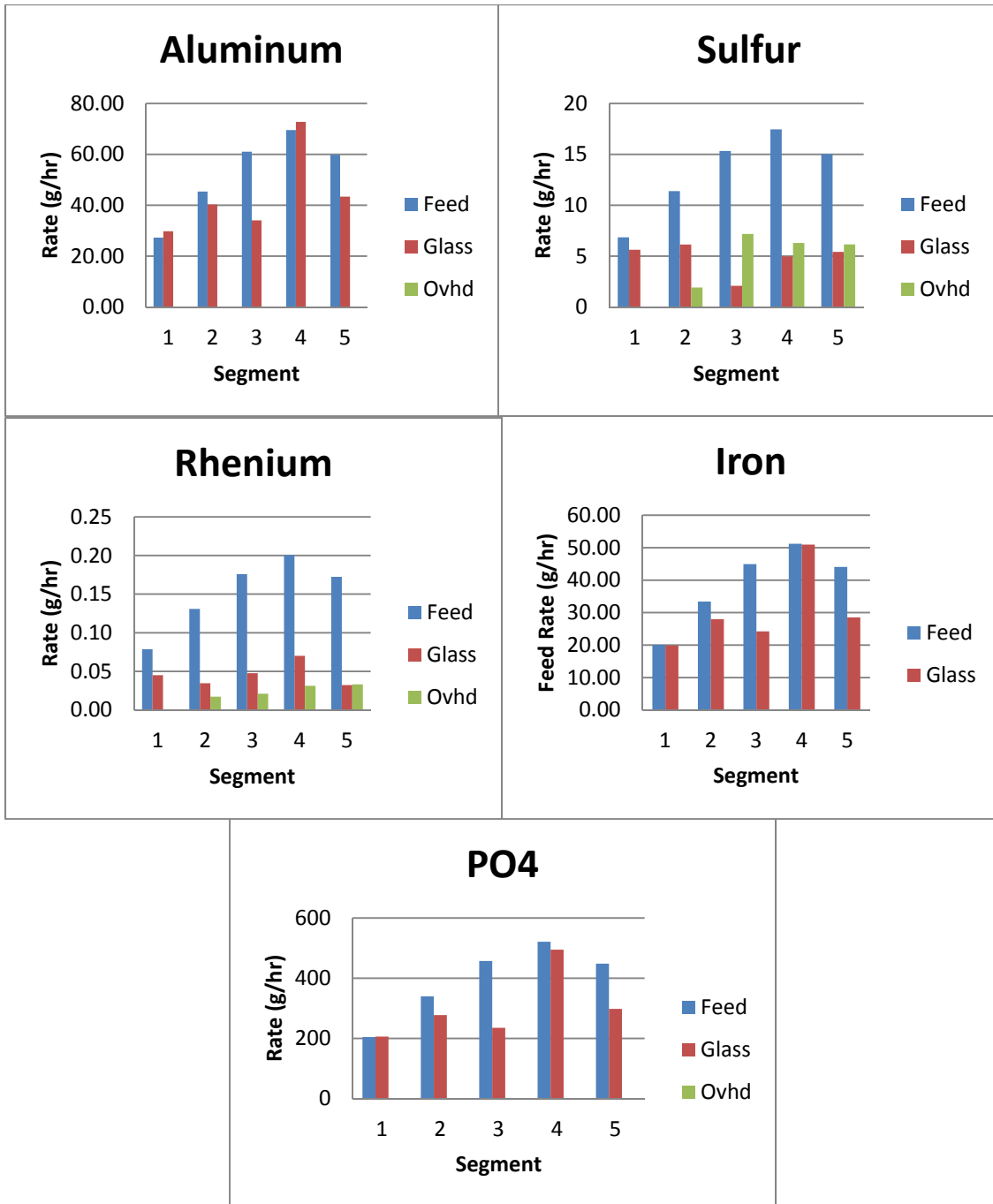
Figure 9.1. Rates of Components of Interest

10.0 Quality Assurance

All work was performed in accordance with best laboratory practices (NQA-1 Subpart 4.2-based) as indicated in work flows and subject areas of the PNNL HDI standards-based management system in effect at the time the work was conducted.

11.0 Conclusions

Overall, the processing of iron-phosphate-based glass was similar to borosilicate glass, although the melter was operated at a lower average temperature (1030°C) with higher levels of sulfur at a target SO_3 concentration of 4.37 wt%. The glass production rates when sugar and/or bubbling were used, were 0.31 to 1 kg/h (411 to 1330 kg/day·m^2), which are similar to borosilicate glasses. The addition of sugar and air bubbling increased the processing rate as expected. The retention of Re_2O_7 in glass ranged from 26 to 70 percent depending on the processing conditions. The SO_3 concentration retained in the glass melted under different processing conditions ranged from 1.0 to 2.8 wt% (23 to 64 percent retention). The addition of sugar increased Re_2O_7 retention in glass while it decreased SO_3 retention. Bubbling decreased the Re_2O_7 retention when sugar was added while it had no or insignificant effect on SO_3 retention.

The product glass met the LAW glass PCT requirement for both quenched and CCC treated glasses, with higher normalized Na releases for CCC treated glasses likely caused by crystallization. The PCT Na release increased as the iron redox of the glass increased. The CCC treated samples had greater alteration rate variability than the quenched samples, with three of the six CCC treated samples failing the VHT requirement. All the quenched glasses showed little sign of alteration. It was suspected that the failure of VHT requirement for some CCC samples may be related to the high crystallinity and low reproducibility of crystallization in those samples. The corrosion of melter components was acceptable with minimal corrosion of Inconel 693 electrodes and Inconel-690 pour spout. Losses to the melter exhaust were typical of other waste glasses. As expected, the crude bubbler system resulted in increased particulate losses to the exhaust system, and the condensate was very acidic.

12.0 References

ASTM—American Society of Testing and Materials. 2008. *Standard Test Methods for Determining Chemical Durability of Nuclear, Hazardous, and Mixed Waste Glasses and Multiphase Glass Ceramics: The Product Consistency Test (PCT)*. ASTM C 1285-02(2008), American Society of Testing and Materials.

ASTM—American Society of Testing and Materials. 2009. *Standard Test Methods for Measuring Waste Glass or Glass Ceramic Durability by Vapor Hydration Test)*. ASTM C 1663-09, American Society of Testing and Materials.

Day DE, RK Brow, CS Ray, and C-W Kim. 2011. *Formulation of Iron Phosphate Glasses with Simulated Hanford LAW for Joule Heated and Cold Crucible Induction Melters*. Missouri University of Science and Technology / Mo-Sci Corporation, Rolla, Missouri.

DOE. 2000. Contract DE-AC27-01RV14136, Section C, as amended, U.S. Department of Energy, Richland, Washington. (http://www.hanford.gov/files.cfm/WTP%20Contract%20Section%20C%20-%20Conformed%20Thru%202301.pdf)

Gan H, AC Buechele, Z Feng, C Wang, C Viragh, IL Pegg, and I Joseph. 2011. *Testing of Iron Phosphate LAW Glass*. VSL-11R2340-1, Vitreous State Laboratory, Washington D.C.

Goles RW and AJ Schmidt. 1992. *Evaluation of Liquid-Fed Ceramic Melter Off-Gas System Technologies for the Hanford Waste Vitrification Plant*. PNL-8109, Pacific Northwest Laboratory, Richland, Washington.

Kim CW, D Zhu, DE Day, DS Kim, JD Vienna, DK Peeler, TE Day, and T Neidt. 2004. *Iron phosphate glass for immobilization of Hanford LAW, Ceramic Transactions* 155 (2004) 309-318.

Kim D, WC Buchmiller, MJ Schweiger, JD Vienna, DE Day, CW Kim, D Zhu, TE Day, T Neidt, DK Peeler, TB Edwards, IA Reamer, and RJ Workman. 2003. *Iron Phosphate Glass as an Alternative Waste-Form for Hanford LAW*. PNNL-14251, Pacific Northwest National Laboratory, Richland, Washington.

Perez Jr. JM, DF Bickford, DE Day, D Kim, SL Lambert, SL Marra, DK Peeler, DM Strachan, MB Triplett, JD Vienna, and RS Wittman. 2001. *High-Level Waste Melter Study Report.* PNNL-13582, Pacific Northwest National Laboratory, Richland, Washington.

Petkus LL. 2003. "Low Activity Container Centerline Cooling Data." Memorandum to C.A. Music, dtd. October 16, 2003, CCN: 074181, River Protection Project, Hanford Tank Waste Treatment and Immobilization Plant, Richland, Washington.

Soelberg N and S Rossberg. 2011. *Melting Hanford LAW into Iron-Phosphate Glass in a CCIM*, Idaho National Laboratory. INL/EXT-11-23251, Idaho National Laboratory, Idaho Falls, Idaho.

Zhu D, CW Kim, and DE Day. 2005. "Corrosion Behavior of Inconel 690 and 693 in an Iron Phosphate Melt." *J. Nucl. Mater.*, 336:47-53.

Appendix A

VHT Sample Images

Appendix A: VHT Sample Images

RSM-FEP-6Q

RSM-FEP-6Q VHT Alteration Thickness Measurement

RSM-FEP-6CCC

Photos of Three RSM-FEP-6CCC(1,2,3) VHT Samples Prior to Testing
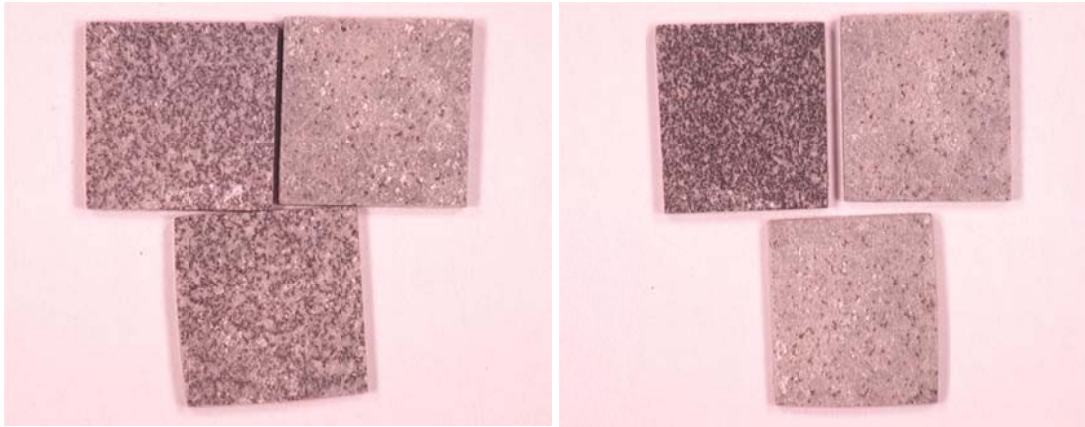
| Side one | Side two |

Photos of RSM-FEP-6CCC(1,2,3) VHT Samples Post Testing
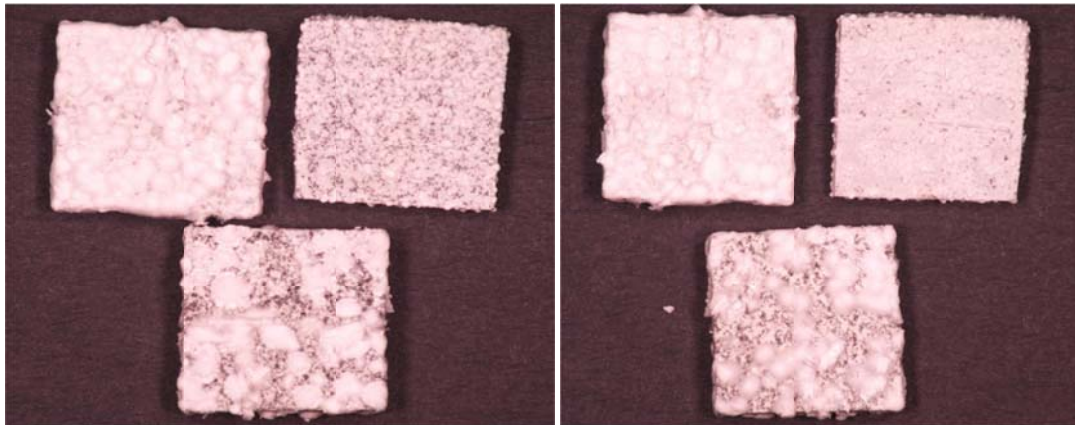
| Side one | Side two |

RSM-FEP-6CCC(1) VHT Alteration Thickness Measurement
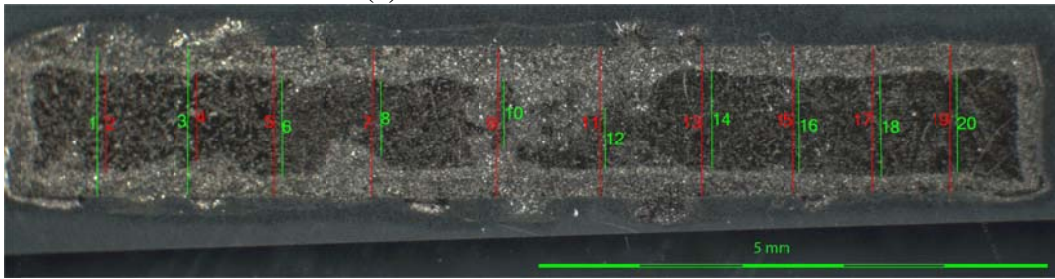
RSM-FEP-6CCC(2) VHT Alteration Thickness Measurement
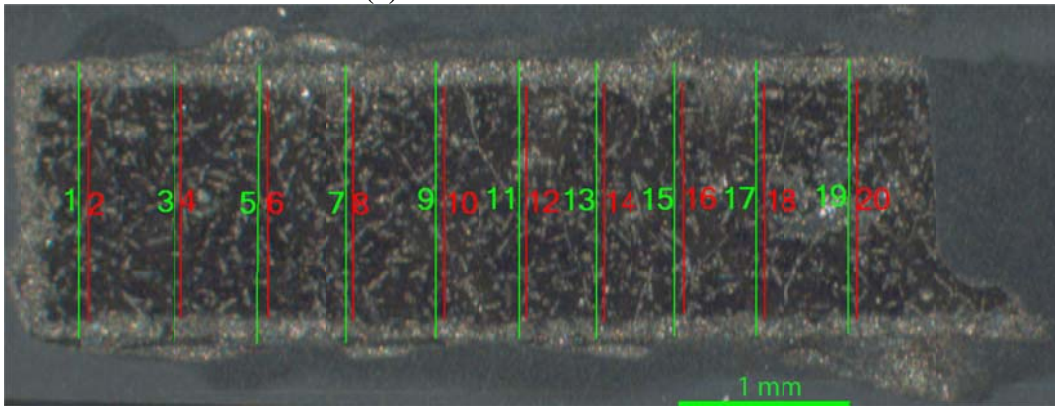
RSM-FEP-6CCC(3) VHT Alteration Thickness Measurement
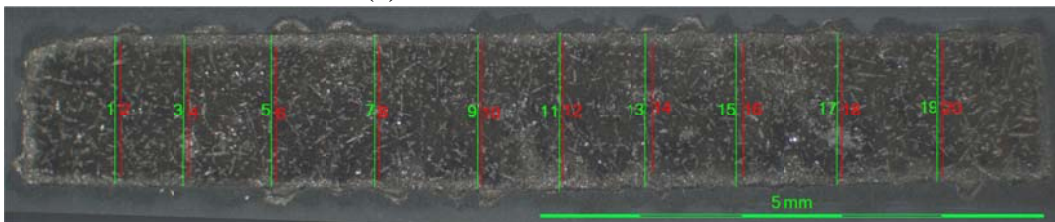
RSM-FEP-6CCC(1) SEM Images of Reacted Surface

20.0 KV EM Mag 1500X   1c - RSM FeP 6   20µm

20.0 KV EM Mag 1000X   1b-RSM FeP-6   20µm

20.0 KV EM Mag 1000X   1- RSM FeP 6   20µm
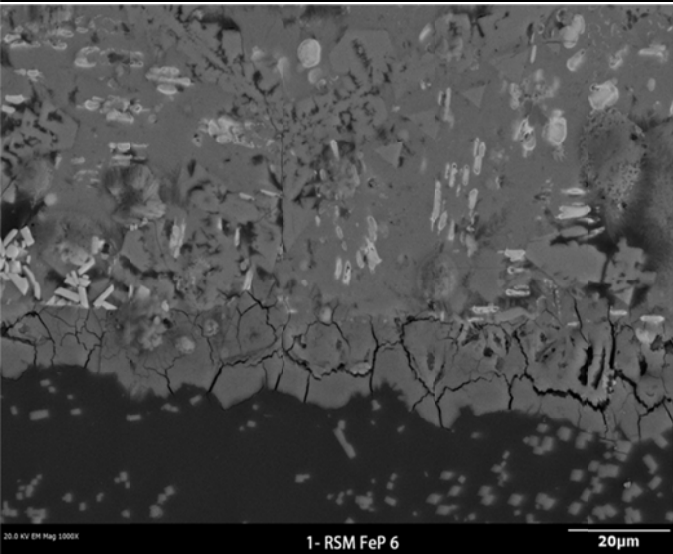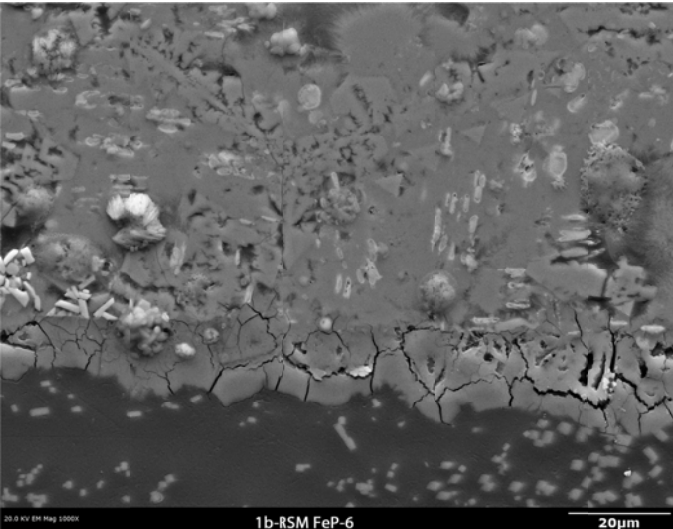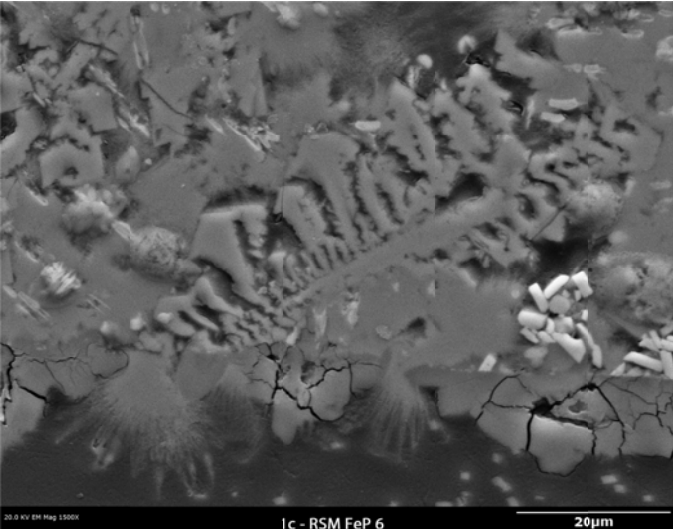
RSM-FEP-6CCC(2) SEM Images of Reacted Surfaces
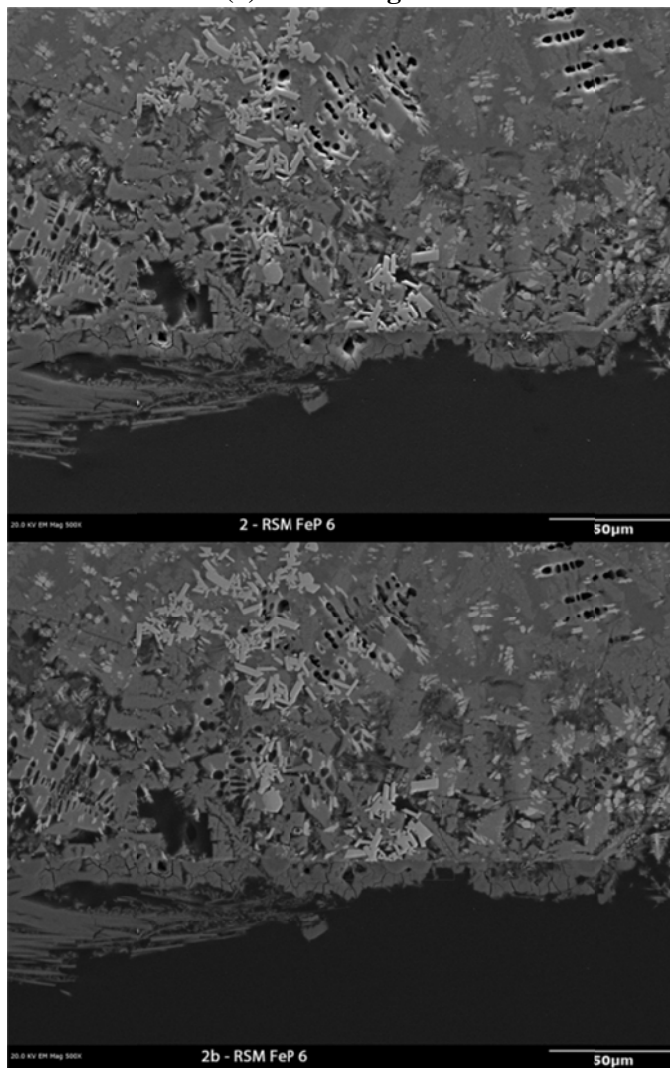
RSM-FEP-6CCC(3) SEM Images of Reacted Surfaces
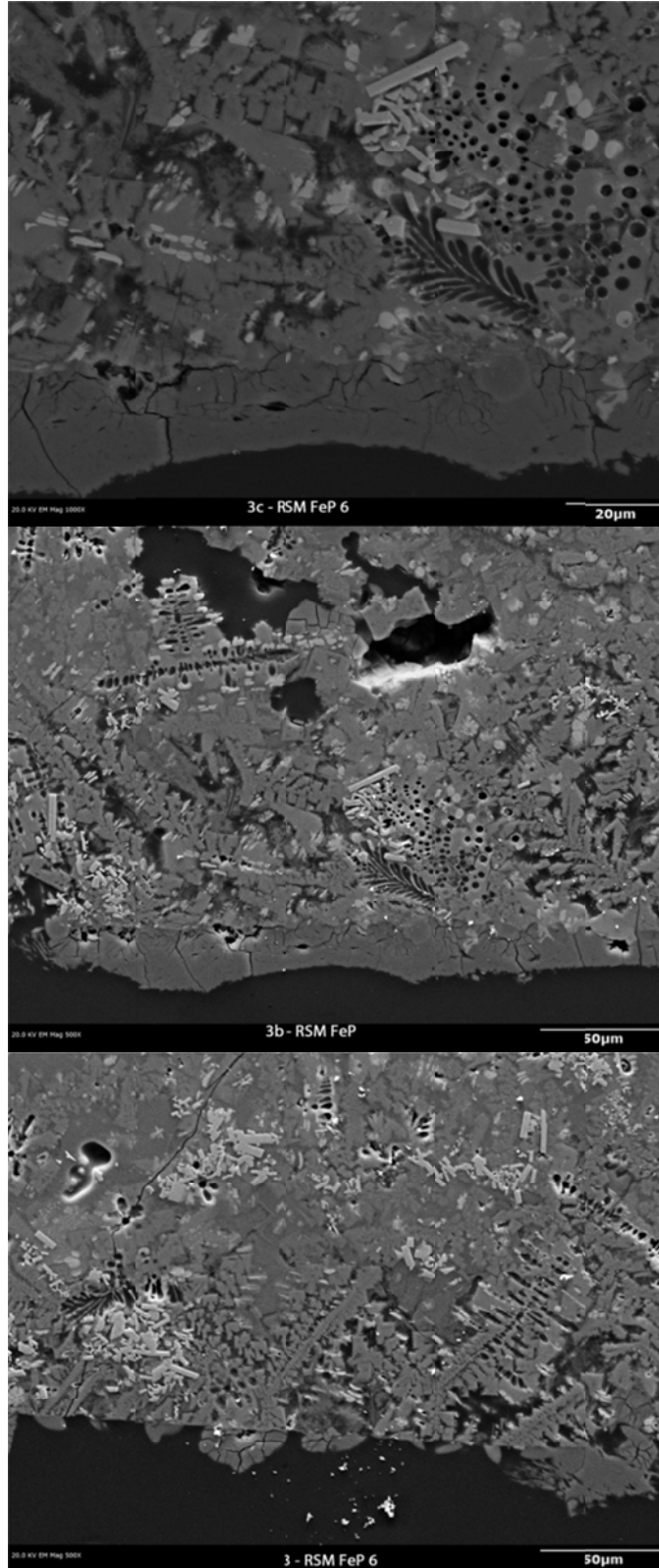
RSM-FEP-16Q

Photos of RSM-FEP-16Q VHT Samples Prior to Testing
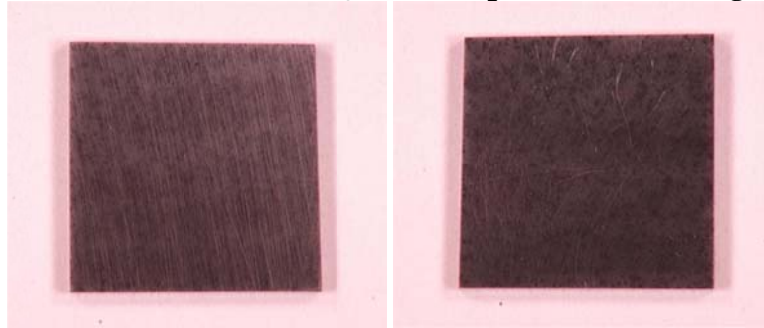
| Side one | Side two |

Photos of RSM-FEP-16Q VHT Samples Post Testing
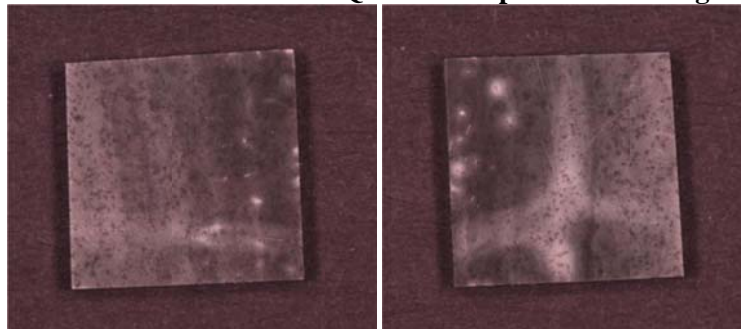
| Side one | Side two |

RSM-FEP-16Q VHT Alteration Thickness Measurement

5 mm

RSM-FEP-16Q SEM Images of Reacted Surfaces
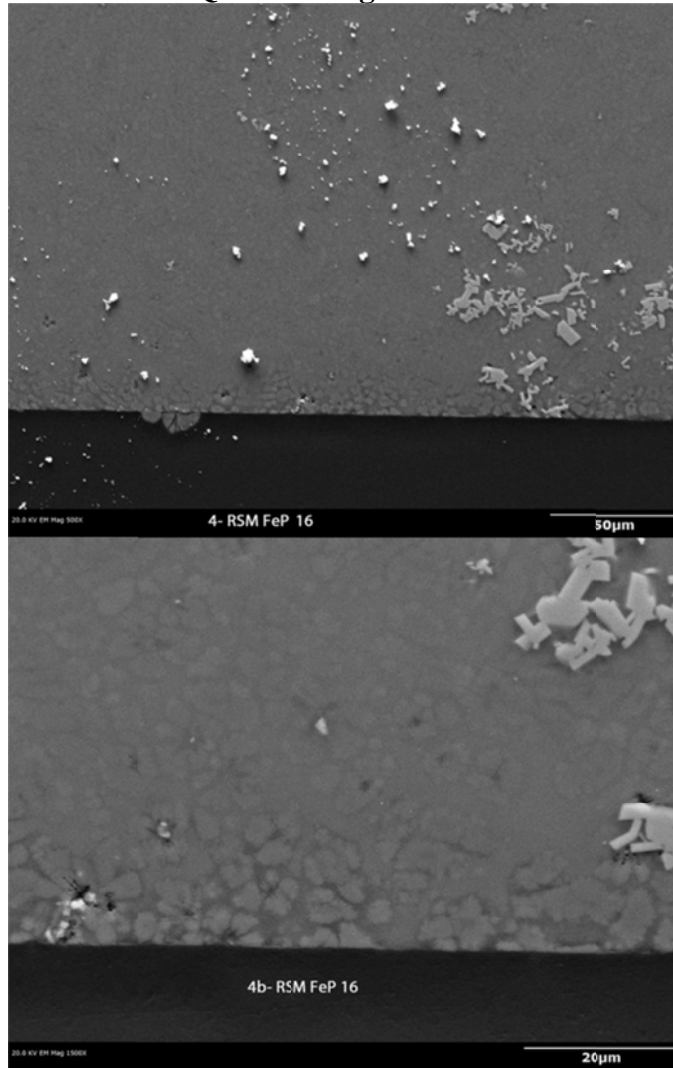
RSM-FEP-31Q

RSM-FEP-31Q VHT Alteration Thickness Measurement
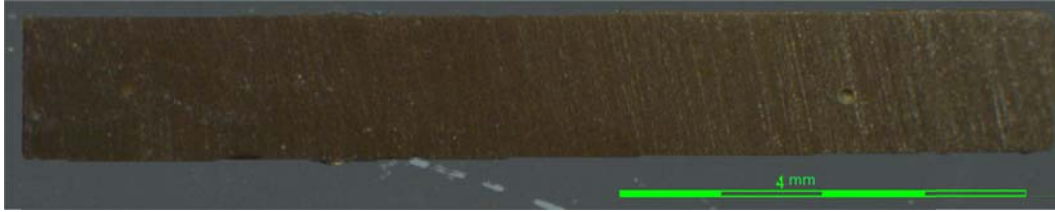
RSM-FEP-54A Q

Photos of RSM-FEP-54A Q VHT Samples Post Testing
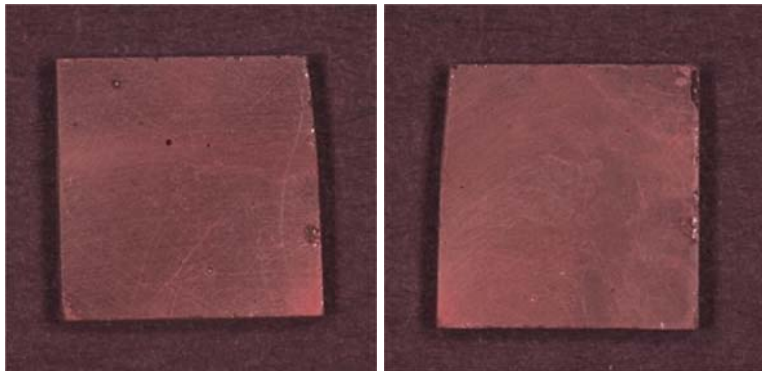
Side One	Side Two

RSM-FEP-54A Q VHT Alteration Thickness Measurement
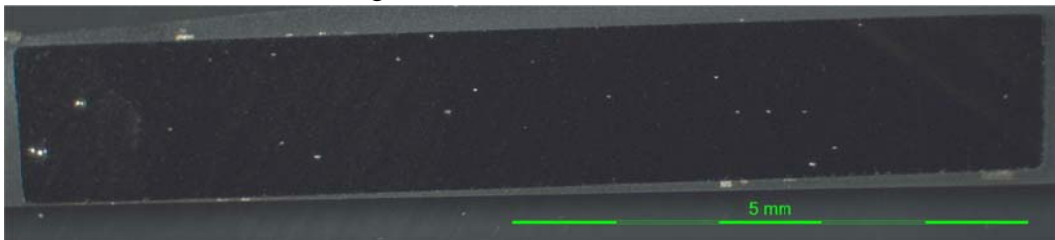
RSM-FEP-54A Q SEM Images of Reacted Surfaces

5-RSM FeP 54A   50 um

5b- RSM FeP 54A   20 um

5c - RSM FeP 54A   10μm

A.9
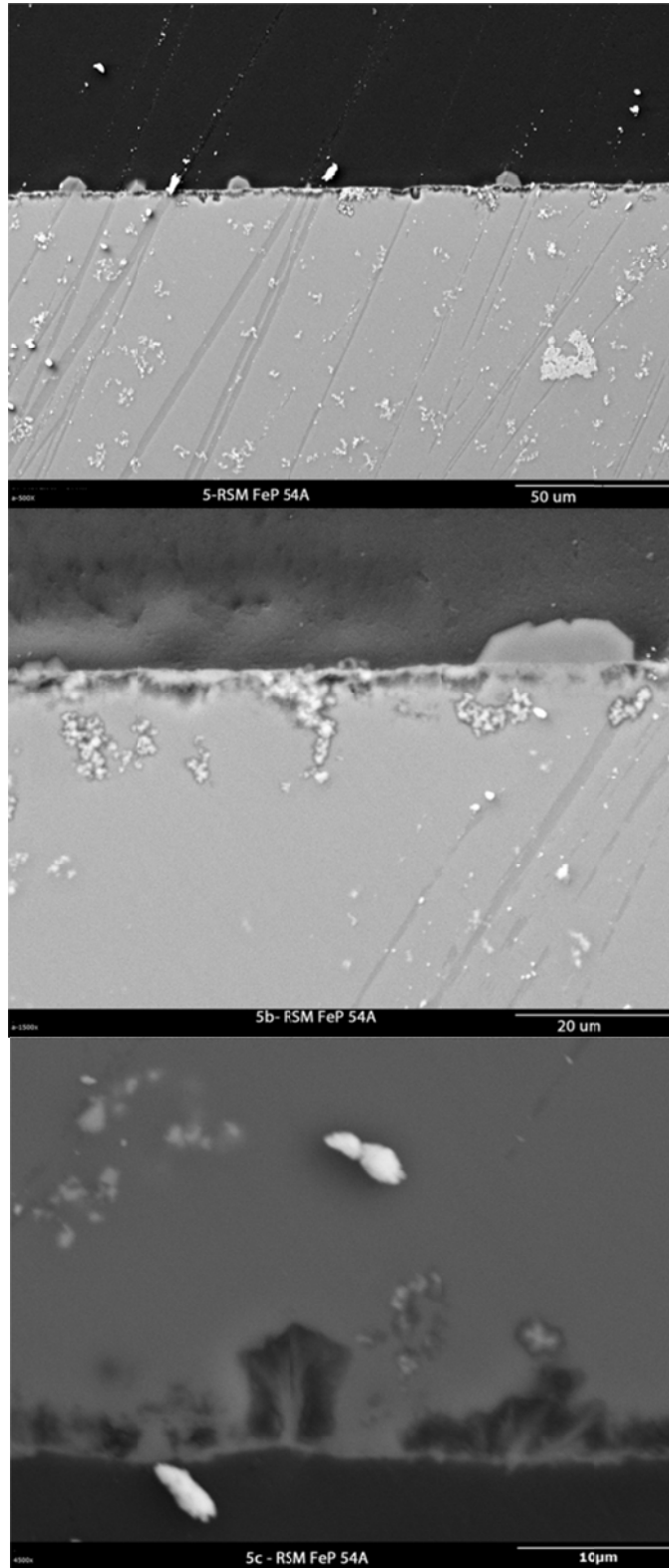
RSM-FEP-54A,CCC

Photos of RSM-FEP-54A CCC VHT Samples Prior to Testing
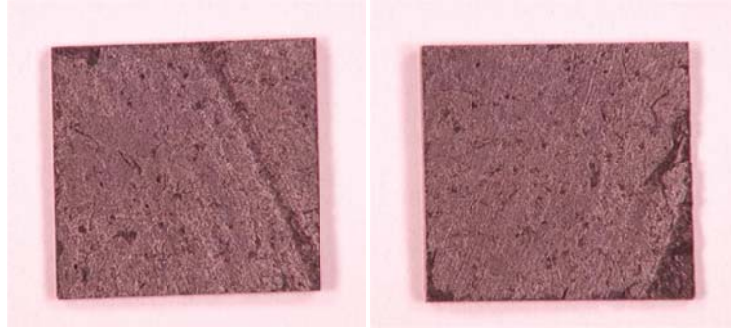
| Side One | Side Two |

Photos of RSM-FEP-54A CCC VHT Samples Post Testing
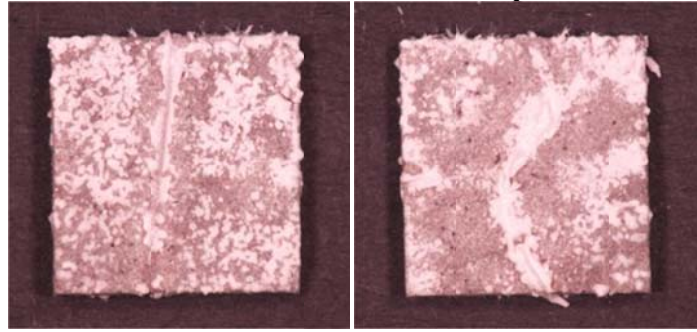
| Side One | Side Two |

RSM-FEP-54A CCC VHT Alteration Thickness Measurement
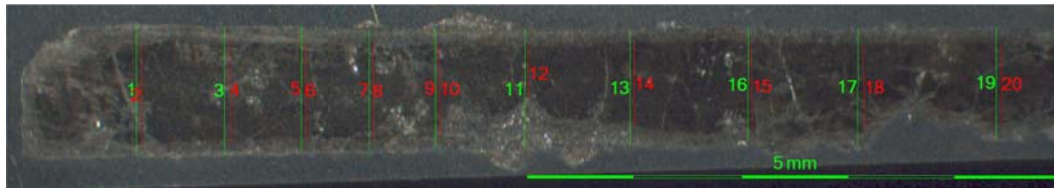
RSM-FEP-54A CCC SEM Images of Reacted Surfaces

6 - RSM FeP 54ACCC

6b-RSM FeP 54ACCC

6c-RSM FeP 54CCC
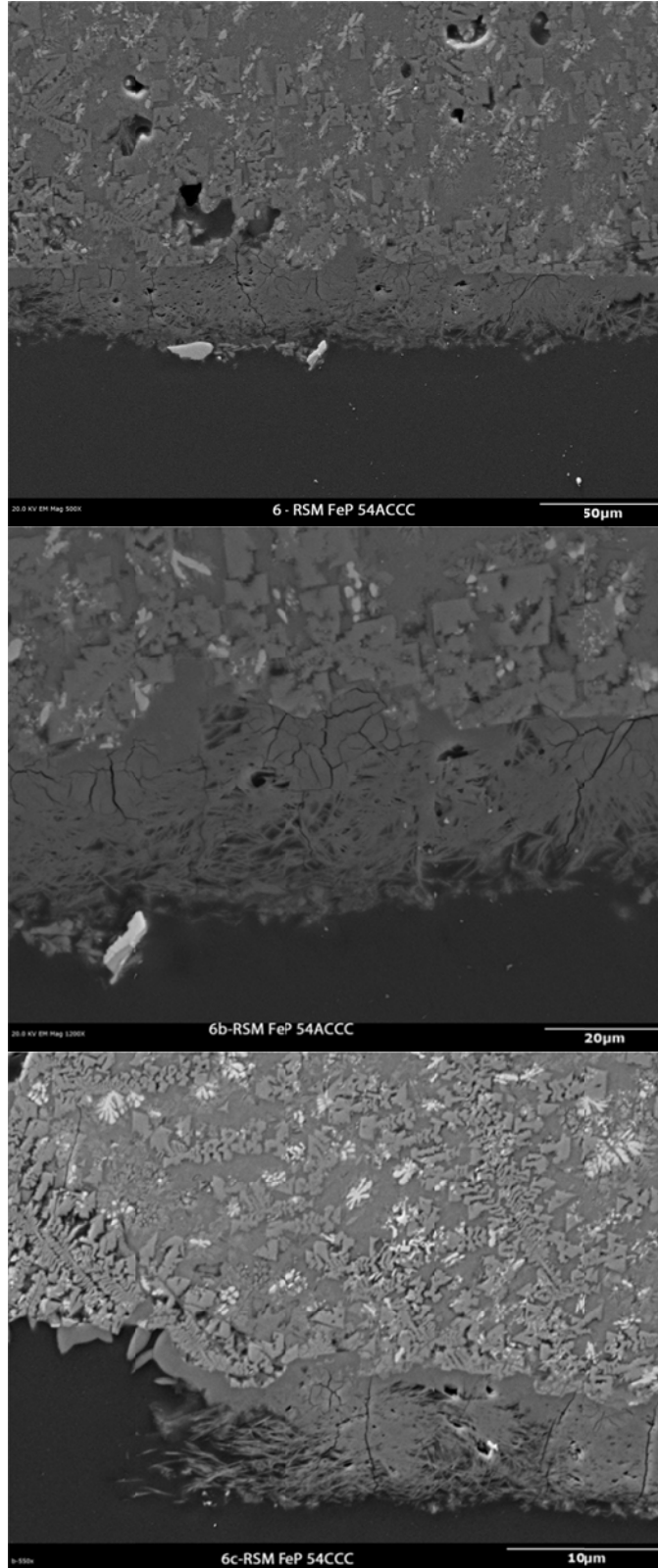
RSM-FEP-63A CCC

Photos of RSM-FEP-63A CCC VHT Samples Prior to Testing
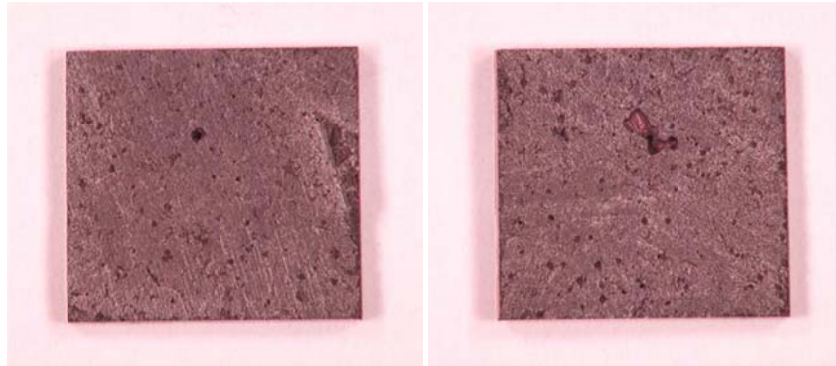
Side One   **Side Two**

Photos of RSM-FEP-63A CCC VHT Samples Post Testing
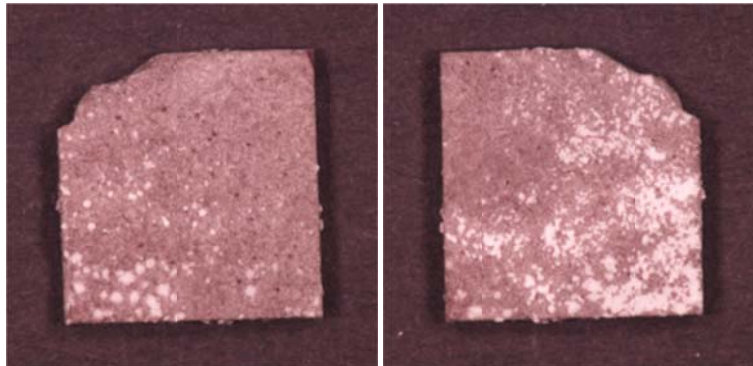
Side One   **Side Two**

RSM-FEP-63A CCC VHT Alteration Thickness Measurement
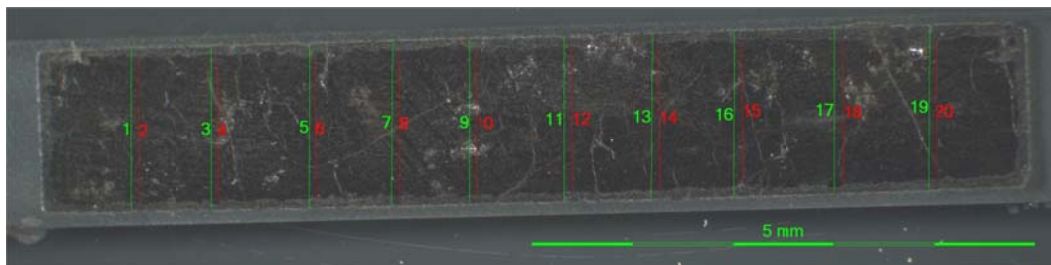
RSM-FEP-63A CCC SEM Images of Reacted Surfaces

7 - RSM FeP 63A   50µm

1100X   7b- RSM FeP 63A   20 um

7 b- RSM FeP 63A   20 um
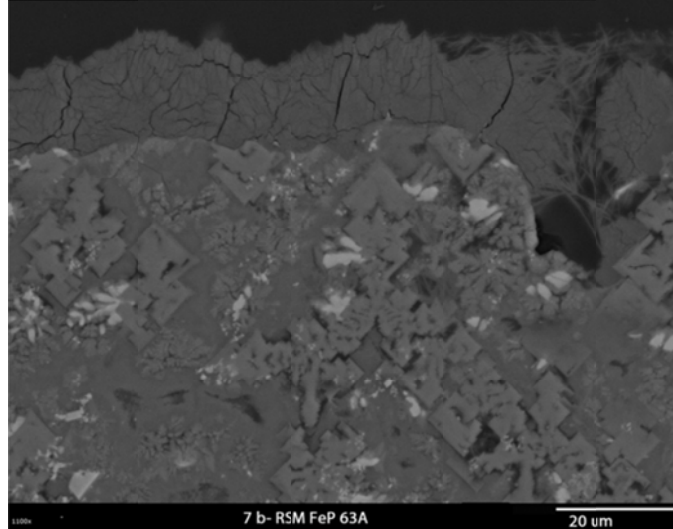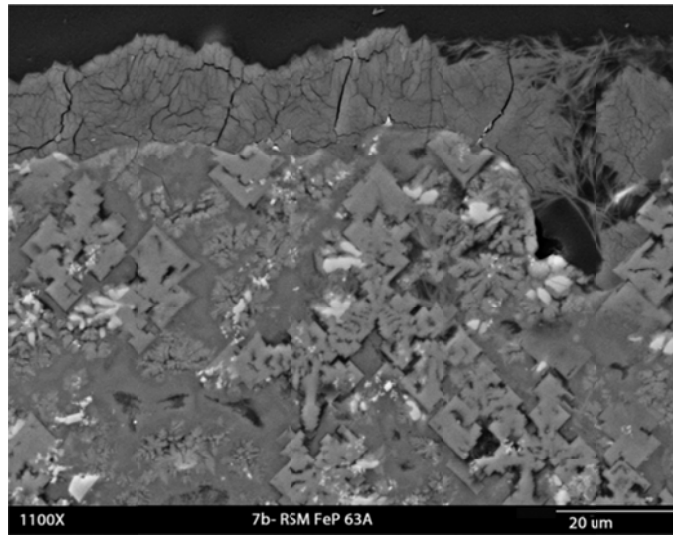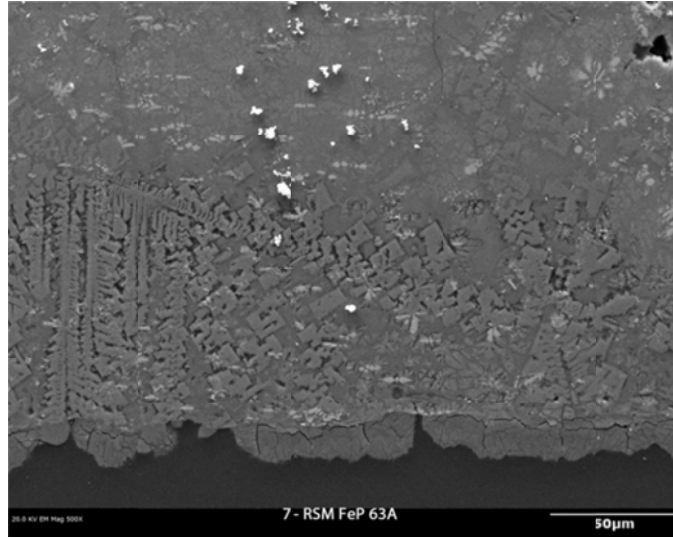
RSM-FEP-70CCC

Photos of RSM-FEP-70CCC VHT Samples Prior to Testing
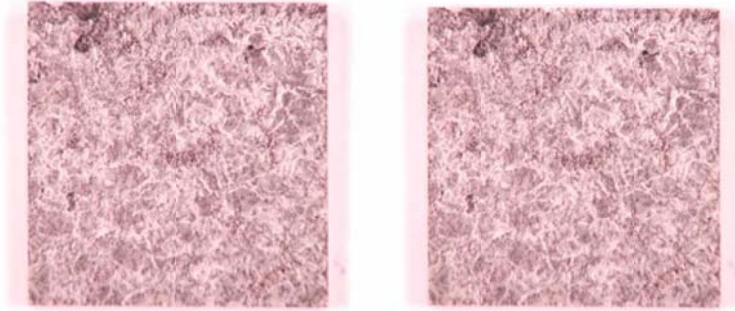
Side One   Side Two

Photos of RSM-FEP-70CCC VHT Samples Post Testing
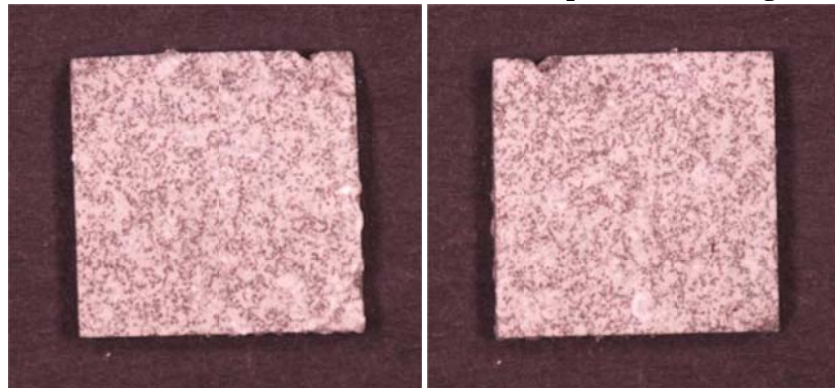
Side One   Side Two

RSM-FEP-70CCC VHT Alteration Thickness Measurement
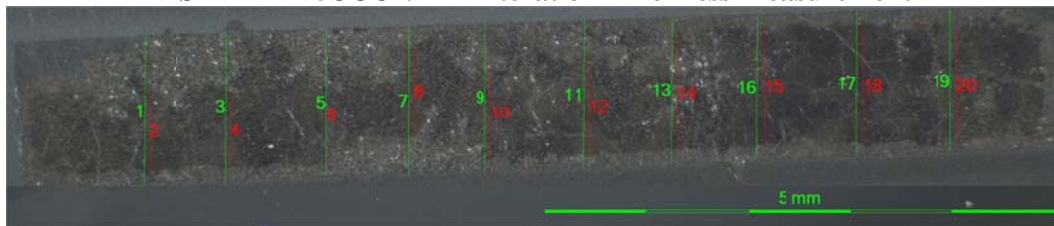
RSM-FEP-70CCC SEM Images of Reacted Surfaces

8b -RSM FeP 70CCC   20µm

8 RSM FeP 70CCC   50µm
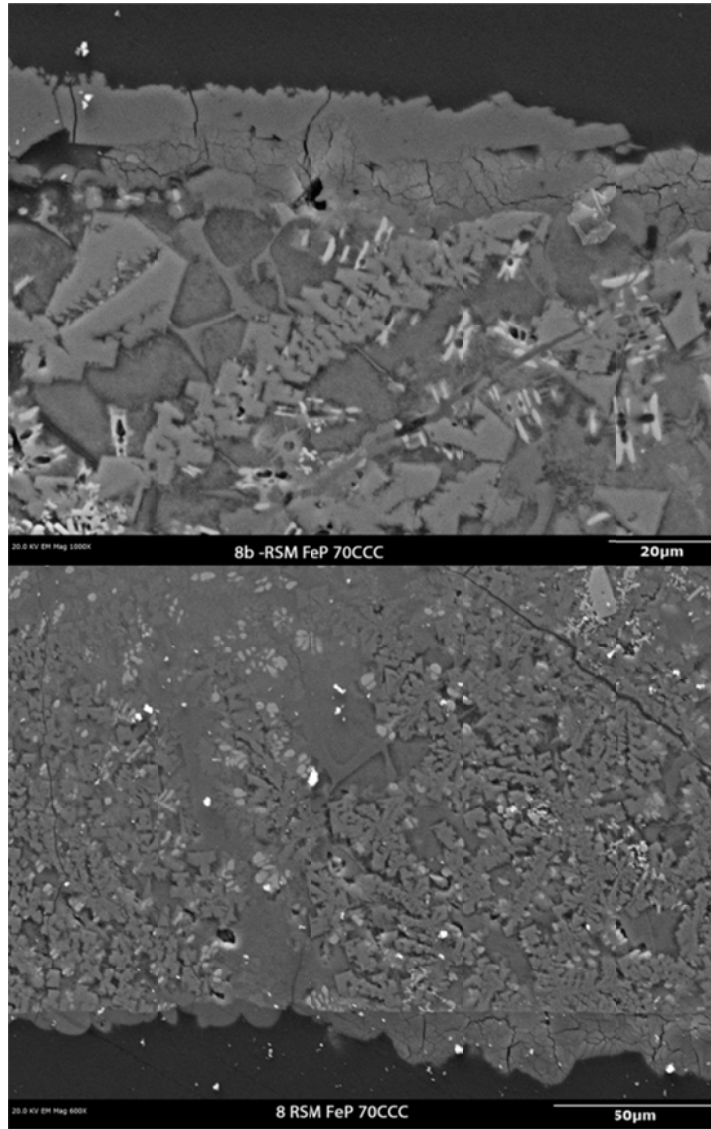
Appendix B

XRD Scan Results

Appendix B: XRD Scan Results

RSM-FEP-07Q
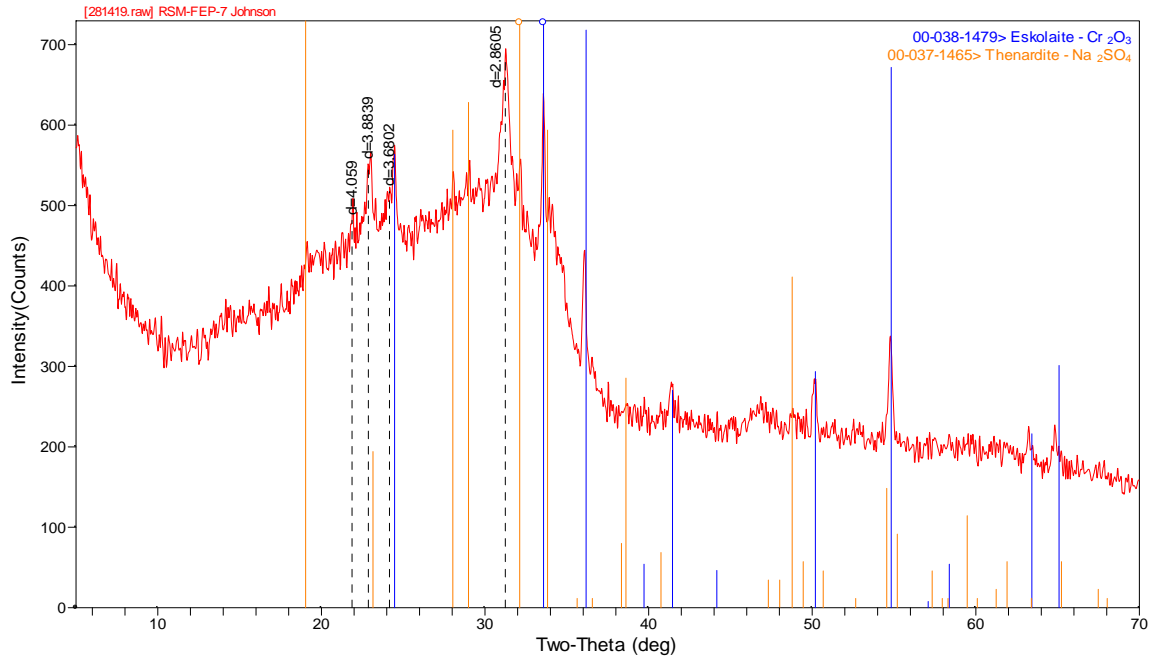
RSM-FEP-12Q
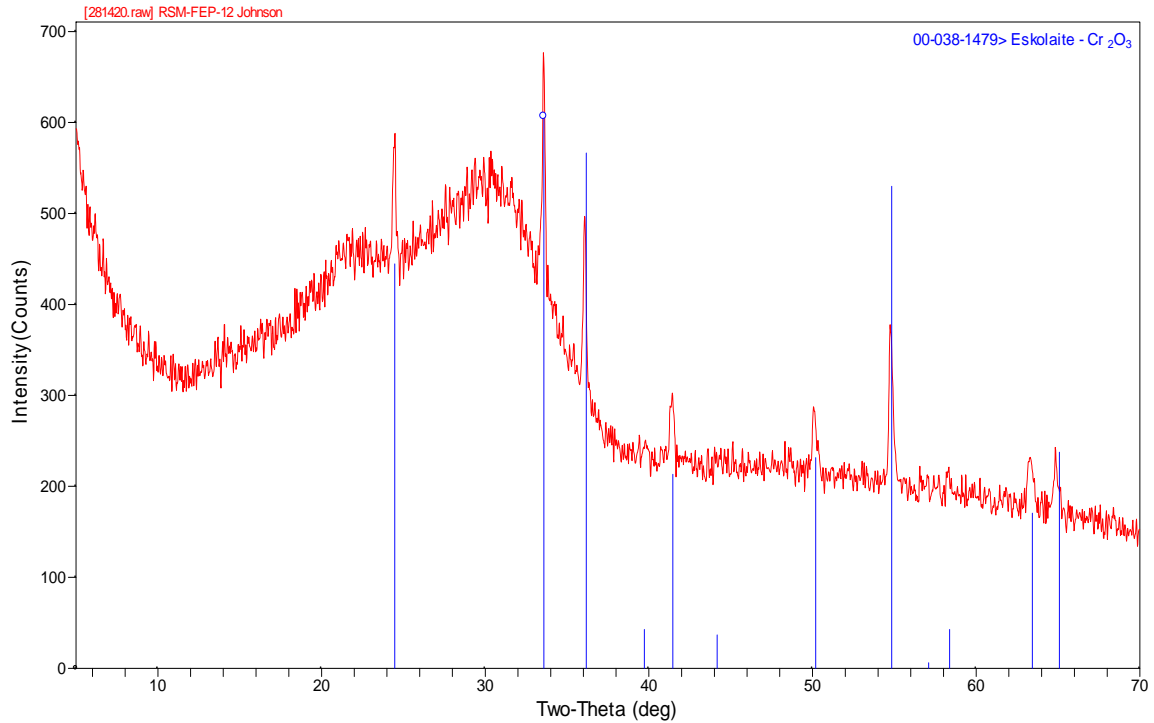
RSM-FEP-15Q
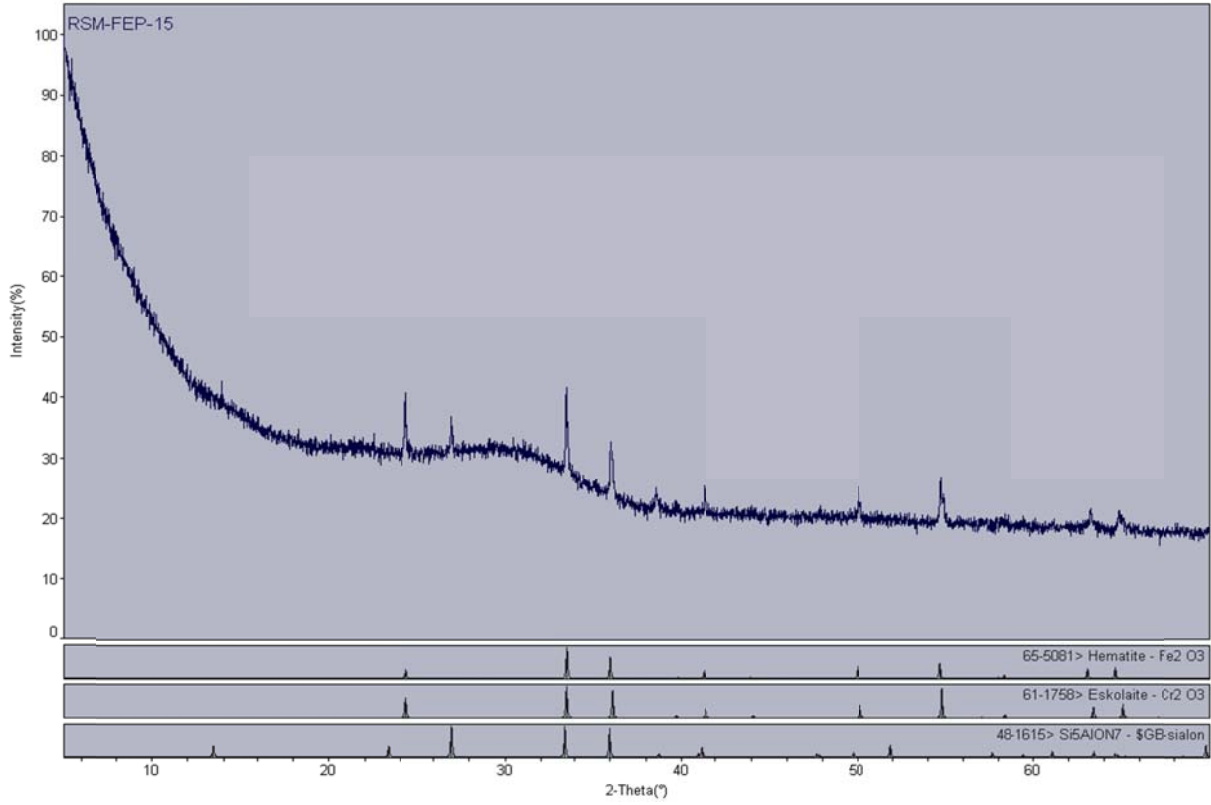
RSM-FEP-34CCC
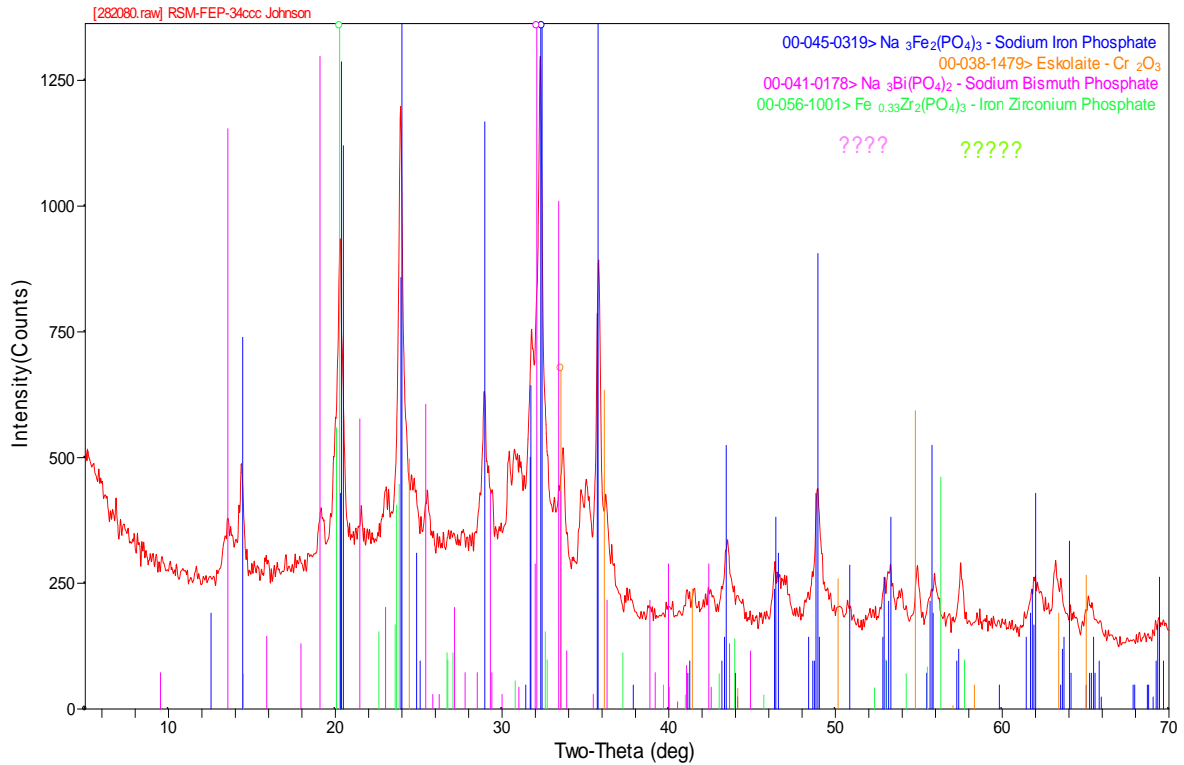
Note: Question marks indicate that the identification of the identified minor phases is questionable.

B.2

RSM-FEP-37Q

RSM-FEP-46Q

B.3
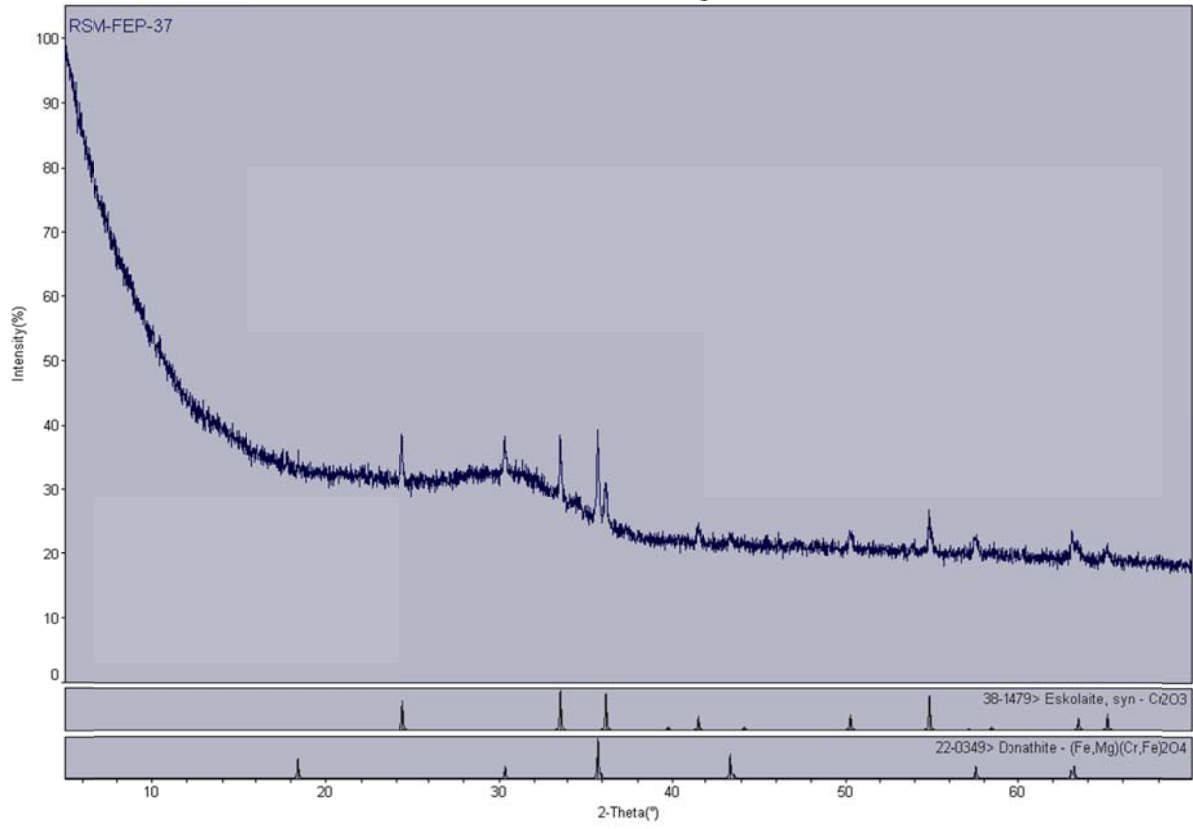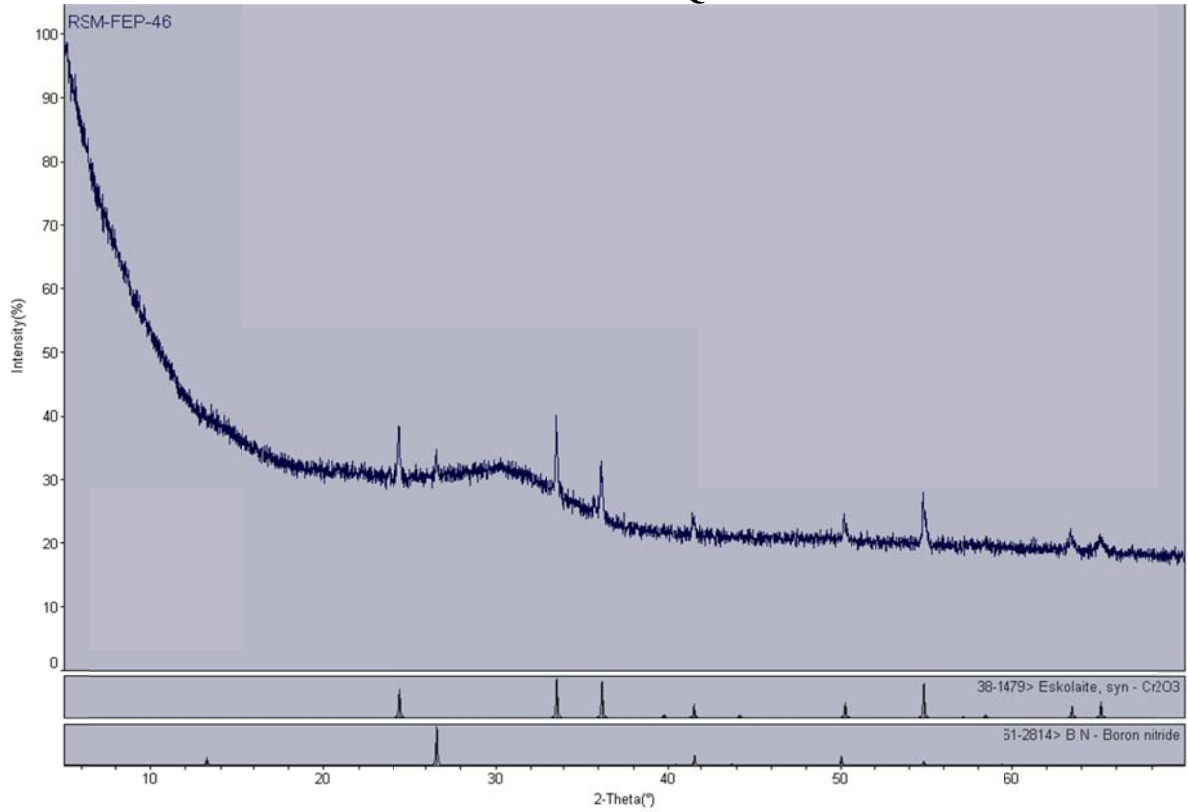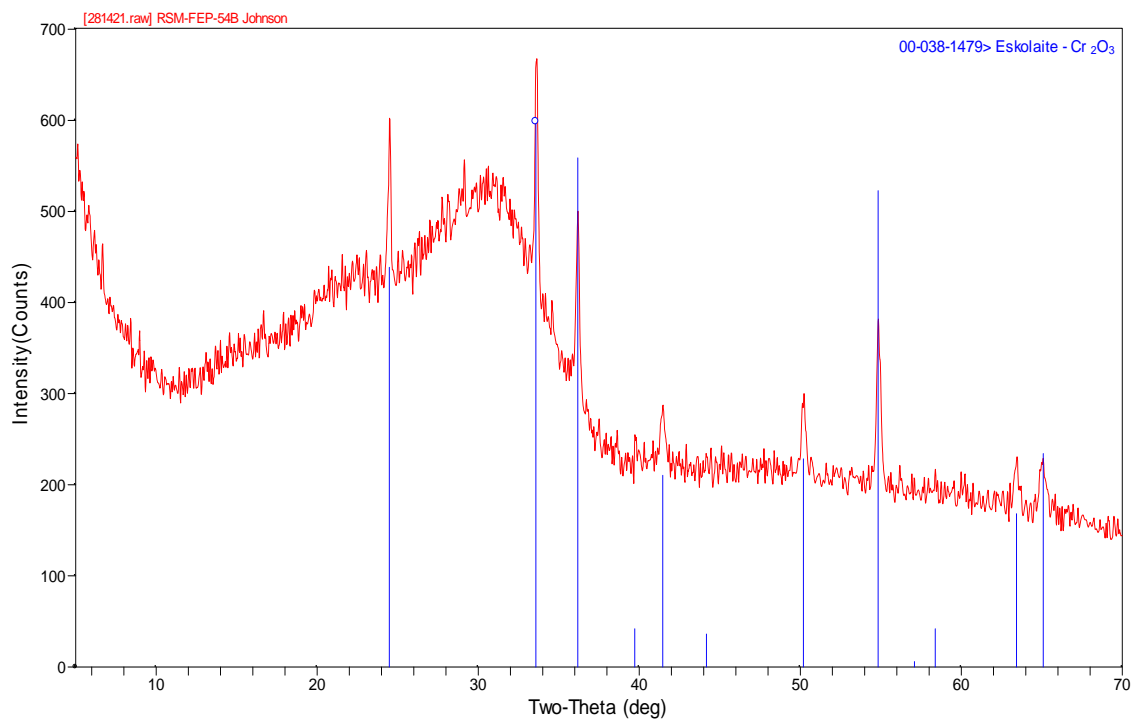
RSM-FEP-54Q

RSM-FEP-59Q
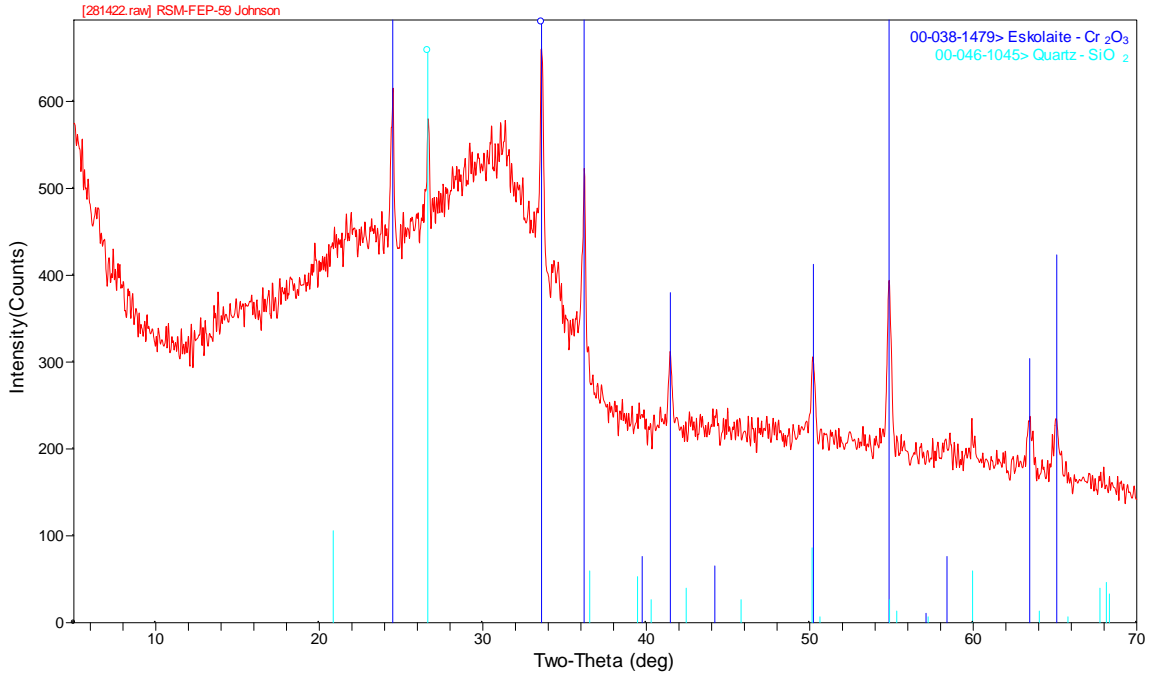
RSM-FEP-59CCC
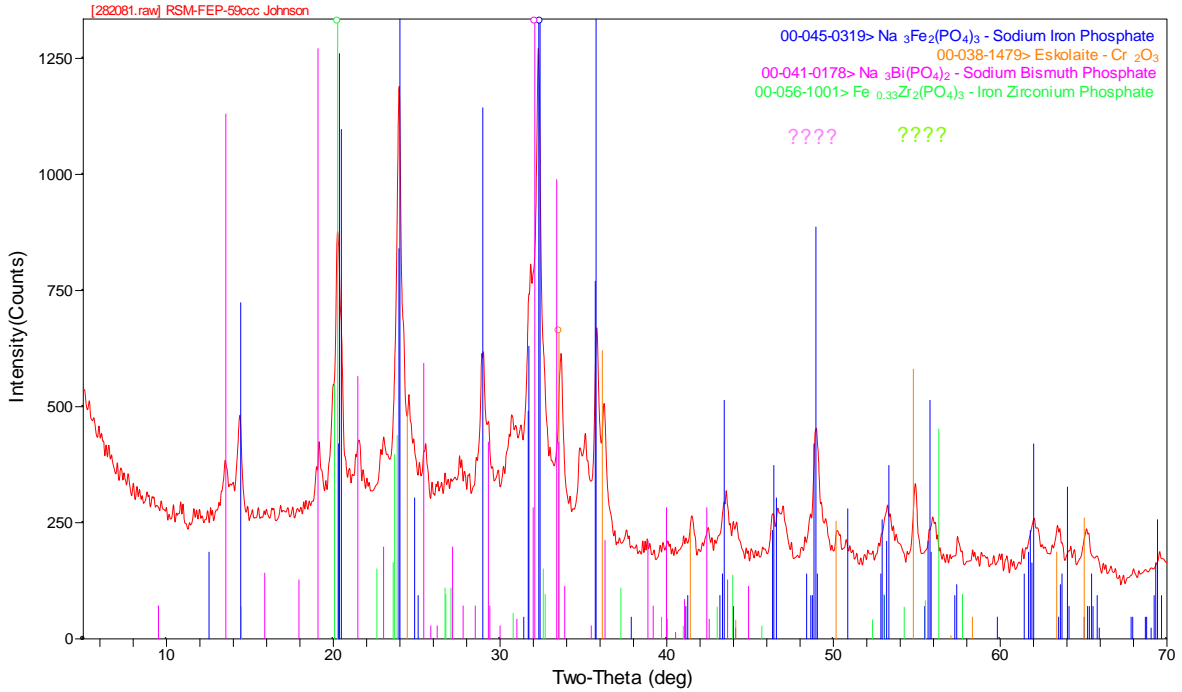
Note: Question marks indicate that the identification of the identified minor phases is questionable.

RSM-FEP-61Q
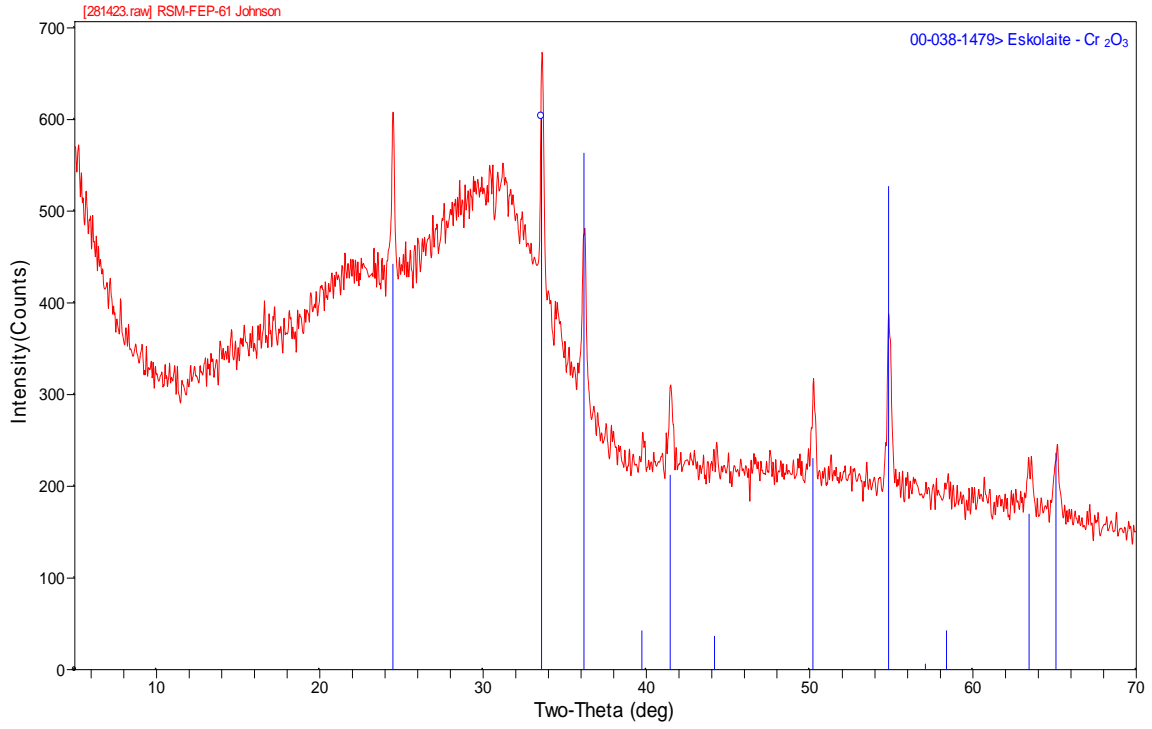
RSM-FEP-61CCC
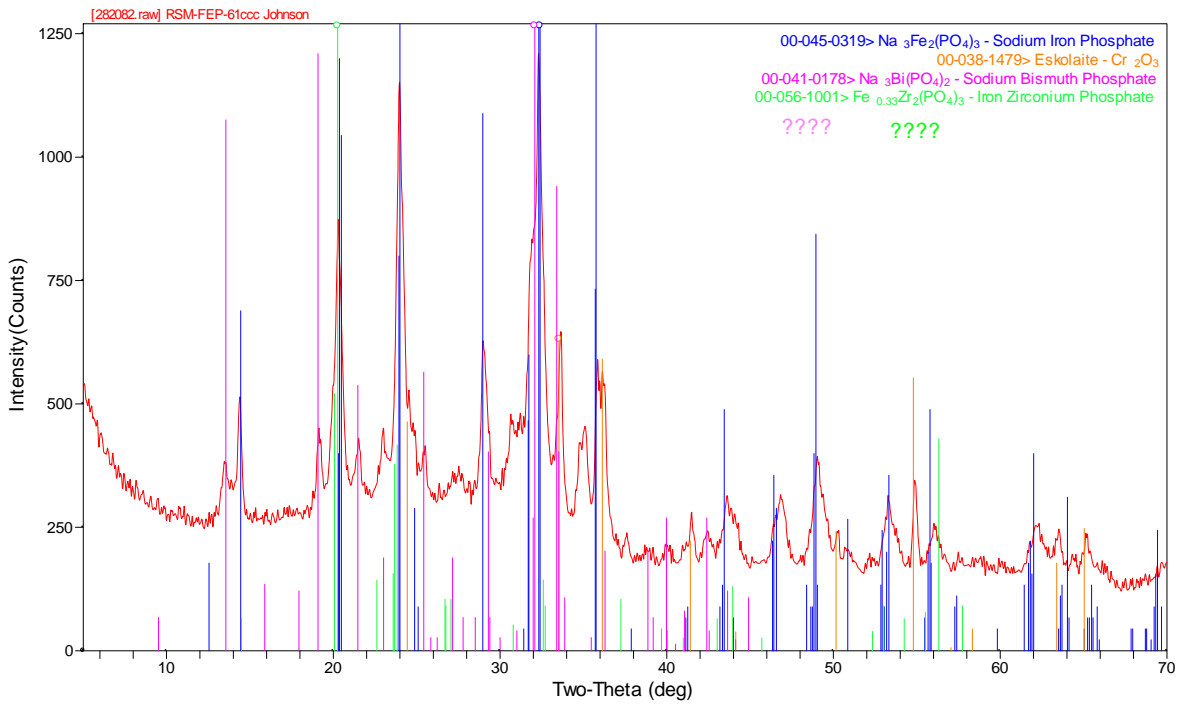
Note: Question marks indicate that the identification of the identified minor phases is questionable.

B.6

RSM-FEP-65Q

[281424.raw] RSM-FEP-65 Johnson

00-038-1479> Eskolaite - Cr $_2$O$_3$

RSM-FEP-65CCC

[282083.raw] RSM-FEP-63Bccc Johnson

00-045-0319> Na $_3$Fe$_2$(PO$_4$)$_3$ - Sodium Iron Phosphate
00-038-1479> Eskolaite - Cr $_2$O$_3$
00-041-0178> Na $_3$Bi(PO$_4$)$_2$ - Sodium Bismuth Phosphate
00-056-1001> Fe $_{0.33}$Zr$_2$(PO$_4$)$_3$ - Iron Zirconium Phosphate

????? ???
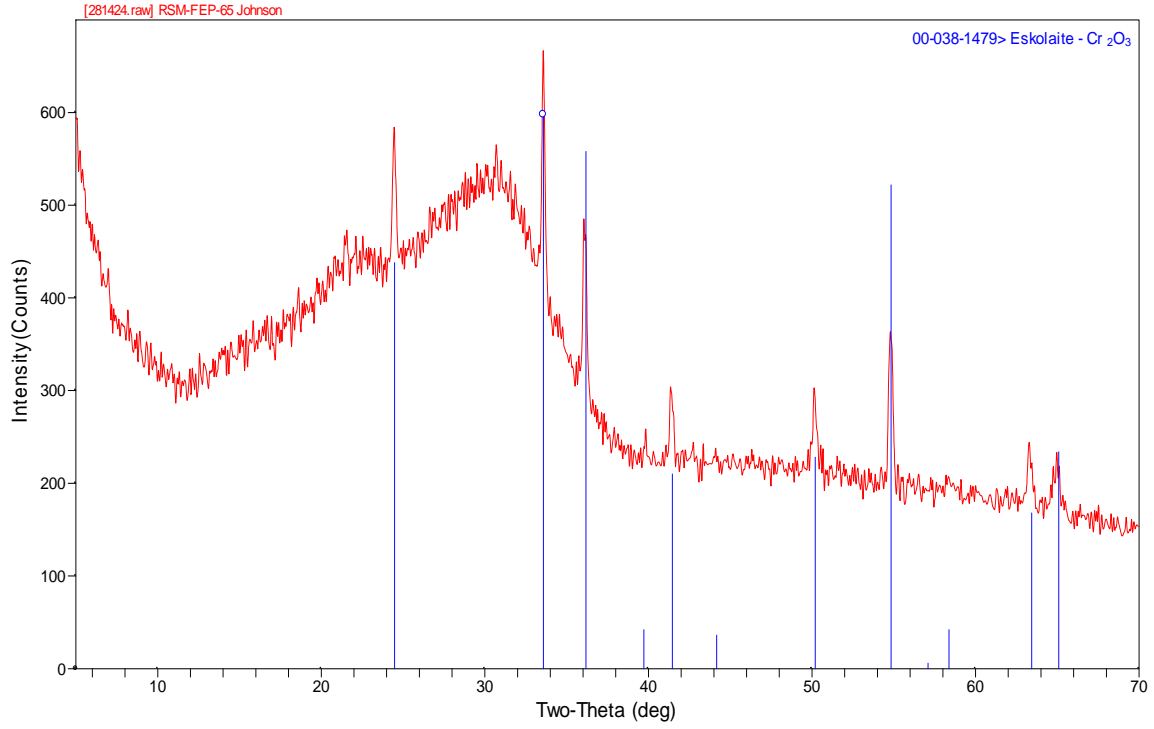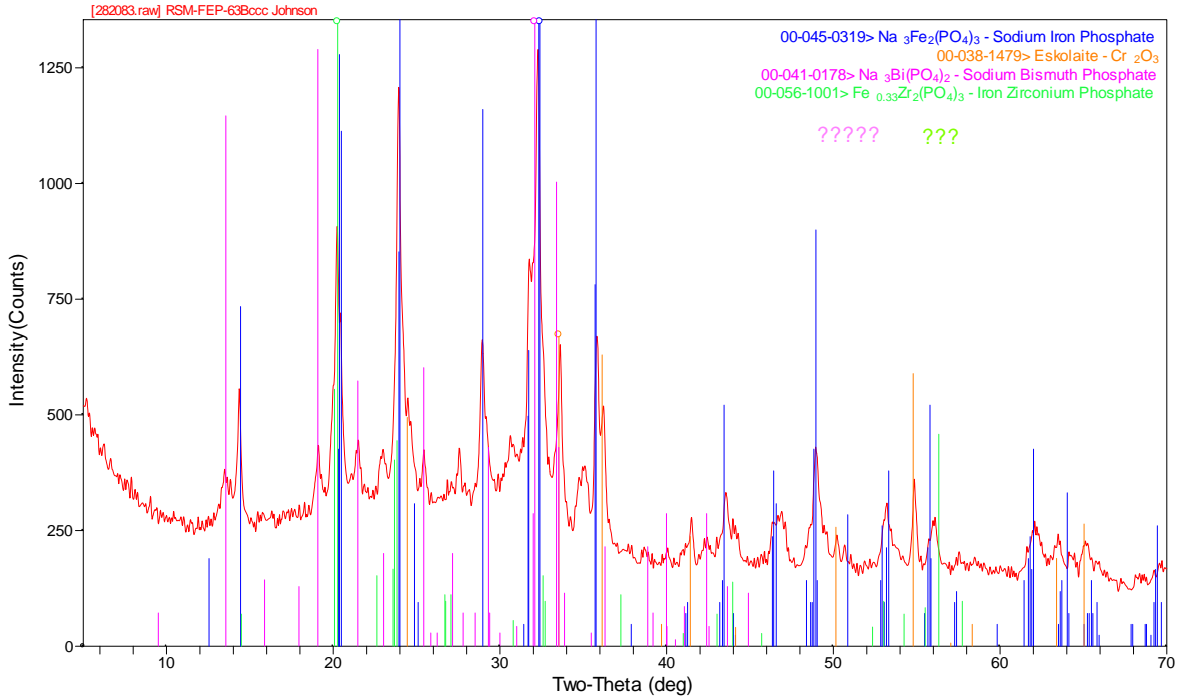
Note: Question marks indicate that the identification of the identified minor phases is questionable.
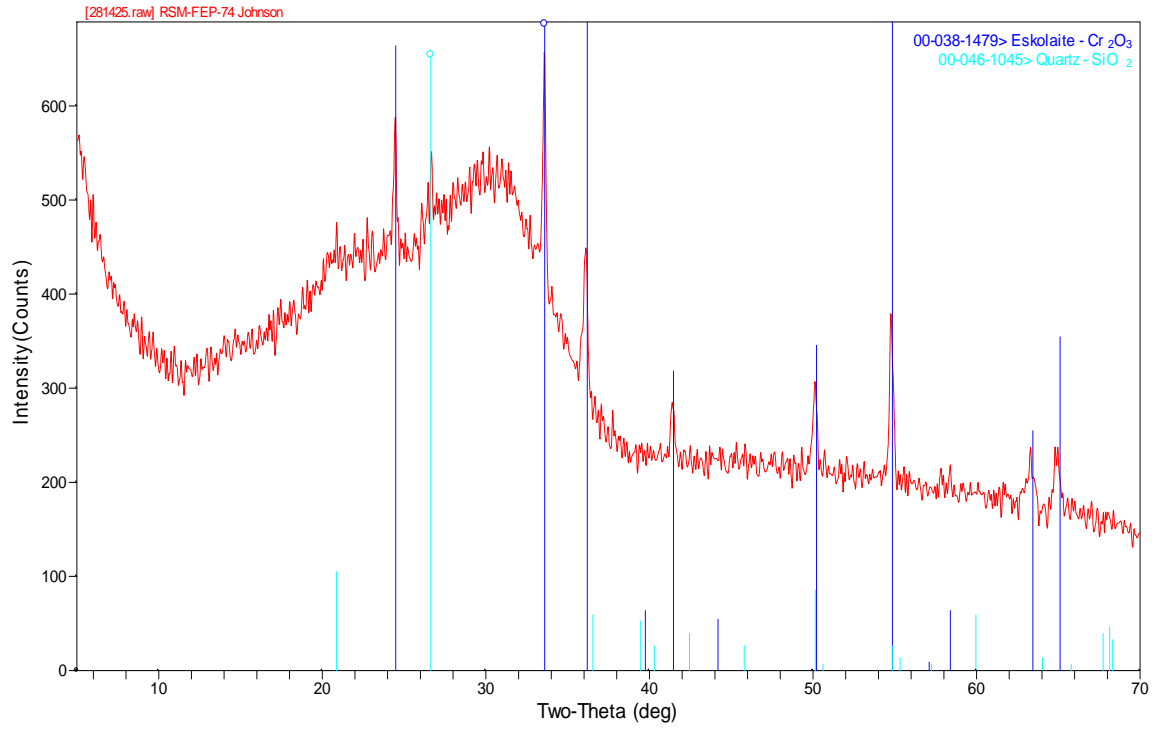
RSM-FEP-74Q

RSM-FEP-74CCC
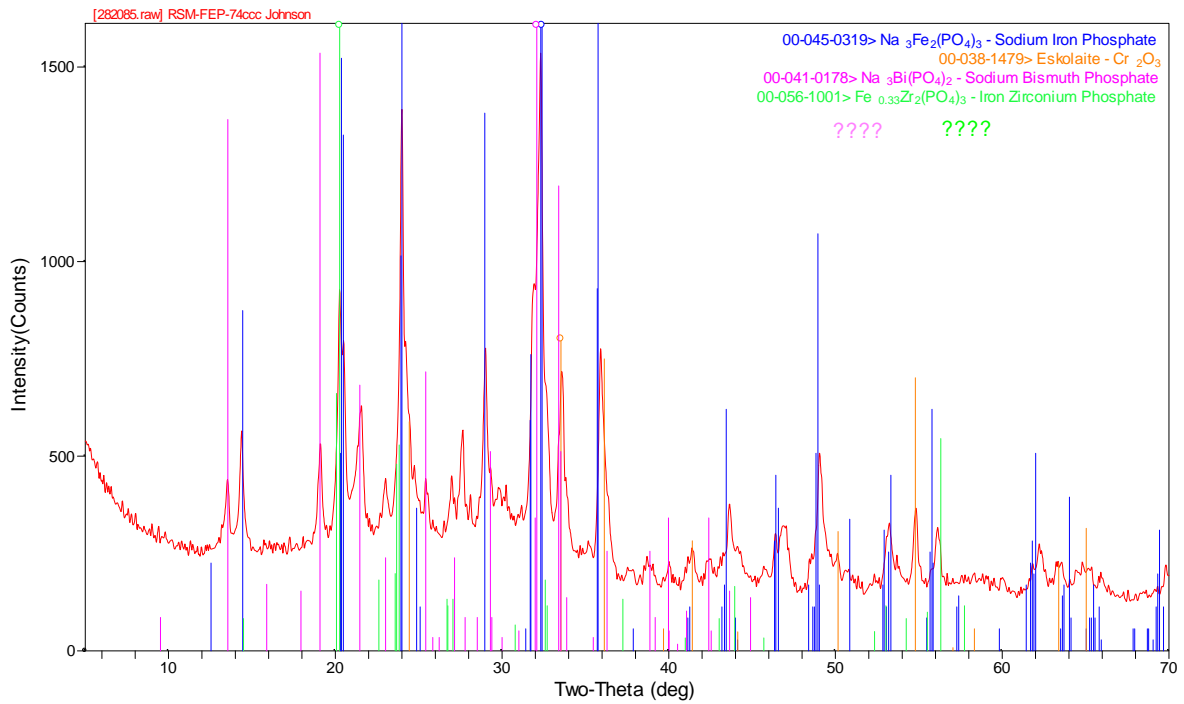
Note: Question marks indicate that the identification of the identified minor phases is questionable.

RSM-FEP-76Q
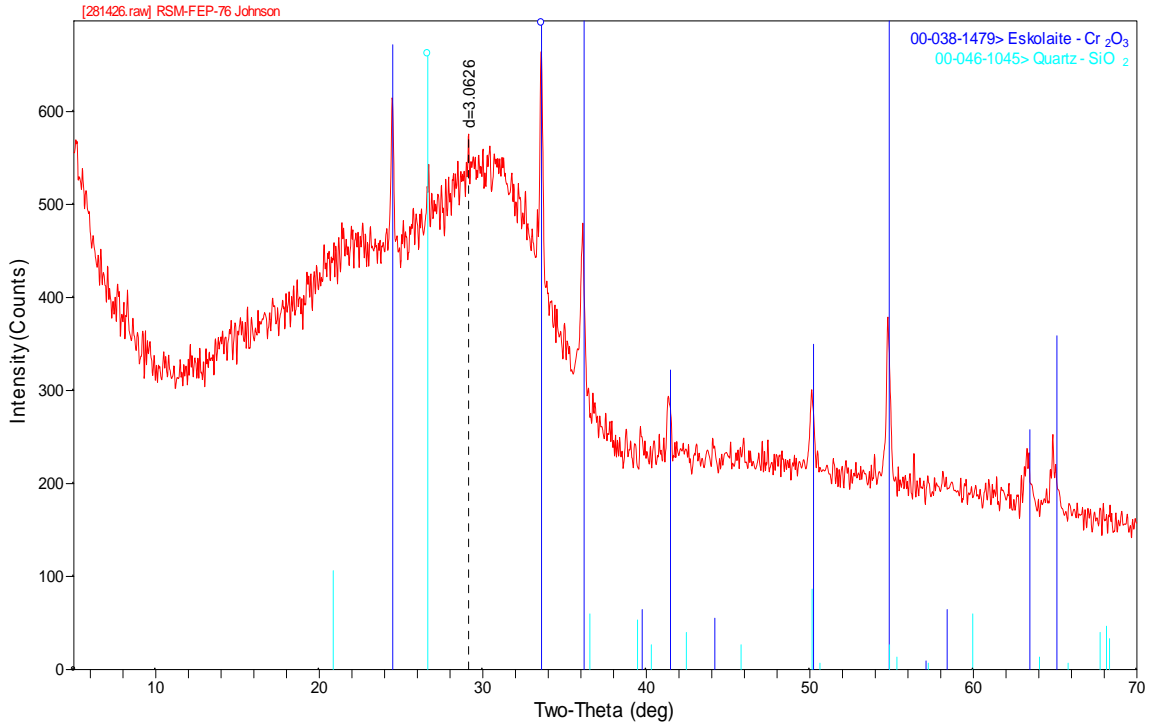
RSM-FEP-76CCC
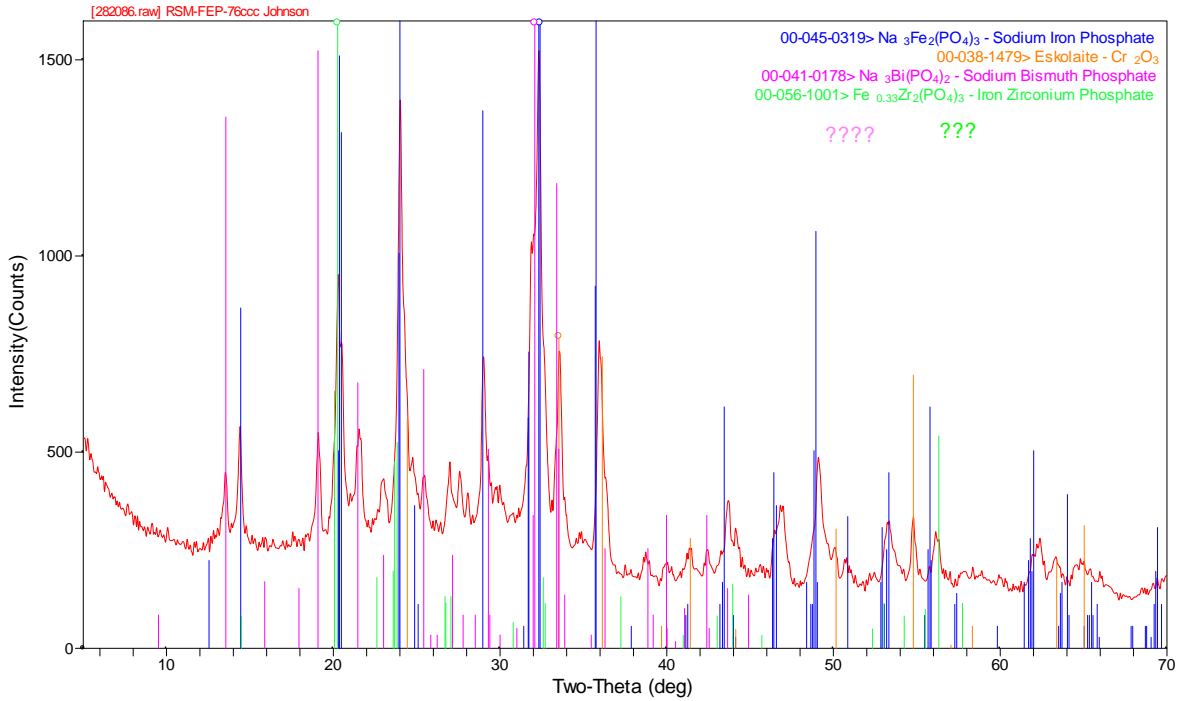
Note: Question marks indicate that the identification of the identified minor phases is questionable.

Appendix C

Research-Scale Melter Measurement and Testing Equipment

Appendix C

Research-Scale Melter Measurement and Testing Equipment

Description	M&TE Description	Location	Calibration Level
Type K thermocouple	Melter glass	Melter electrode	Cat 1
Type K thermocouple	Post EVS off-gas temperature	In EVS/HEME off-gas jumper	Indication only
Type K thermocouple	Scrub liquid temperature after heat exchanger	Spray nozzle supply line	Indication only
Weigh scale	Feed tank weight	Feed station stand	User calibrated
Weigh scale	Glass scale weight	Under RSM kiln	Indication only

Appendix D

Operating Parameters Data Plots from RSM Test

Appendix D

Operating Parameters Data Plots from RSM Test
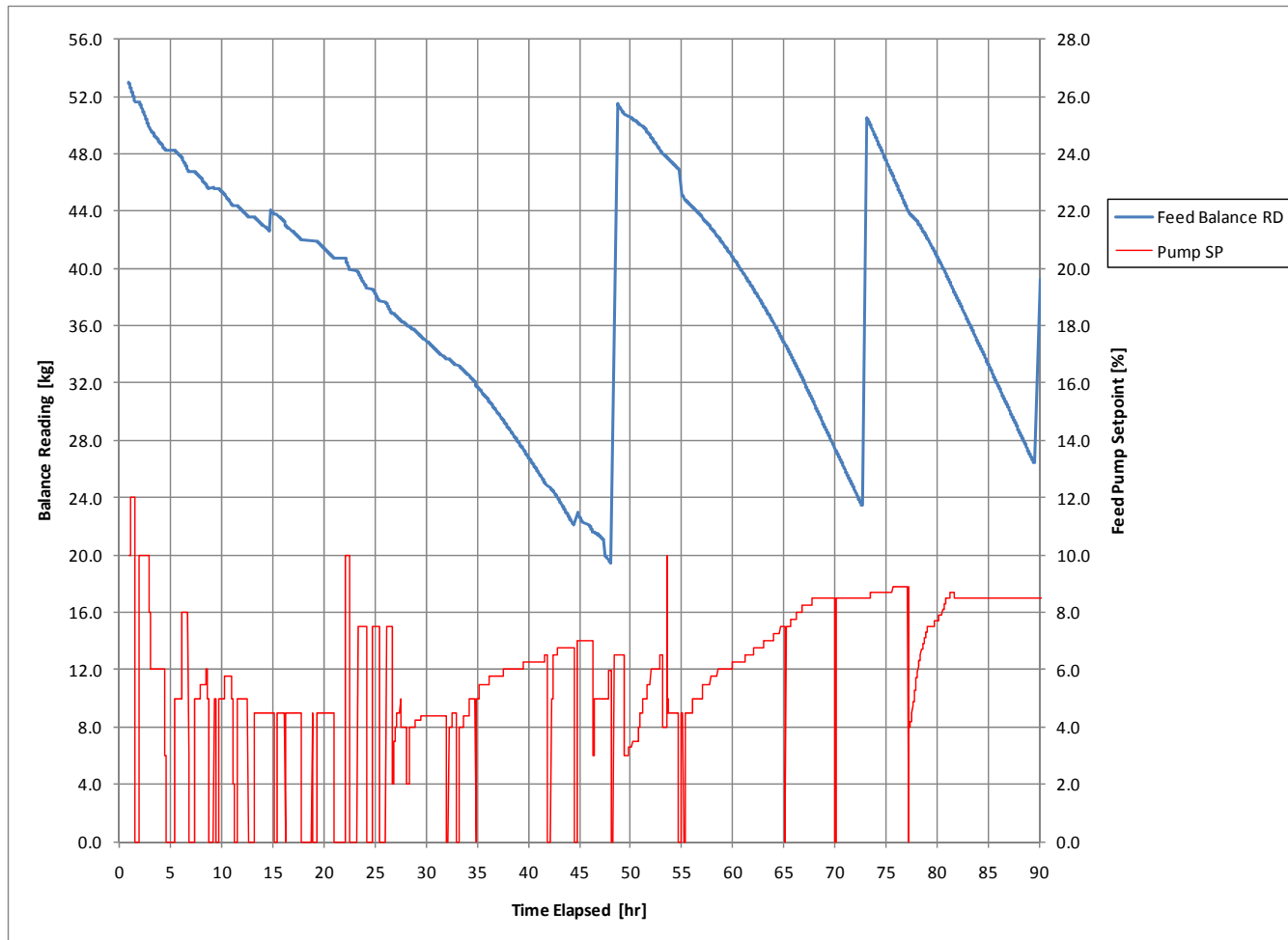
Figure D.1. Simulant Feed Pump Set Point and Balance Reading (0 to 90 hr)
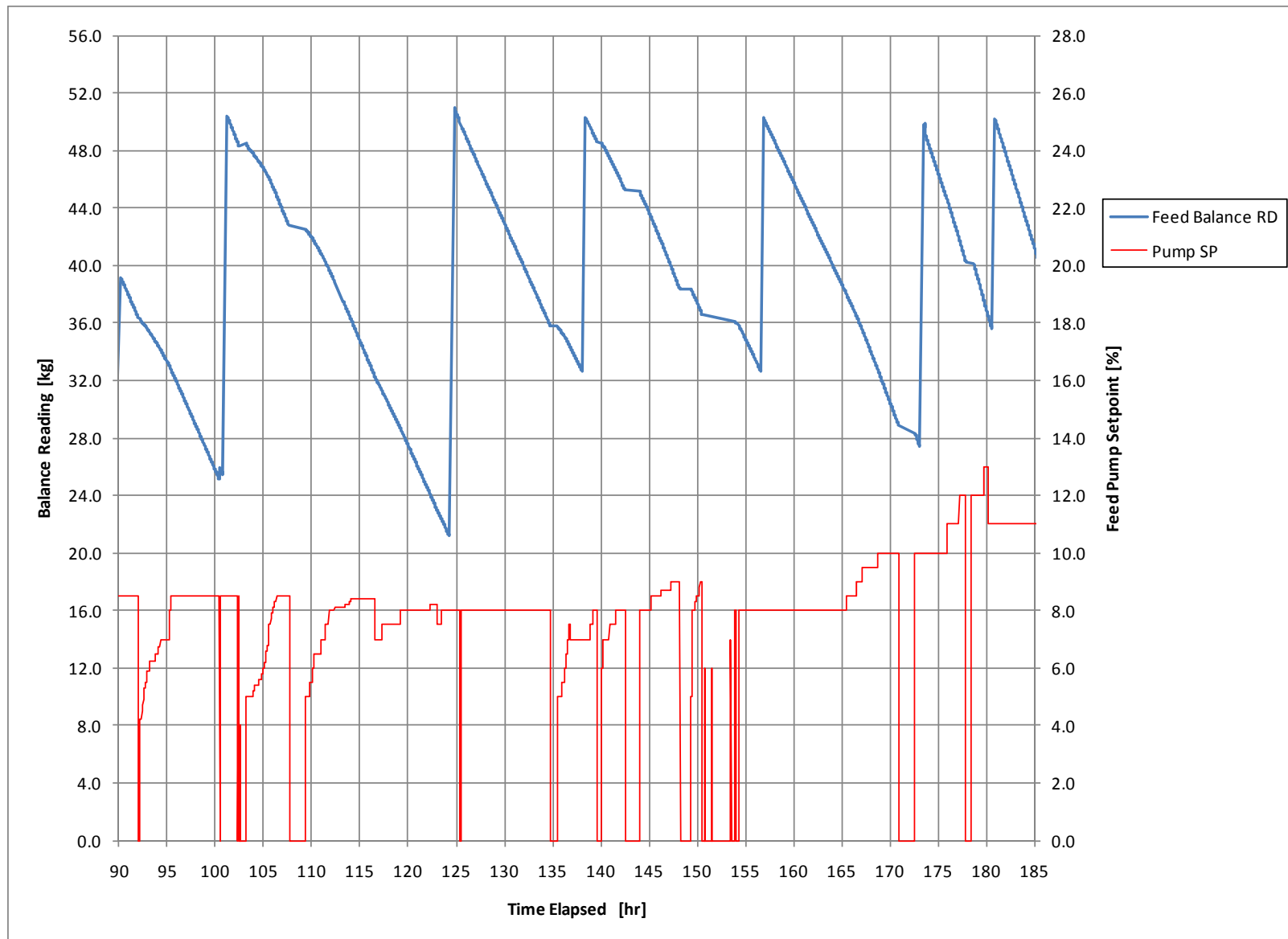
Figure D.2. Simulant Feed Pump Set Point and Balance Reading (90 to 185 hr)
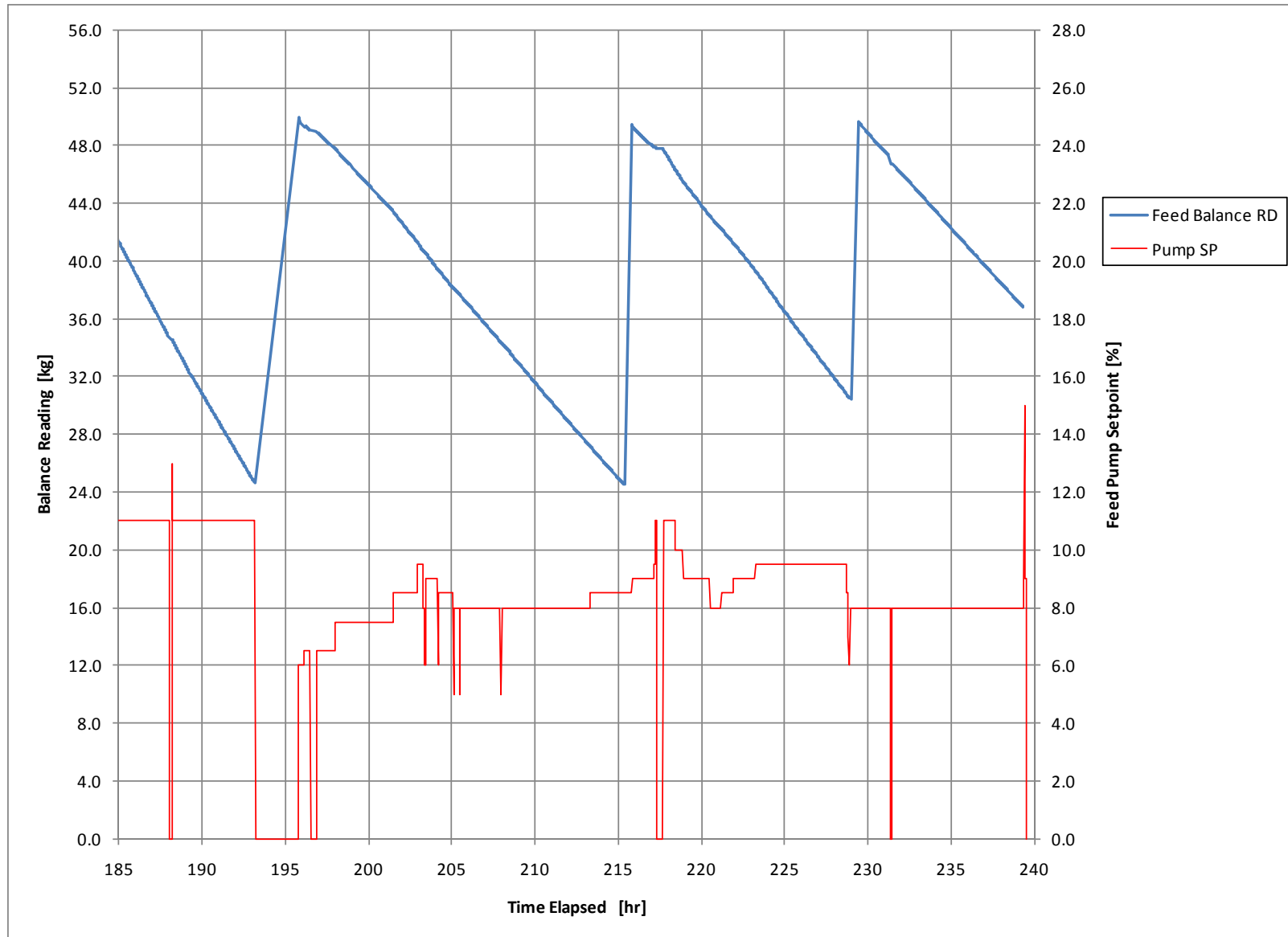
Figure D.3. Simulant Feed Pump Set Point and Balance Reading (185 hr to end of test)
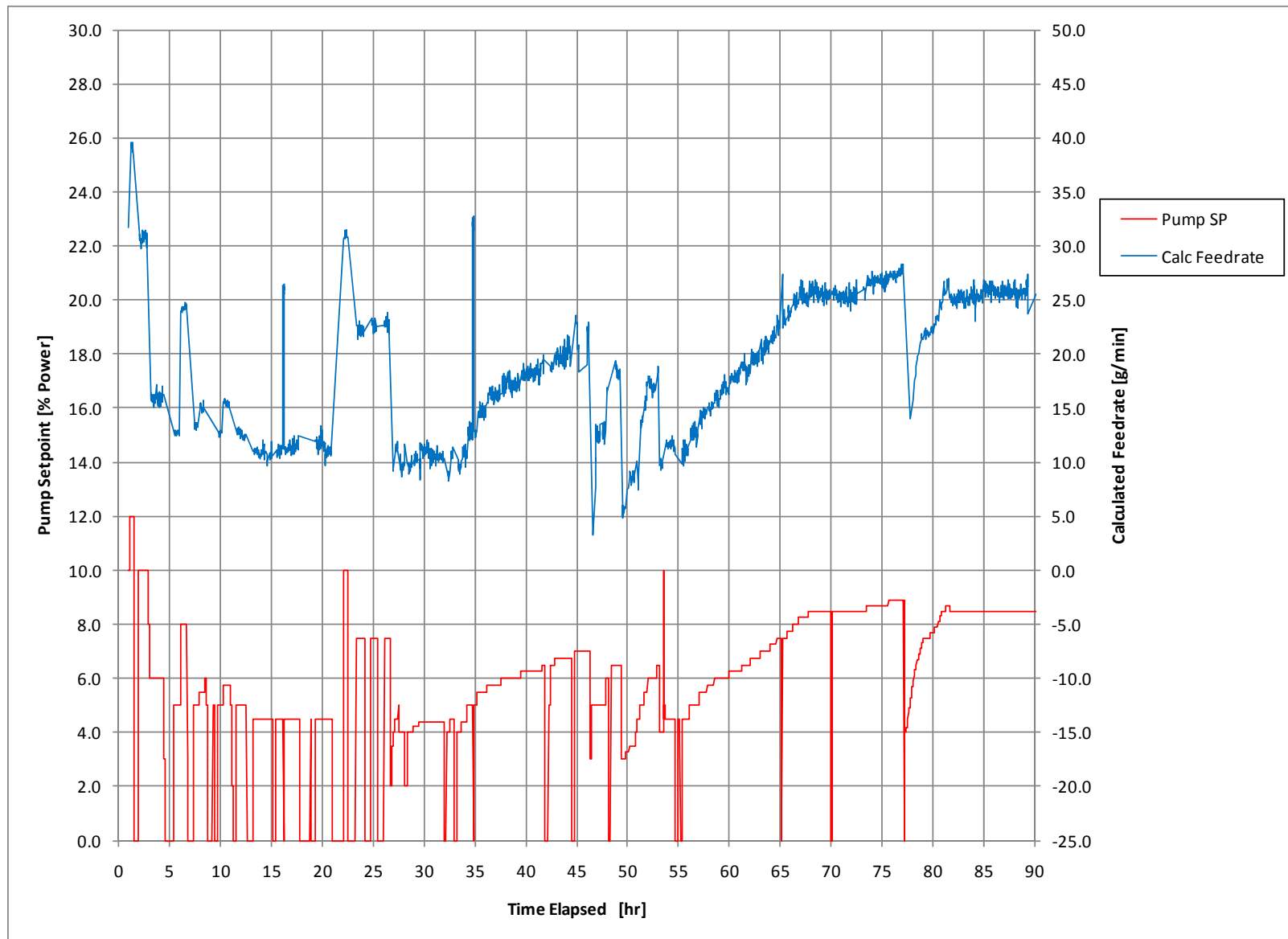
Figure D.4. Simulant Feed Pump Set Point and Calculated Feed Rate (0 to 90 hr)
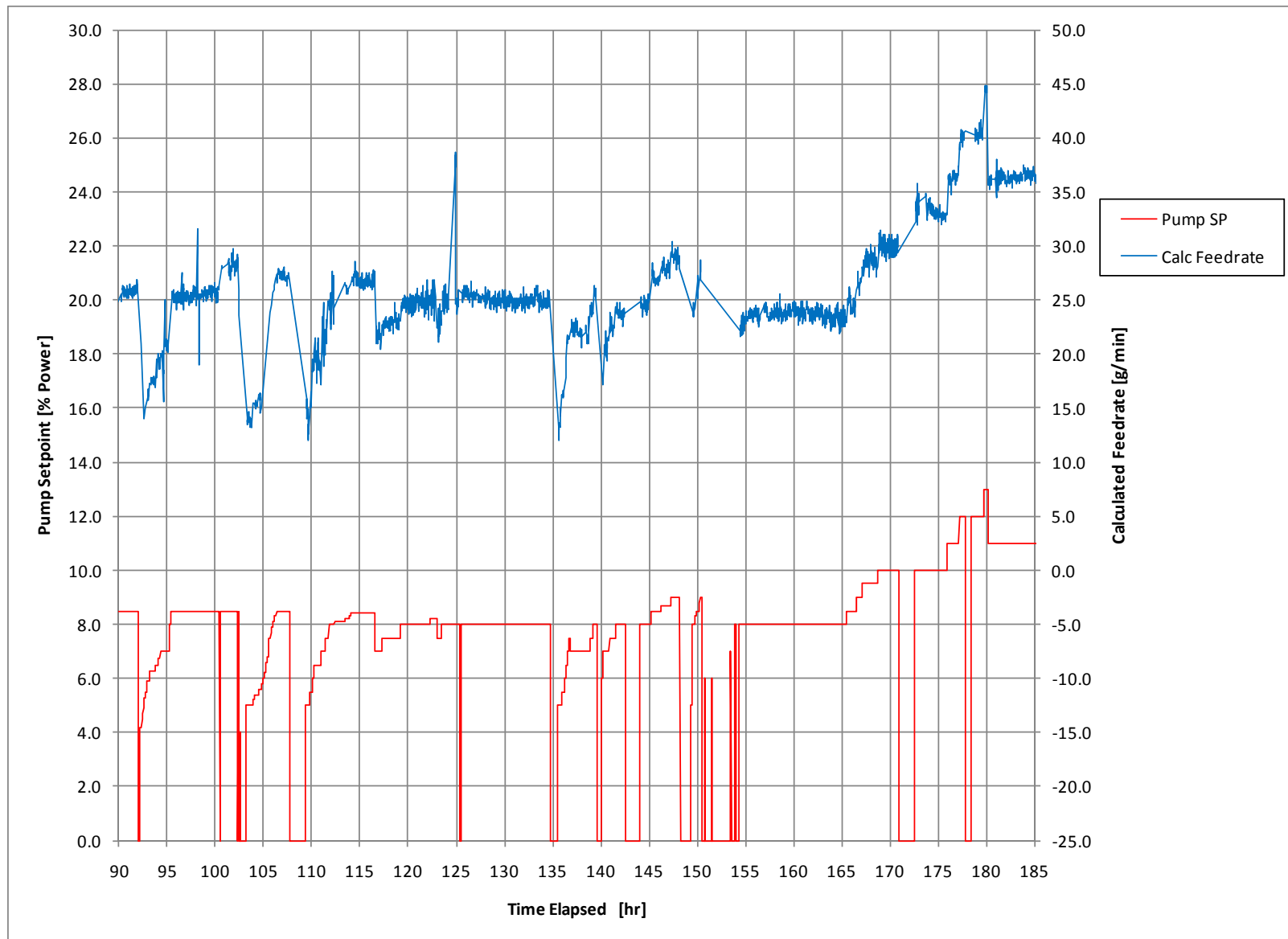
Figure D.5. Simulant Feed Pump Set Point and Calculated Feed Rate (90 to 185 hr)
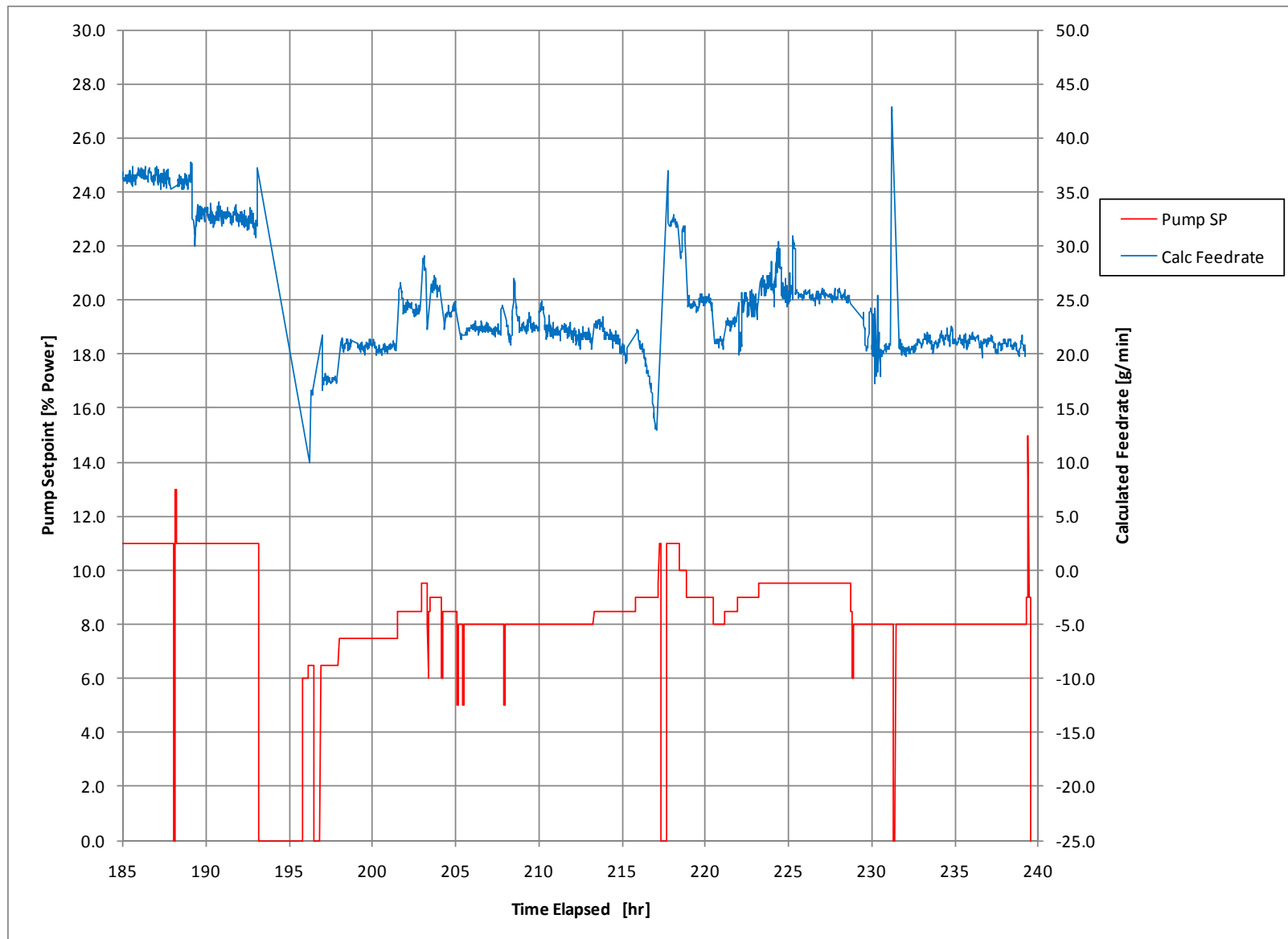
Figure D.6. Simulant Feed Pump Set Point and Calculated Feed Rate (185 hr to end of test)
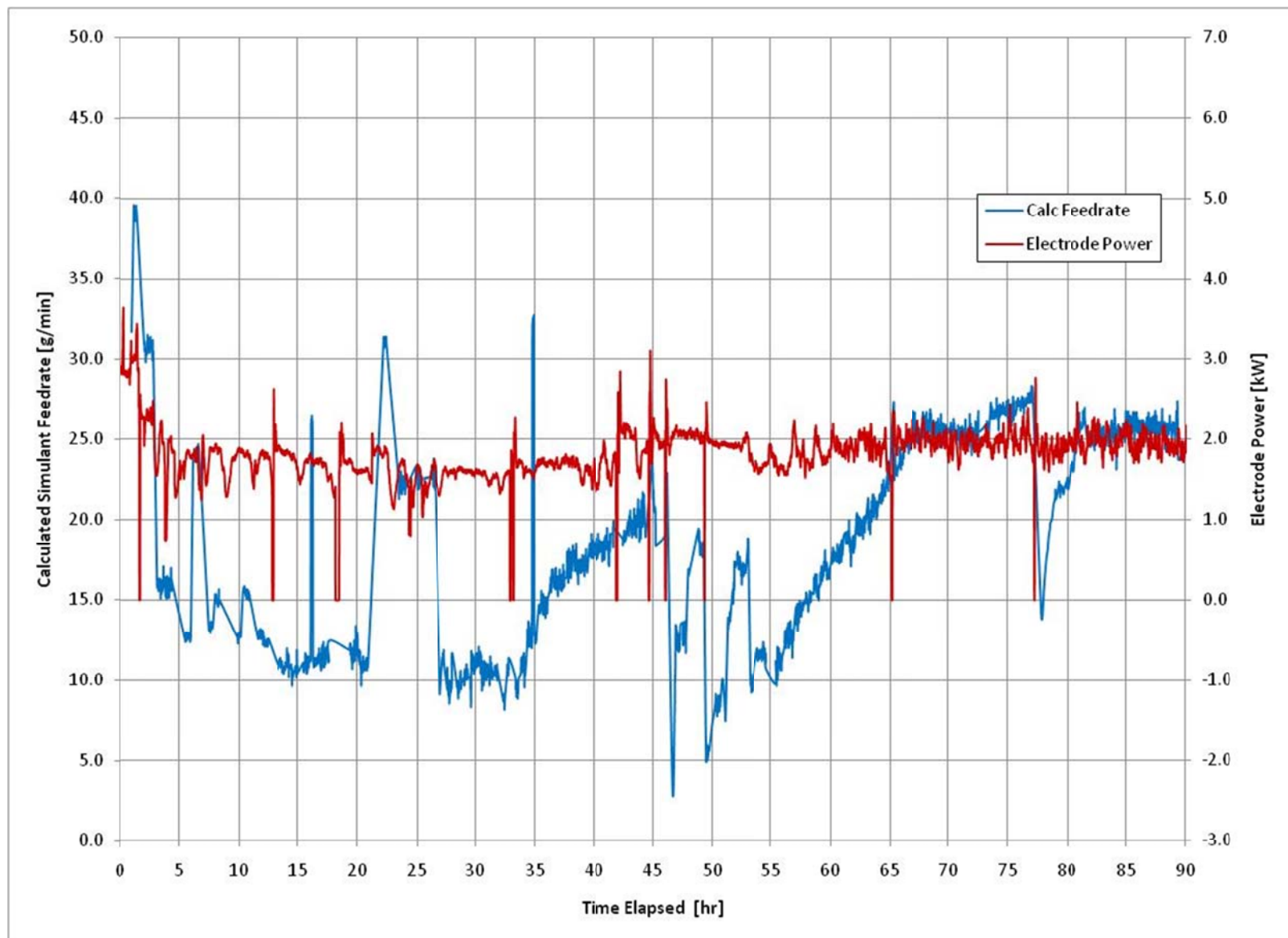
Figure D.7. Calculated Simulant Feed Rate and Electrode Power (0 to 0 hr)
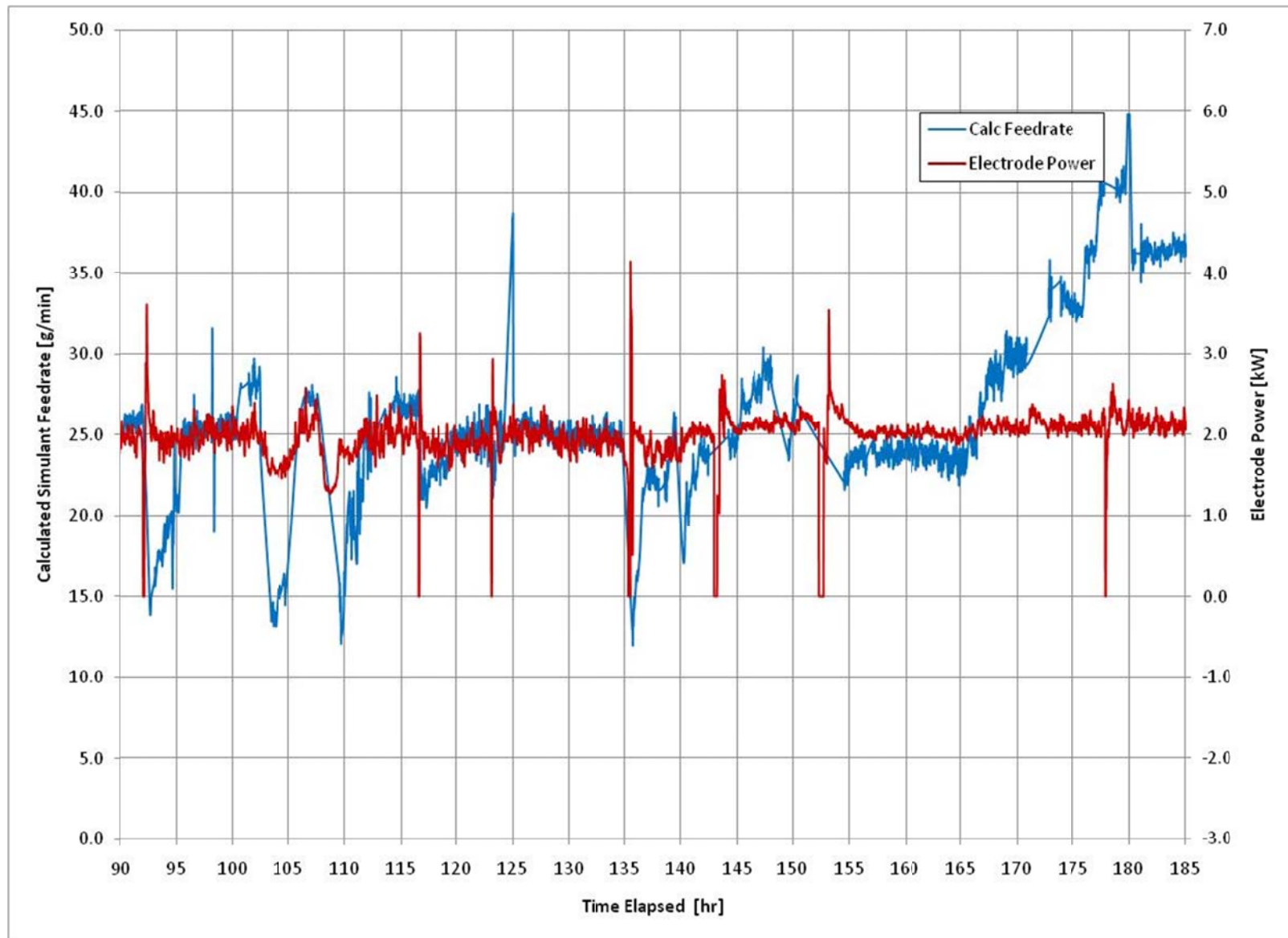
Figure D.8. Calculated Simulant Feed Rate and Electrode Power (90 to 185 hr)
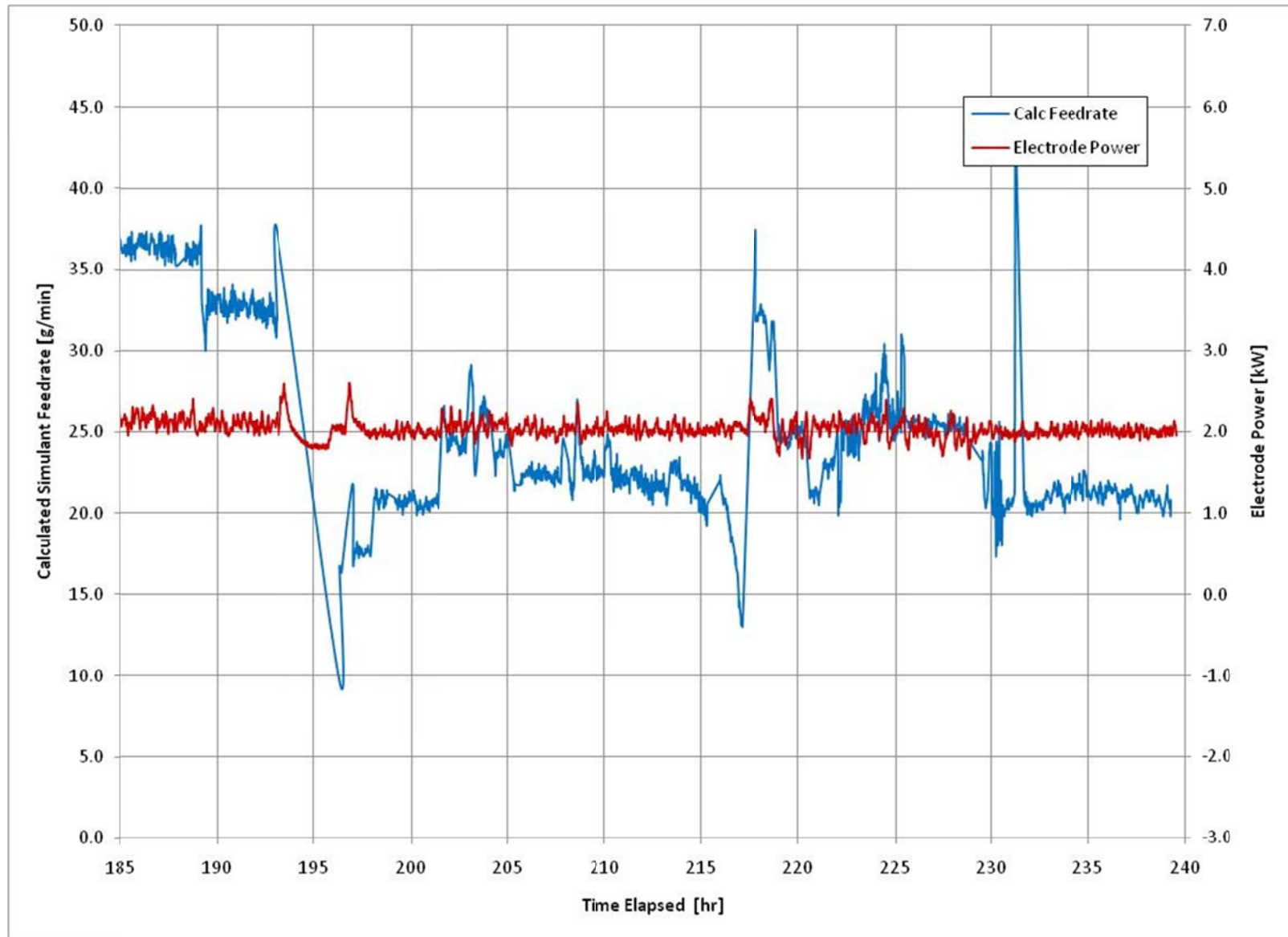
Figure D.9. Calculated Simulant Feed Rate and Electrode Power (185 hr to end of test)
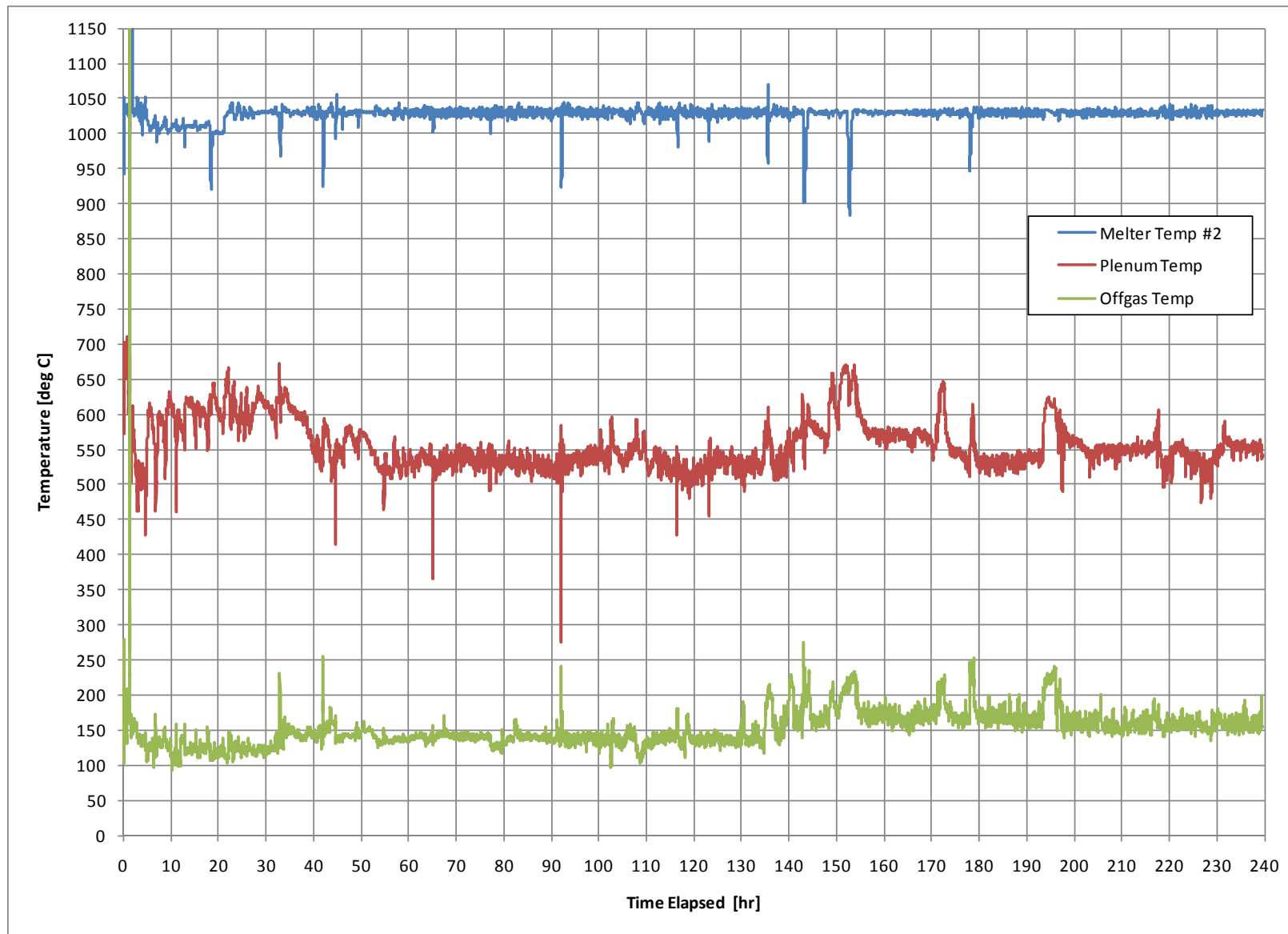
Figure D.10. Melter, Plenum, and Off-Gas Temperatures
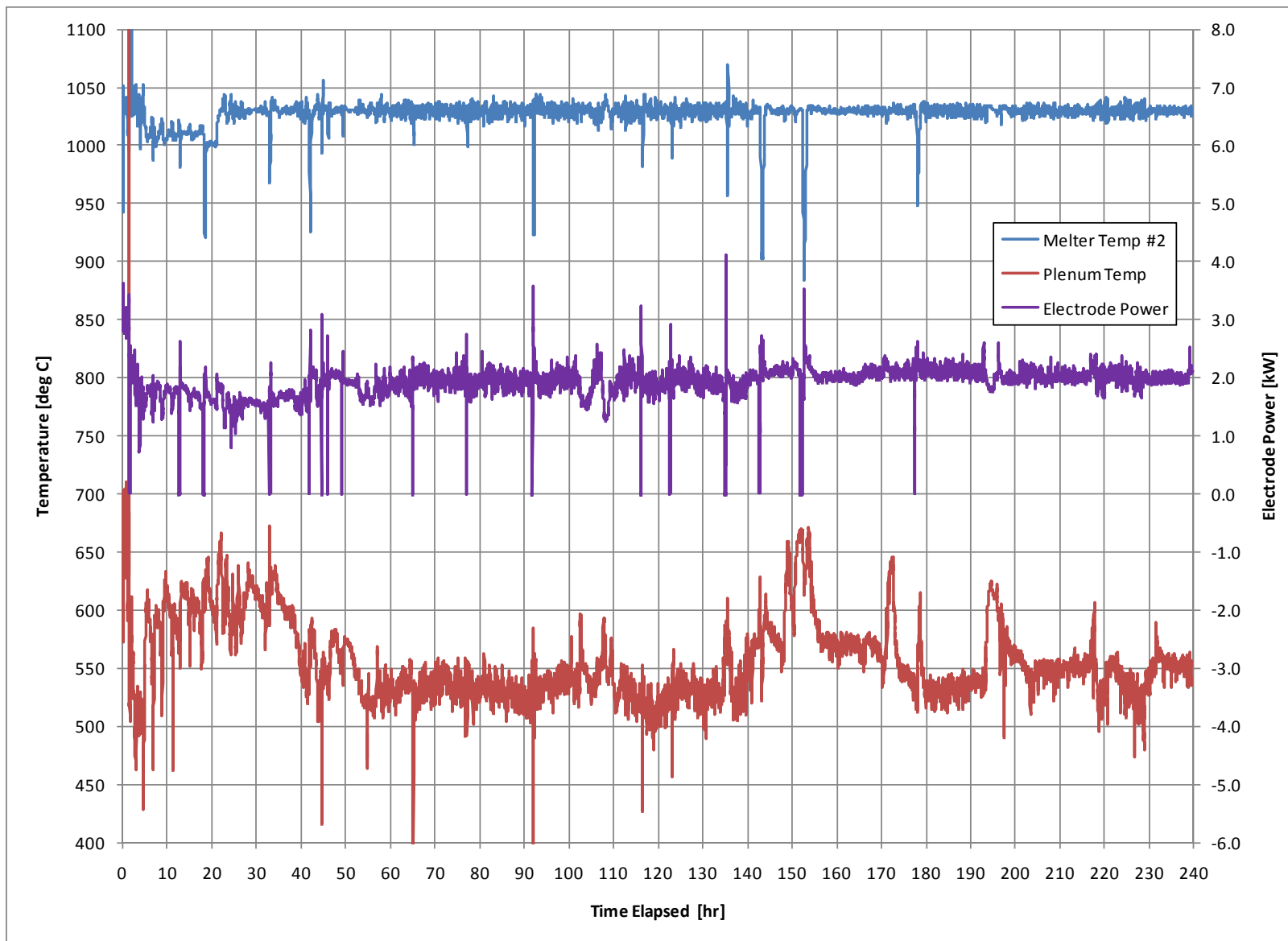
Figure D.11. Melter/Plenum Temperatures and Electrode Power
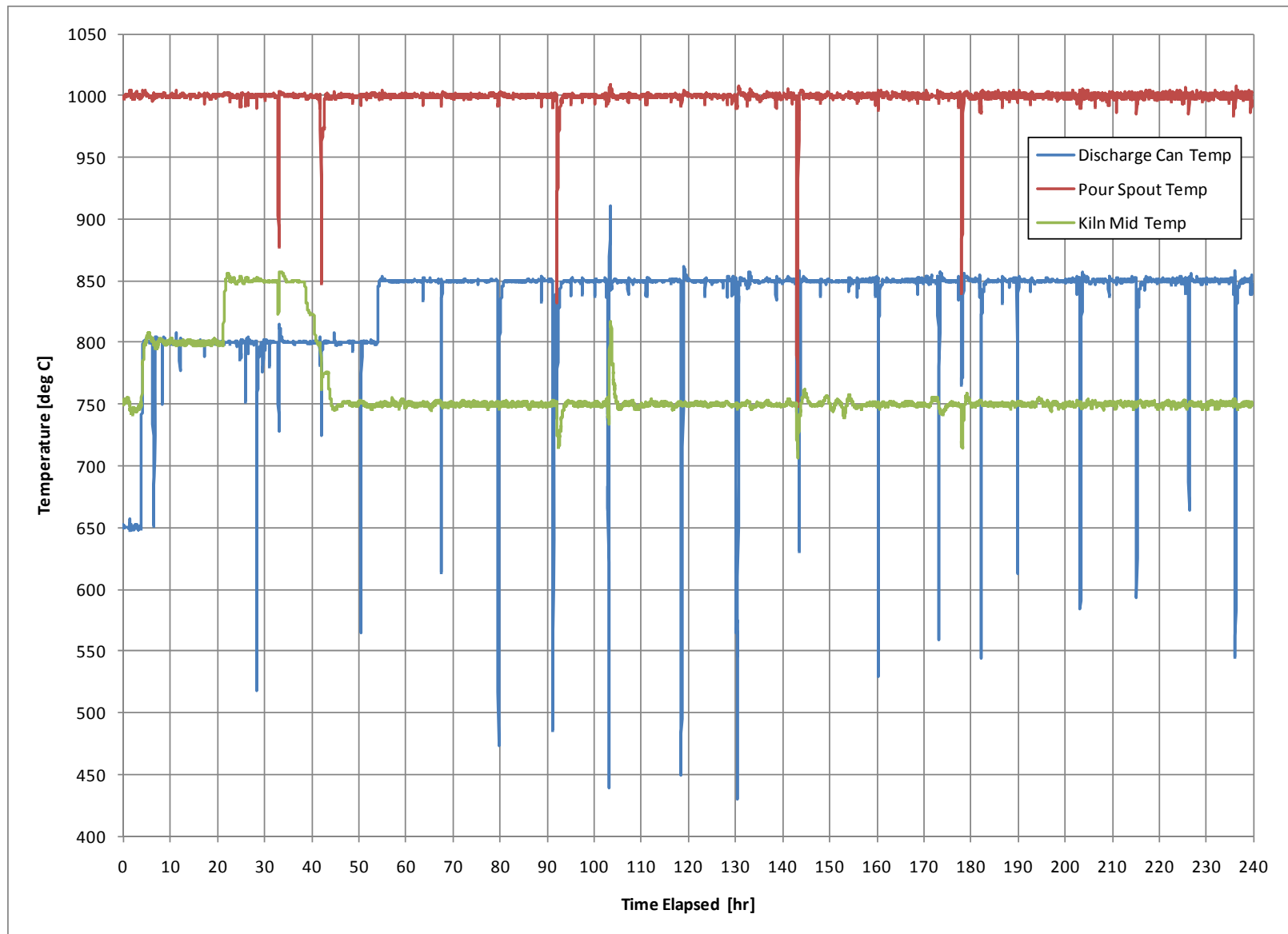
Figure D.12. Discharge Can, Pour Spout, and Kiln (Mid) Temperatures
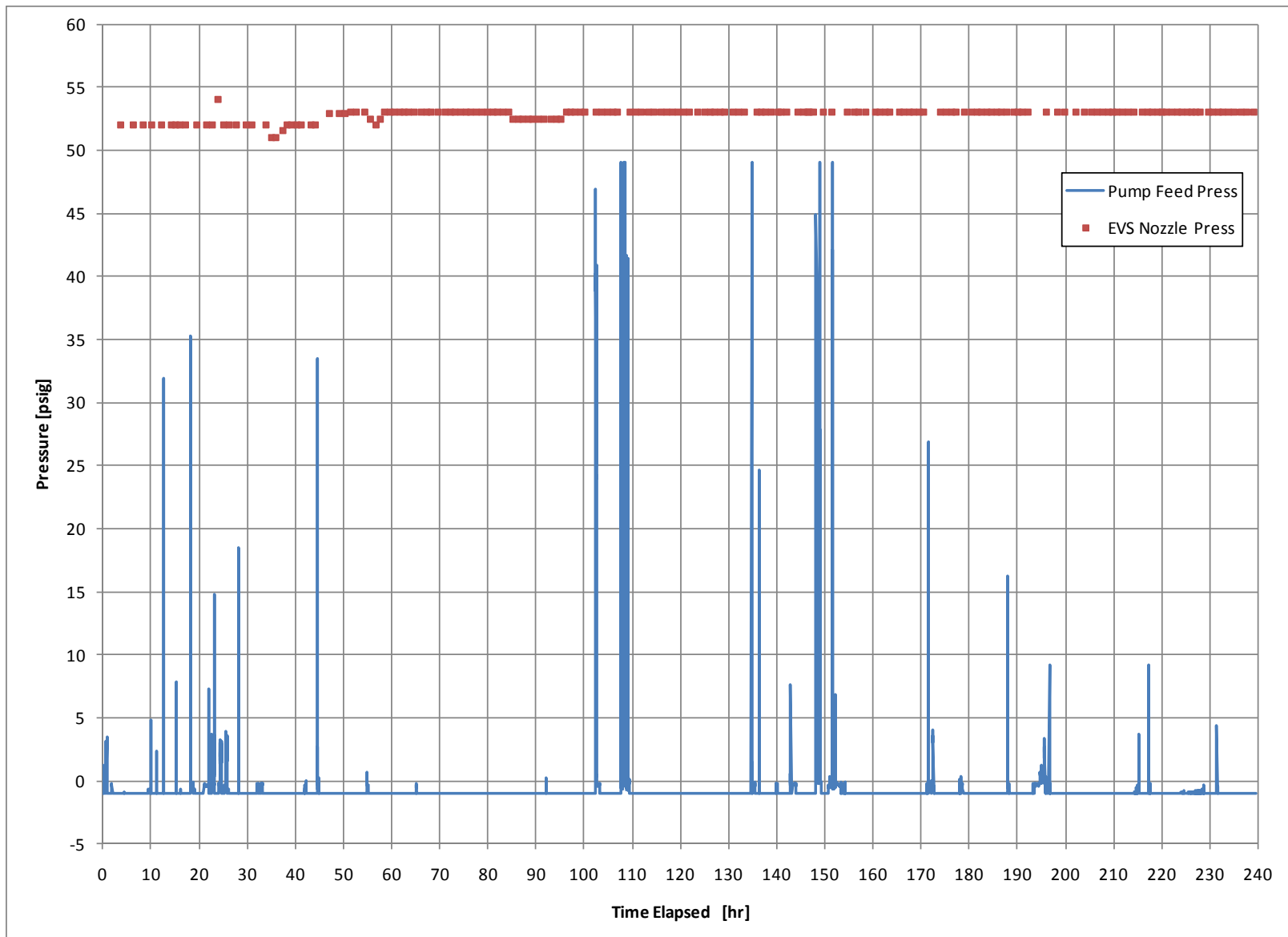
Figure D.13. Feed Pump and EVS Nozzle Pressure
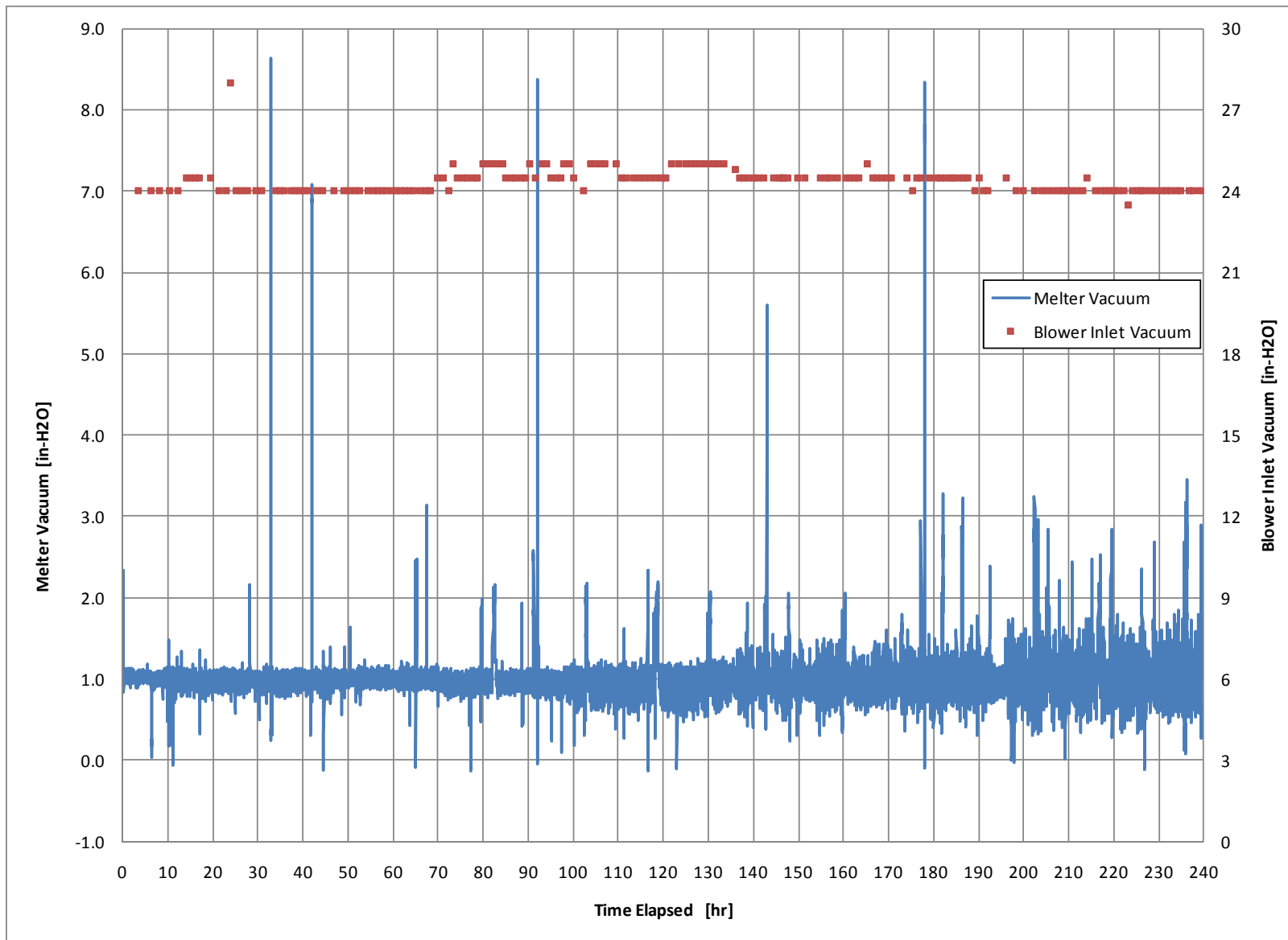
Figure D.14. Blower and Melter Vacuum
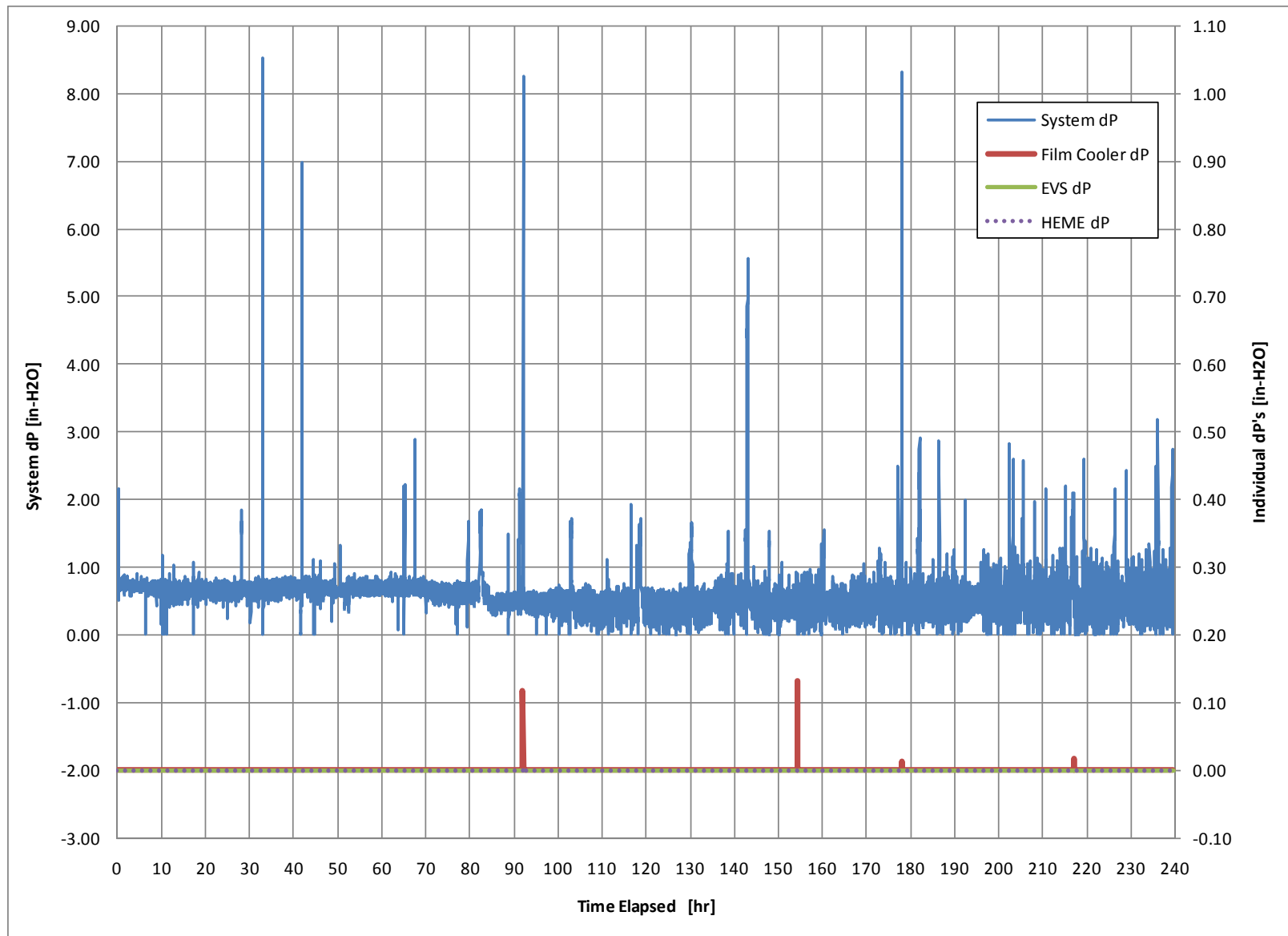
**Figure D.15**. System, Film Cooler, EVS, and HEME Pressure Drop
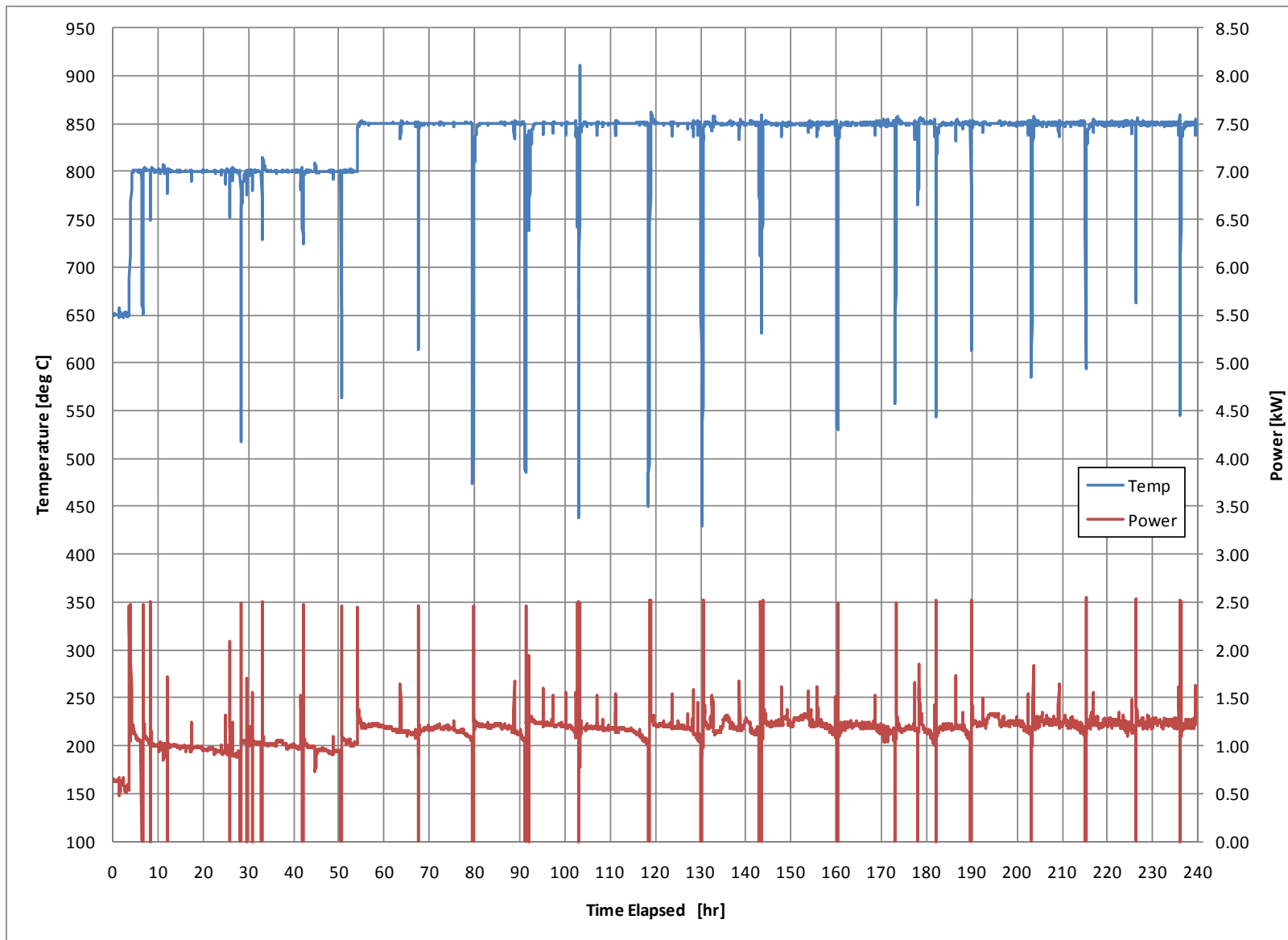
**Figure D.16**. Discharge Canister Power and Temperature
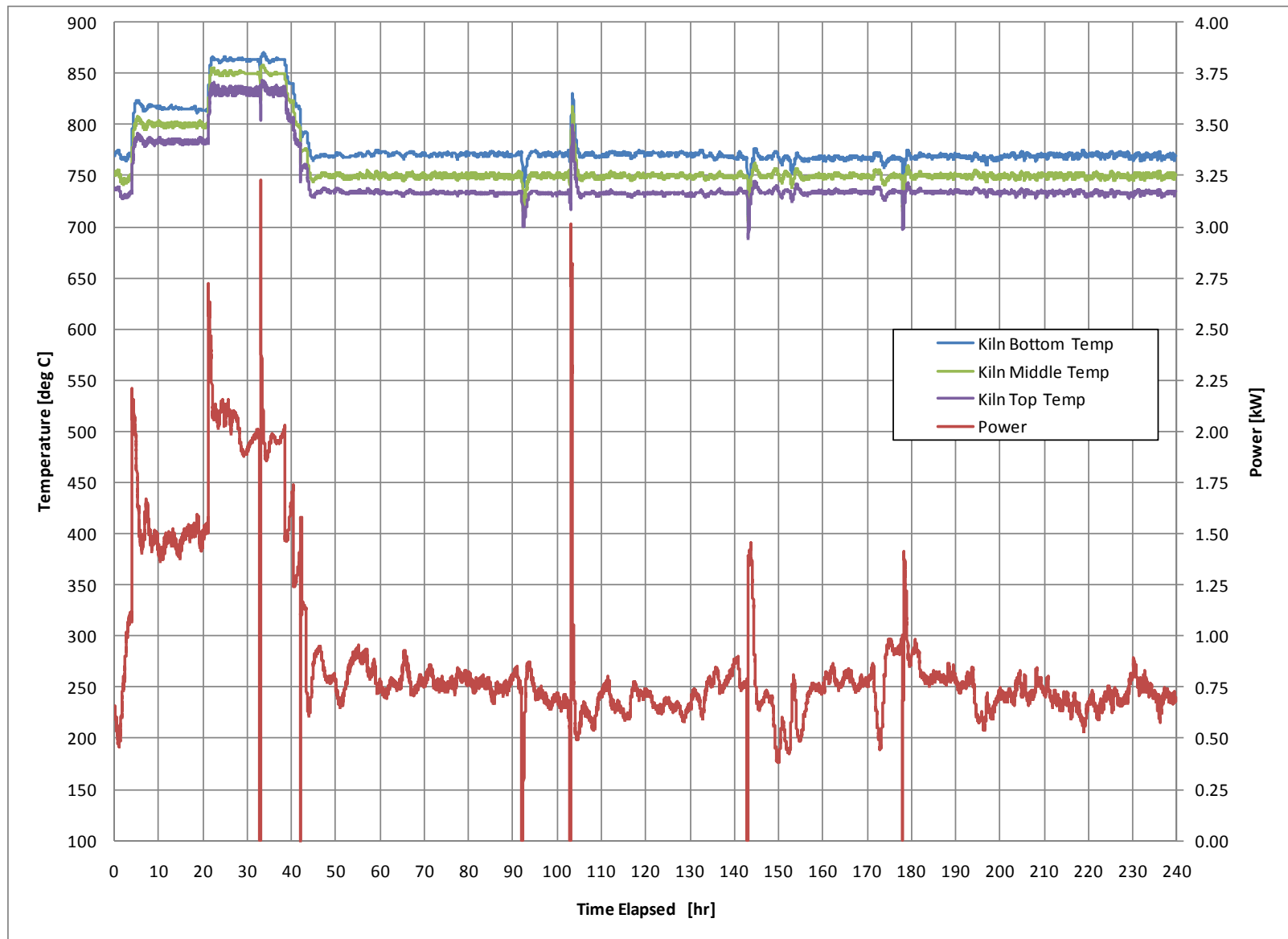
Figure D.17. Kiln Power and Temperature
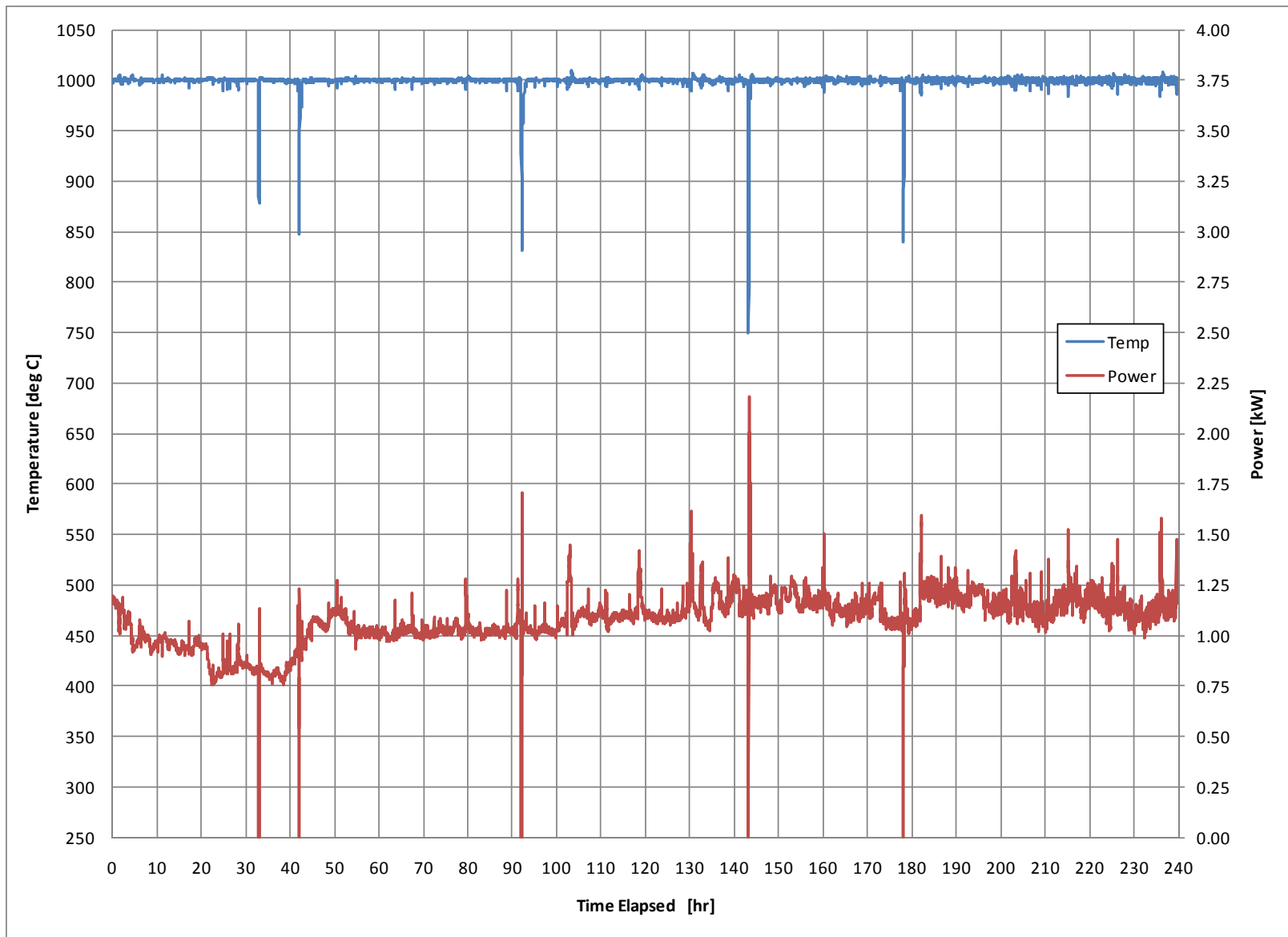
**Figure D.18**. Pour Spout Power and Temperature
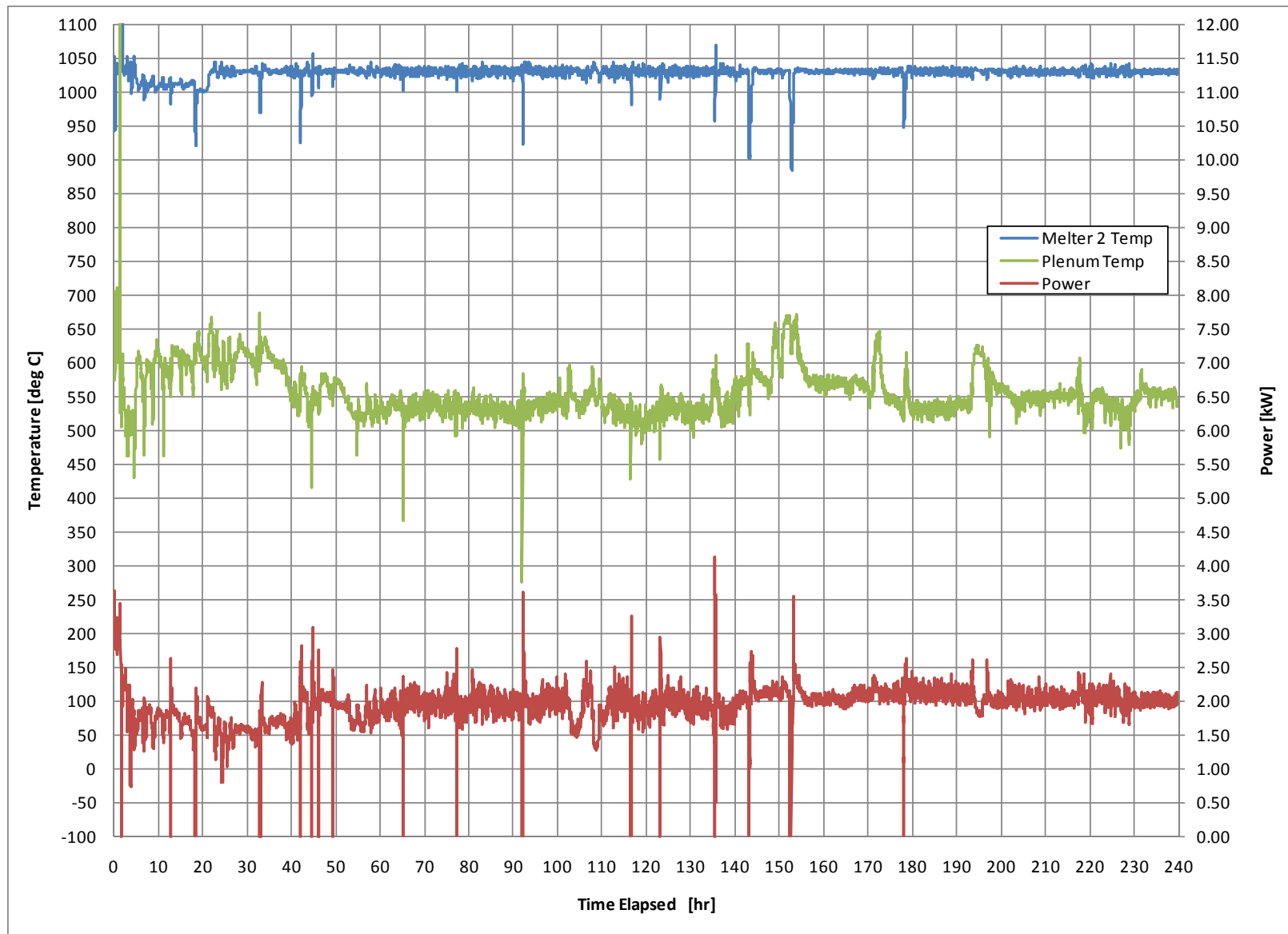
Figure D.19. Melter Electrode Power and Temperature (plenum temperature included)
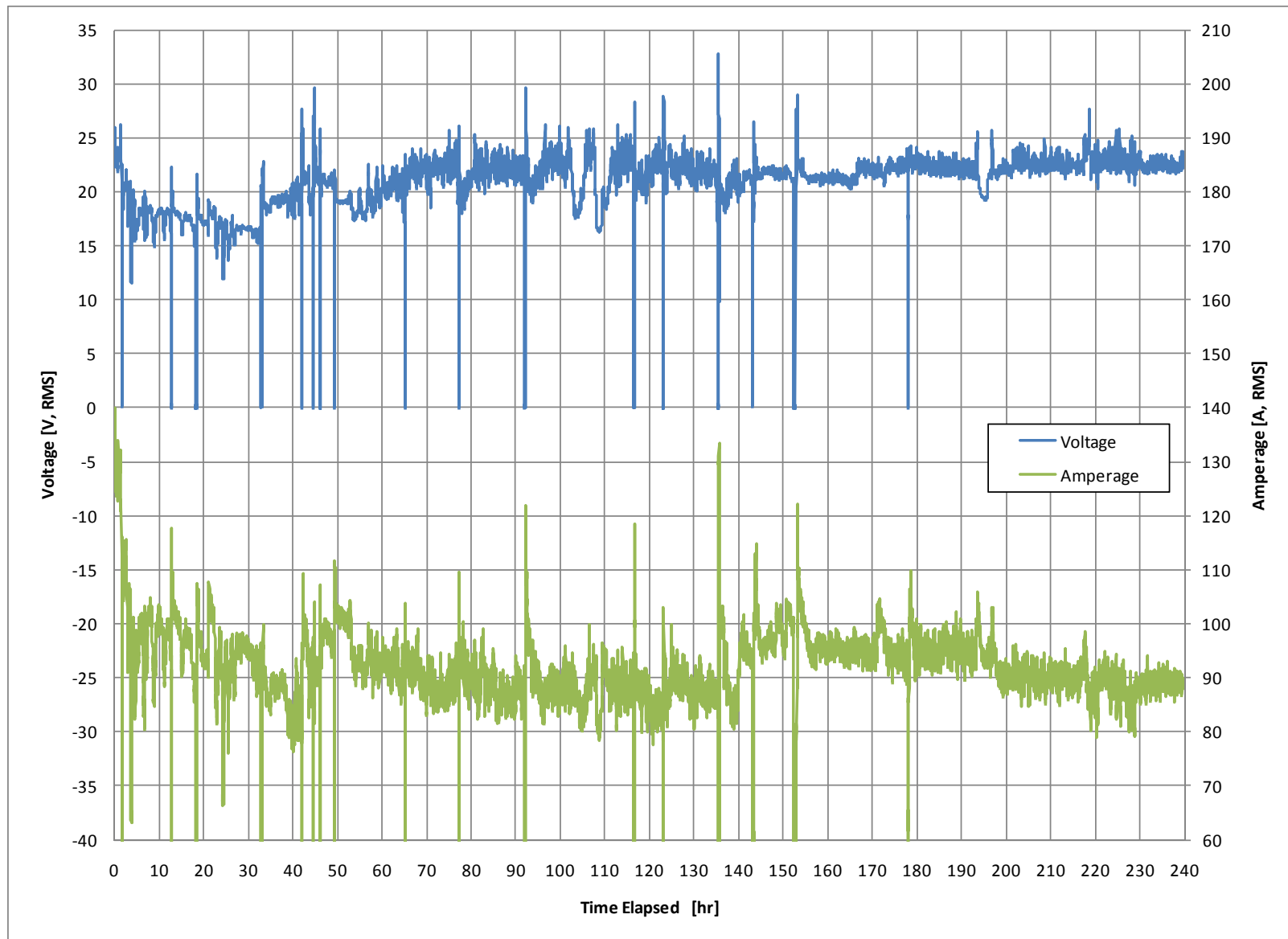
Figure D.20. Melter Electrode Voltage and Amperage
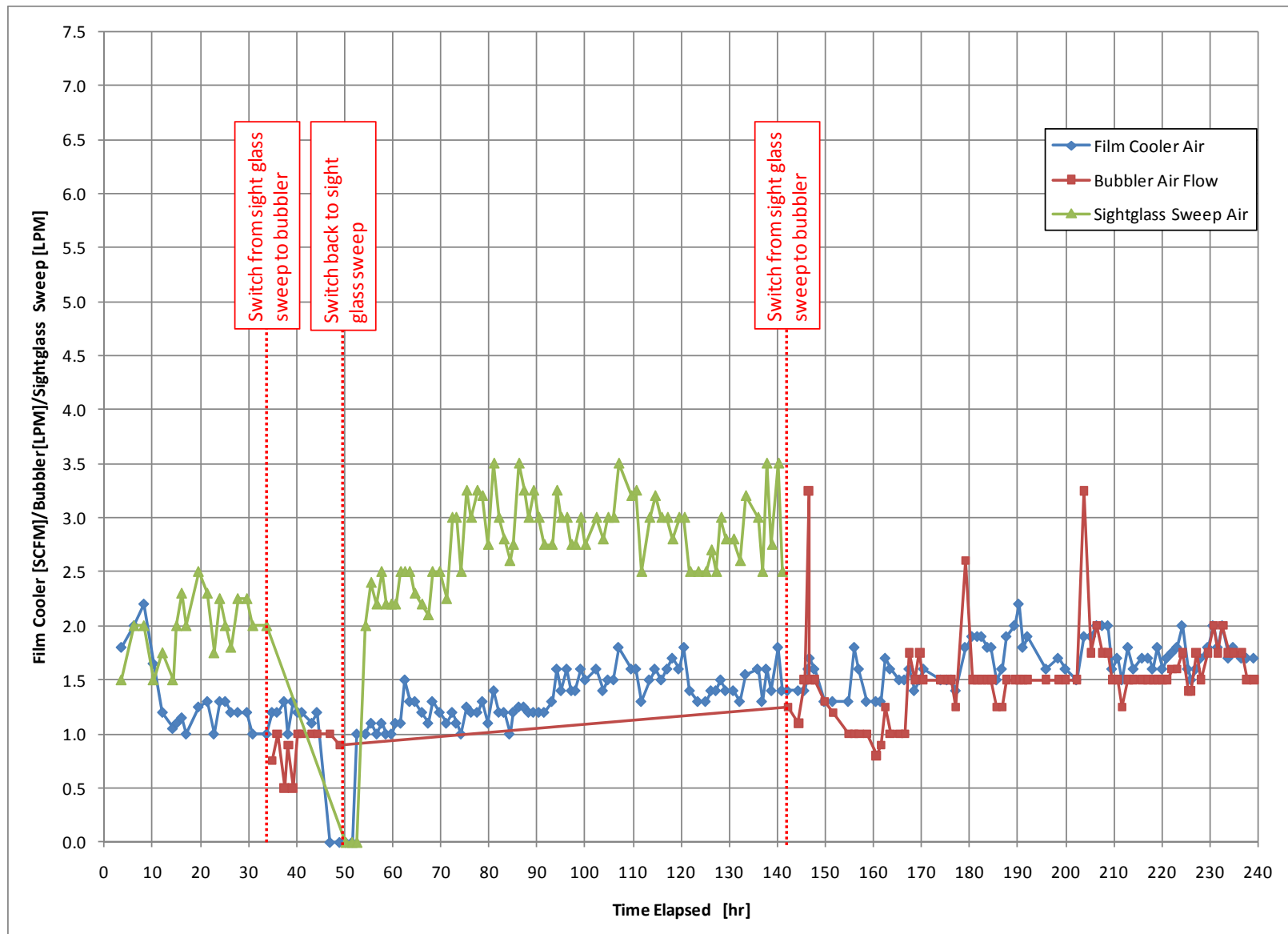
Figure D.21. Film Cooler, Bubbler, and Sight Glass Sweep Flow Rates
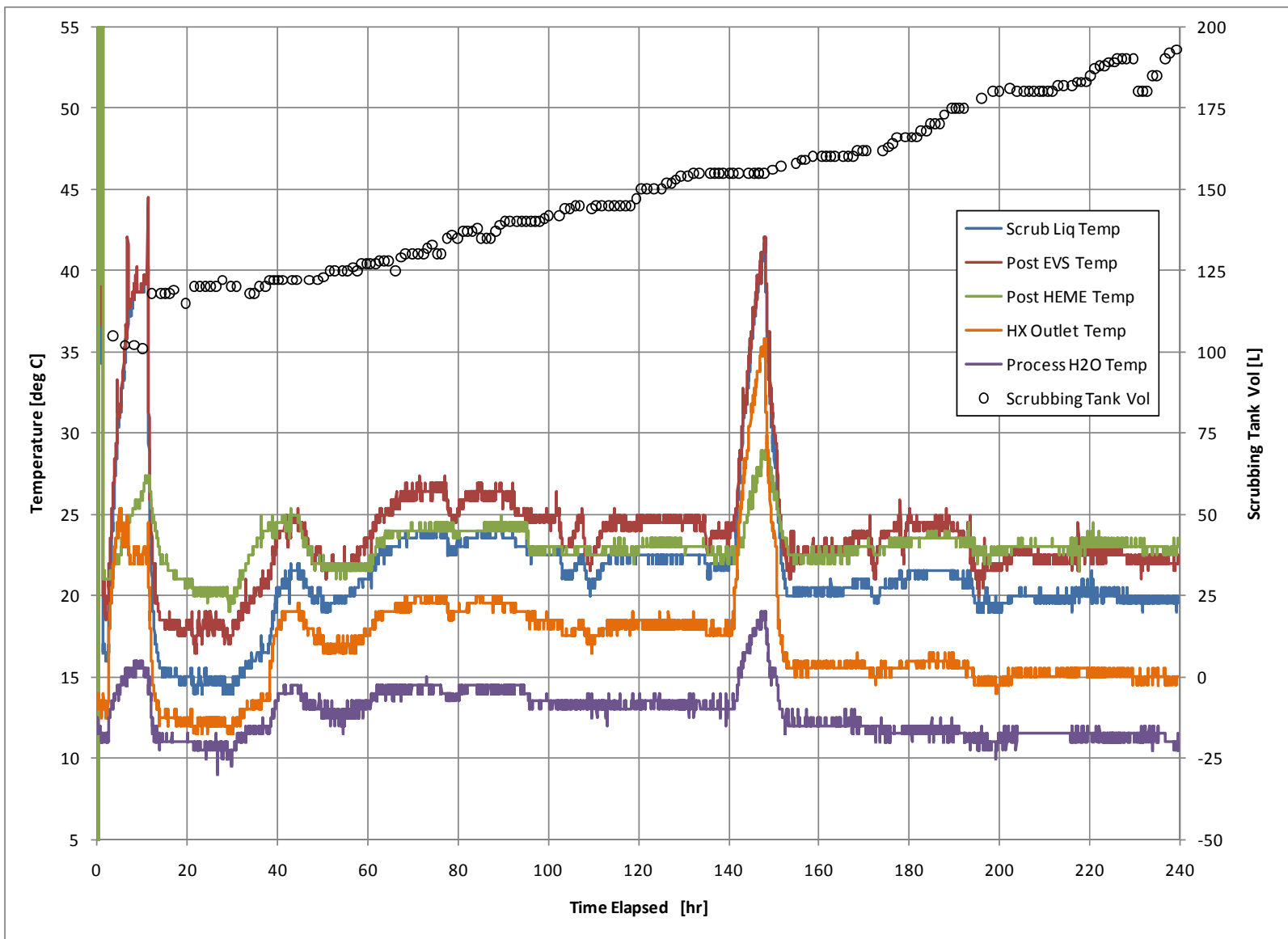
Figure D.22.   Scrubbing Liquid, Post EVS, Post HEME, Heat Exchanger Outlet, and Process Water Temperatures. Scrubbing Liquid Tank Volume Included.

Distribution*

No. of
Copies

No. of
Copies

3 U.S. Department of Energy
    Office of Environmental Management
        KD Gerdes
        SP Schneider
        GL Smith

3 U.S. Department of Energy
    Office of River Protection
        TW Fletcher
        RA Gilbert
        AA Kruger
        BM Mauss
        SH Pfaff

3 Savannah River National Laboratory
        F Johnson
        J Marra
        D Peeler

3 Vitreous State Laboratory
        W Kot
        K Matlack
        I Pegg

2 Washington River Protection Solutions
        WG Ramsey
        LE Thompson

4 Waste Treatment and Immobilization Plant
        SM Barnes
        CC Chapman
        JL Nelson
        LL Petkus

24 Pacific Northwest National Laboratory
        PR Bredt
        WC Buchmiller
        JL Buelt
        J Chun
        JV Crum
        PR Hrma
        A Goel
        BR Johnson
        GB Josephson
        JB Lang
        W Lepry
        DS Kim
        J Matyas
        JS McCloy
        RA Peterson
        LM Peurrung
        BJ Riley
        CP Rodriguez
        JV Ryan
        MJ Schweiger
        GJ Sevigny
        D Skorski
        JD Vienna
        JH Westsik, Jr.

*All distribution will be made electronically.